מכון ויצמן למדע
WEIZMANN INSTITUTE OF SCIENCE

Thesis for the degree
Doctor of Philosophy

חבור לשם קבלת התואר
דוקטור לפילוסופיה

By
Tamir Klein

מאת
תמיר קליין

אקו-פיזיולוגיה של ניצול מים באורן ירושלים: מרמת העלה ועד רמת היער

Eco-physiology of water use in *Pinus halepensis*: from leaf to forest scale

Advisor: Prof. Dan Yakir

מנחה: פרופ' דן יקיר

Co-mentored by Dr. Shabtai Cohen (ARO Volcani)

בשיתוף ד"ר שבתאי כהן (מינהל המחקר החקלאי מכון וולקני)

November 2012

תמוז תשע"ב

Submitted to the Scientific Council of the
Weizmann Institute of Science
Rehovot, Israel

מוגש למועצה המדעית של
מכון ויצמן למדע
רחובות, ישראל

This work has been conducted under the supervision of

Prof. Dan Yakir

Department of Environmental Sciences and Energy Research
Weizmann Institute of Science
Rehovot, Israel

And

Dr. Shabtai Cohen

Institute of Soil, Water and Environmental Sciences
Volcani Center ARO
Beit Dagan, Israel

Acknowledgements

I was blessed with two exceptional mentors, Prof. Dan Yakir and Dr. Shabtai Cohen, whose positive, passionate approach to scientific research and to any learning in general, has been an inspiration to me. Their enthusiasm about plant eco-physiology together with the highest level of professionalism has made a profound impact on my work.

I wish to thank my advisory committee, Profs. Brian Berkowitz and Amram Eshel for their interest in the work and advice for improvements. I have had the privilege of illuminating discussions with Prof. Gabi Schiller, Dr. Jose Gruenzweig, Dr. Gilboa Arye, Dr. Ron Milo, Prof. Harvey Scher, Prof. Yohai Carmel and Dr. Yagil Osem, that broadened my knowledge and understanding.

The members of Dan's group with whom I have worked: Fyodor, David, Uri, Hemu, Naama, Keren, Gil and Amir; have been research collaborators and good friends. Special thanks go to Dr. Eyal Rotenberg, with whom I had many interesting discussions and good research ideas, and Yakir Preisler, a lasting companion to the field operations. Hagay, Manuela, Ruthi and Efrat are greatly acknowledged for their help at the lab. The work would not have been possible without the assistance of many 'secret helpers': the undergraduate students Yoav, Gil, Ehud, Shani and Mika, and the WIS security personnel. Around the department, Ishay, Ruthi, Dalia, Ofra, Avram, Hila and Dror have always been a source of help accompanied with a smile.

I express my gratitude to a number of excellent, foreign scientists with whom I had the benefit to learn from and collaborate. This includes Prof. Katarina Strelcova, Dr. Jiri Kucera, Dr. Giovanni Di Matteo, Dr. Jerome Ogee, Dr. Lisa Wingate, Prof. Nate McDowell, Dr. Christopher Reyer, Dr. Sebastian Leuzinger, Dr. Guenter Hoch and Prof. Christian Koerner. These collaborations, facilitated by meetings with the support of various EU travel grants, have undoubtedly left a prominent footprint on my research.

Finally, my wife Yasmin, who always encouraged and took an interest in my work, our little Tom (who was born amidst this term), and my parents Hanna and Yoel, I thank you for everything.

Declaration

This Thesis summarizes my own research.

Dr. Eyal Rotenberg, a research associate in our group, has contributed to the discussion of results from the provenance trial (chapter 5.2) and the study of soil and tree hydraulics (chapter 5.3).

Yakir Preisler, an MSc student in our group, performed the deep soil survey in Yatir forest which facilitated the root distribution analysis in the study of soil and tree hydraulics (chapter 5.3). Yakir also established and maintained the stand density experiment in Yatir forest, enabling the study of stand density effects on leaf gas exchange (chapter 5.4.9-11).

The study of soil and tree hydraulics (chapter 5.3) involved additional contributors. Ella Cohen-Hilaleh, an MSc student, participated in soil sampling and analysis. The soil moisture measurement system was established by Naama Raz-Yaseef, a former PhD student. Soil moisture simulations using the model MuSICA were performed together with Dr. Fyodor Tatarinov of our group, and the model developer, Prof. Jérôme Ogée of INRA, Bordeaux, France.

Dr. Giovanni Di Matteo of CRA, Rome, Italy, has participated in tree coring as part of the provenance trial (chapter 5.2).

Interpretation and analysis of the data is my own.

All other work presented in this Thesis is also my own.

Tamir Klein
Rehovot, November 2012.

Table of Contents

1. List of abbreviations **7**

2. Abstract **8**

3. Introduction **10**

3.1. Forests under change 10

3.2. Water transport in trees 10

3.3. Xylem embolism and refilling 12

3.4. Forests and the hydrological cycle 13

3.5. Aleppo pine as a model forest tree 14

3.6. A forest in the dry timberline 15

3.7. Research Objectives 15

4. Materials and Methods **16**

4.1. Forest sites and plant material 16

4.2. Experimental set-up and design of the greenhouse experiment 18

4.3. Experimental design of the thinning experiment 18

4.4. Tree water use 19

4.5. Xylem hydraulic conductivity and cavitation 20

4.6. Leaf gas exchange and water potential 21

4.7. Field Performance and growth phenology 21

4.8. Tree- ring $\delta^{13}C$ 22

4.9. Leaf chlorophyll concentration 23

4.10. Soil mechanical arrangement and water retention 23

4.11. Root depth distribution 24

4.12. Simulation of soil water content dynamics 25

4.13. Upscaling from leaf- to forest stand-scale transpiration 25

4.14. Statistical analysis 26

5. Results **27**

5.1. Hydraulic adjustments underlying drought resistance of *Pinus halepensis*.

Klein T, Cohen S, Yakir D. 2011. Hydraulic adjustments underlying drought resistance of *Pinus halepensis. Tree Physiology* **31**:637-48. 28

5.1.1. Seasonal shifts in xylem hydraulics on the diurnal scale 40

5.1.2. Comparison with previous reports of cavitation and refilling 45

5.1.3. Stomata, VPD, leaf water potential and cavitation 46

5.2. The role of trait plasticity in sustaining growth and survival of *Pinus halepensis* under climate change in the Mediterranean. **50**

Klein T, Di Matteo G, Rotenberg E, Cohen S, Yakir D. 2012. Differential ecophysiological response of a major Mediterranean pine species across a climatic gradient. *Tree Physiology*, in press. 51

5.3. The role of soil and tree hydraulics in the success of a water-limited pine forest. **62**

5.3.1. Soil water content dynamics and mechanical structure 62

5.3.2. Soil water retention properties 63

5.3.3. Transpirable soil water content and tree water use 65

5.3.4. Annual soil water budget is influenced by depth-dependent infiltration 69

5.3.5. Root depth distribution 70

5.3.6. Water $\delta^{18}O$ of soil and tree sap 71

5.3.7. Relationship between soil texture and water content from ecosystem model simulations 72

5.3.8. Depth-dependent water availability 74

5.3.9. Inter-annual variations in transpirable soil water content 75

5.4. From leaf to forest scale: water use of *P. halepensis* and the coexisting, anisohydric *Quercus calliprinos* and the impact of a semi-arid pine forest on local water yield. **79**

5.4.1. Stomatal regulation in *P. halepensis* and *Q. calliprinos* 79

5.4.2. Stomatal adjustments and transpiration 79

5.4.3. Seasonal gas exchange patterns of *P. halepensis* and *Q. calliprinos* 80

5.4.4. Tree-ring $\delta^{13}C$ 83

5.4.5. Stand-scale water use of *P. halepensis* and *Q. calliprinos* 84
5.4.6. Relationship between stomatal regulation and leaf gas exchange 85
5.4.7. Relationship between tree-ring $\delta^{13}C$ and leaf gas exchange 87
5.4.8. Water-use of *Pinus halepensis* and *Quercus calliprinos* and the forest water balance 87
5.4.9. Stand density effects on leaf-scale conditions and gas exchange rates 90
5.4.10. Upscale to stand-scale gas exchange rates using leaf area index (LAI) 90
5.4.11. The thinning bias 91

6. Discussion **93**
6.1. Eco-physiology of water use in *P. halepensis* 93
6.2. A broader perspective 94
6.3 Implications for forest management under change 96

References **98**

1. List of abbreviations

Abbreviation	Definition	Units
A	Net carbon assimilation	µmol CO_2 m^{-2} s^{-1}
BAI	Basal area increment	cm
DBH	Diameter at breast height	cm
E_s	Evaporation from soil	mm
ET	Evapotranspiration	mm
g_s	Leaf stomatal conductance	µmol H_2O m^{-2} s^{-1}
I	Interception	mm
K_s	Specific hydraulic conductivity	kg m^{-1} MPa^{-1} s^{-1}
L_a	Leaf area	m^2
P	Annual precipitation	mm
PAR	Photosynthetically active radiation	µmol m^{-2} s^{-1}
PDI	Plant drought index	(dimensionless)
PLC	Percent loss of conductivity	%
RH	Relative humidity	%
SF	Sap flow rate	kg hr^{-1}
SFD	Sap flux density	cm^3 d^{-1} cm^{-2}
SWC	Soil water content (volumetric)	m^3 m^{-3}
T	Leaf transpiration	mmol H_2O m^{-2} s^{-1}
T_d	Diurnal tree water use	mm
tSWC	Transpirable soil water content	mm
T_t	Tree water use	mm
T_u	Understory water use	mm
VPD	Vapor pressure deficit	kPa
WUE_i	Intrinsic water-use efficiency	µmol CO_2 mol^{-1} H_2O
$\delta^{13}C$	^{13}C fractionation	‰
$\Delta^{13}C$	Discrimination against ^{13}C	‰
Ψ_l	Leaf water potential	MPa
Ψ_s	Soil water potential	MPa

2. Abstract

Tree water use and transport are fundamental eco-physiological processes with major implications on phenomena of various scales. Among these are the biological mechanisms underlying tree drought resistance; the interactions between hydraulic and physiological traits; and the differences of water use with forest type, with important implications for water yield under increasing water limitations. In this study, these processes were measured in *Pinus halepensis* trees growing in the dry timberline, where they are regularly challenged by seasonal drought. The field study at Yatir forest (southern Israel) was complemented by provenance trials across a climatic gradient including Rome, Italy and Beit Dagan (central Israel); comparison to a coexisting oak species; a forest thinning experiment; and a greenhouse experiment. We found that the regulation of water use in *P. halepensis* is isohydric: stomata typically limit water potential to above -2.8 MPa. At -3.1 MPa, there is already 50% loss of xylem conductivity due to cavitation, leaving a narrow safety margin of ~0.3 MPa. This risky behavior, near or beyond the safety margin, allows prolonged CO_2 uptake under drought. We demonstrated that this is possible because it is complemented by efficient cavitation reversal. In summer, the refilling of cavitated xylem was completed within 1-2 hr., two times during the day, a dynamic that has not been previously reported. Sap flow lagged behind leaf transpiration, indicating that the stem xylem system buffers long (up to 9 hr.) and large (3-5 kg) water deficits during a day. Differences between *P. halepensis* provenances indicated that drought-induced mortality was related to a 2-7 fold higher sensitivity to cavitation. A cavitation-resistant provenance had a longer growth season than a sensitive provenance (200 and 140 days, respectively). Wood $\delta^{13}C$ analysis showed that water use efficiency increases with drying from 80, to 95, to 110 μmol CO_2 mol^{-1} H_2O along the climatic gradient from Rome, through Beit Dagan, to Yatir, respectively. An equation was developed to quantify the amount of soil water available for tree transpiration at a given soil layer and time (tSWC), calculated from its water retention properties and root uptake water potential threshold. tSWC=0 defined, empirically, the onset and the termination of the growth season. Water use of the isohydric *P. halepensis* in the dry season was 50-70% lower than that of the coexisting, anisohydric *Quercus calliprinos*. Finally, the relatively high resistance to water flow of *P. halepensis* together with a conservative water use, mostly unaffected by stand density, means moderate effect of pine afforestation on water yield in a semi-arid site.

תקציר

ניצול והובלת מים בעצים הינם תהליכים אקו-פיזיולוגיים בסיסיים בעלי השלכות נרחבות על תופעות במספר רמות. ביניהן, התהליכים הביולוגיים המקנים לעץ עמידות לבצורת; קשרי הגומלין בין תכונות הידראוליות ופיזיולוגיות; והשפעת סוג היער על ניצול המים, עם השלכות חשובות על המים בקרקע תחת מגבלת מים מחריפה. במחקר זה נמדדו תהליכים אלו בעצי אורן ירושלים הגדלים על סף המדבר ונחשפים לבצורת עונתית מידי שנה. לעבודת השטח ביער יתיר שבדרום הארץ התווספו ניסויי אקוטיפים לאורך גרדיאנט אקלימי הכולל את רומא, איטליה, ובית דגן, במרכז הארץ; השוואה לאלון מצוי; ניסוי דילול ביער; וניסוי חממה. מצאנו כי הבקרה על ניצול המים באורן ירושלים הינה איזוהידרית: הפיוניות בד״כ מגבילות את פוטנציאל המים לערכים שמעל 2.8- מגה-פסקל. ב-3.1- מגה-פסקל יורדת מוליכות העצה ב-50% עקב קביטציה, תו״כ השארת טווח ביטחון צר של ~0.3 מגה-פסקל. התנהגות מסוכנת זו, קרוב או מעבר לטווח הביטחון, מאפשרת המשך הטמעת פחמן דו-חמצני גם בעקת יובש. הראנו כי התנהגות זו אפשרית בעזרת תהליך יעיל של מילוי מחדש. בקיץ, מילוי של עצה הנמצאת בקביטציה הושלם תוך שעה עד שעתיים פעמיים במהלך היום, דינמיקה אשר טרם תוארה. זרימת המים בגזע פיגרה אחר הדיות בעלים , תופעה המצביעה על תפקידה של מערכת העצה בגזע כתווך למחסור ממושך (עד 9 שעות) וגדול (3-5 ק״ג) במים במהלך היום. הבדלים בין אקוטיפים של אורן ירושלים הראו כי תמותה עקב בצורת הייתה קשורה לרגישות לקביטציה הגבוהה פי 2-7. עונת הגידול הייתה ארוכה יותר באקוטיפ עמיד לקביטציה מאשר באקוטיפ רגיש (200 ו-140 יום, בהתאמה). ניתוח של ההרכב האיזוטופי של הפחמן בגזע הראה כי יעילות ניצול המים עולה עם היובש מ-80, ל-95, ל-110 מיקרומול פחמן דו-חמצני למול מים לאורך הגרדיאנט האקלימי מרומא, דרך בית-דגן, ועד יתיר, בהתאמה. פותחה משוואה לכימות זמינות המים לדיות העצים לכל שכבת קרקע וזמן (״מים זמינים לדיות״), שחושבה מתוך תכונות תאחיזת המים של שכבת הקרקע וסף פוטנציאל המים לכניסת מים לתוך השורש. סף זמינות המים לדיות הגדיר, באופן אמפירי, את תחילתה ואת סיומה של עונת הגידול. ניצול המים של אורן ירושלים האיזוהידרי במהלך הקיץ היה נמוך ב-70-50% מזה של האלון המצוי האנאיזוהידרי באותם אתרים. לסיום, ההתנגדות הגבוהה יחסית לזרימת מים בעצה של אורן ירושלים יחד עם ניצול מים שמרני, אשר לרוב איננו מושפע מצפיפות היער, משמעותה השפעה מתונה יחסית של יער האורנים על המים בקרקע, גם באתר תת-מדברי.

3. Introduction

3.1. Forests under change

Water deficiency is the main factor limiting plant productivity worldwide (Boyer 1982, Flexas et al. 2004) and drought is an important driver of eco-physiological adaptations in plants. Future climate warming is expected to elevate atmospheric water demand; however changes will not be restricted to increases in mean temperature, but will also include increases in the frequency and intensity of droughts (Christensen et al. 2007, Seager et al. 2007, Sterl et al. 2008). Climate predictions indicate drying trends associated with reduced precipitation in the Mediterranean and other regions (Alpert et al. 2006, Burke et al. 2006). Observed increases in global drought severity since 1952 and in evaporative demand in Israel since 1964 are expected to intensify during the 21st century (Cohen et al. 2002, Burke et al. 2006). The fate of many forest ecosystems will depend on the ratio of the rate of the climate changes to the rate of adaptation to such changes. A ratio larger than one means that the rate of climate change exceeds the rate of plant adaptation. Accumulating evidence of drought-induced tree mortality in recent years (Allen et al. 2009 and references therein) might be the result of this scenario. In 2008 alone at least five examples of distinct drought-induced forest stand dieback and decline were observed. This includes *Abies cephalonica* forests in Greece (Raftoyannis et al. 2008); *Cedrus atlantica* in Algeria and Morroco; *Quercus*, *Pinus*, and *Juniper* spp. in Turkey; and *Quercus suber* in France (Allen et al. 2009). Impacts on *Pinus* sect. *halepensis* (including *P. brutia*) following the drought years of 1999-2000 are evident in Israel as well as in Greece (Koerner et al. 2005, Sarris et al. 2007) and Spain (Penuelas et al. 2001, Martinez-Vilalta and Pinol 2002). Additional implications of climate change on tree growth include reduced ability of forests to sequester carbon (Ciais et al. 2005) as well as shifting the timing of the growth season (Chmielewski and Rotzer 2001).

3.2. Water transport in trees

The mechanism of water transport in plants is known as the cohesion–tension theory, first proposed in the late 19th century (Boehm 1893, Dixon and Joly 1894). Although this theory is still being challenged (Zimmermann et al. 2004), it is the only widely accepted theory of water transport in plants (Angeles et al. 2005).

Trees, like other vascular plants, have developed a very specific tissue devoted to long-distance water transport, i.e. the xylem. The xylem contains cells that have

evolved to specialize in water transport: the lateral walls have been reinforced by a deposit of hydrophobic lignin and the cytoplasm has been dissolved. This type of cells is called tracheids. In broadleaves trees, cell end walls are partly or completely dissolved, thus forming very long conduits: the vessels. Tracheids and vessels are hence capillaries of various dimensions (1 mm to several meters in length and 10 to 400 μm in diameter). These pipes are made of dead cells and water moves from one conduit to another across cell walls without crossing any membrane. Water movement is caused by differences in hydrostatic pressures ΔP (Sperry et al. 2003, Domec et al. 2009):

(1) $F = K*\Delta P$

where F is the bulk water flow (kg s^{-1}) and K a diffusive coefficient. To account also for water movement across a membrane (e.g. between two cytoplasts) we must consider the difference of osmotic potential ΔΠ between the two compartments and the reflection coefficient of the membrane:

(2) $F = K*(\Delta P + \sigma*\Delta\Pi)$

If the membrane is perfectly hemi-permeable (σ=1), $\Delta P + \sigma*\Delta\Pi$ represents the difference in water potential Ψ, namely, the chemical potential of water μ divided by its partial molar volume. Hence:

(3) $F = K*\Delta\Psi$

The entire water flux crossing the tree comes from the soil, which is a porous media made of small aggregates and particles retaining water between them. Water enters the root xylem by reverse-osmosis (Eq. 2) and flows to the leaves in the xylem conduits, according to difference in hydrostatic pressures (Eq. 1). This xylem pathway represents about 99% of the total water path length in the tree. Hydrostatic pressures in the soil are at most zero and usually under negative pressures. The force of gravitation lowers this pressure by −0.1 MPa every 10 m of tree height, and hence the xylem conduits are under negative pressures (i.e., under tension; Tyree and Sperry 1988, Holbrook 1995, Holbrook and Zwieniecki 1998). Hence, at the top of a 100 m tall *Sequoia*, the xylem pressure is lower than −1 MPa (Cochard 2006). When water evaporates in the leaves, the radius of air/water meniscusi tend to decrease, thus increasing the capillary forces due to the surface tension of water. These forces pull upwards the water molecules at the meniscusi, but because the cohesive forces between water molecules are much larger, it is the entire water column which is pulled upwards. Because water has to find a path through pores and membranes, there

is a resistance to the water flow. This resistance further lowers the negative xylem pressure proportionally to the water flow (Domec et al. 2009). As a consequence, xylem pressures of most temperate trees typically reach values as low as −2 MPa in the middle of the day. Much more negative values are measured in Mediterranean trees.

3.3. Xylem embolism and refilling

Since the sap pressure is most of the time under large negative pressures, trees live under the threat of cavitation. Cavitation would break the continuity of water columns and hence the water supply to transpiring leaves. Xylem embolism and cavitation inhibit hydraulic conductance and are therefore among the most prominent threats to plant function worldwide. In theory, without the risk of hydraulic failure, plants could potentially increase their leaf gas exchange up to the limits of photosynthetic capacity, thereby augmenting primary productivity and reducing the occurrence of drought-induced mortality. This is because cavitation can be fatal (e.g. Tyree and Sperry 1988, Brodribb and Cochard 2009) and irreversible (Tyree and Sperry 1988). Since water is transported in the xylem under constant tension (water potential, $\Psi<0$) the possibility of refilling was ruled out by pioneering research. However, empiric evidence for the reversibility of cavitation and the refilling of xylem conduits became available from experimental data on induced and native embolism (Tyree 1999, Holbrook and Zwieniecki 1999, respectively). The proposed refilling mechanism overcame the tension enigma by segregation, i.e. the refilling process is preceded by isolation of the cavitated section from the water conducting system (Holbrook and Zwieniecki 1999). Cavitation removal was shown in garpevine (*Vitis vinifera*, Zufferey et al. 2011) and visualization of the refilling mechanism confirmed the segregation hypothesis and showed water influx from surrounding living cells (Brodersen et al. 2011). The refilling process is triggered by the osmotic properties of sucrose in walls of embolized vessels (Secchi and Zwieniecki 2011). An alternative mechanism was described in the desert woody shrub *Sinarundinaria nitida*, where embolism repair occurs at night while stomata are open and transpiring, without the need to isolate the cavitated section (Schenk and Espino 2011). A third mechanism was proposed for Bamboo (*Sinarundinaria nitida*), where nocturnal root pressure was sufficient to recover embolism in the leaves (Yang et al. 2012).

The ability of trees to function normally with cavitation and recover from it suggested a certain degree of immunity (Cochard 2006, Klein et al. 2011, Klein et al. 2012). This immunity also means that (1) leaf transpiration (T) and xylem sap flow (SF) must be partially temporally decoupled; and (2) once xylem conductivity is impaired, T must rely on water storage (S). A T-SF decoupling was discussed (Cruiziat et al. 2002) but not frequently tested, presumably due to the differentiation between gas (T) and liquid (SF) phase measurement techniques. Two exceptions are Zweifel et al. (2001) and Fisher et al. (2007), who showed time lags between T and SF of 0.5-3 hr. Comparing SF rates at the bottom and high crown of large tropical trees, Meinzer et al. (2003) found up to 2 hr. decoupling. The role of tree water storage was shown in many studies (Zweifel et al. 2001, Meinzer et al. 2003, McLaughlin et al. 2003, Fisher et al. 2007, Meinzer et al. 2009), some showing major contribution, where S accounts for 10-75% of daily T in potted, young Norway spruce (*Picea abies*, Zweifel et al. 2001), or a more minor contribution of 2-10% in adult yellow poplar (*Lirodendron tulipifera*, McLaughlin et al. 2003) and down to zero stem storage in the woody monocot Bamboo suffering from cavitation (Yang 2012).

3.4. Forests and the hydrological cycle

In an ecological context, resolving the relationships between soil water dynamics and tree water use requires several considerations. Firstly, soil water retention properties usually vary with depth (Breda et al. 1995, Oren et al. 1998, Granier et al. 1999, Warren et al. 2005, Domec et al. 2010), so that amounts of transpirable water are not necessarily homogeneously distributed. Secondly, the point of stomatal closure is species-specific (Tardieu and Simonneau 1998, Bond and Kavanagh 1999, Klein et al. 2011) and depends on leaf water potential rather than bulk soil water content. This leads to species-specific differences in the ability to sustain transpiration under soil hydraulic limitations (Sperry et al. 1998, Heiskanen and Makitalo 2002). Finally, in order to quantify the amounts of transpirable water, one must account for the relevant soil profile, as well as the complete ecosystem water balance (Williams et al. 1996, Oren et al. 1998, Siqueira et al. 2008, Schwarzel et al. 2009).

Forests are not only influenced by soil water availability, but also bear large impact on the regional water balance. The critical role that forests play in the hydrological cycle has raised some concerns about their negative impact on water

yield (WY), with evidence that afforestation reduced downstream water availability (Farely et al. 2005, Jackson et al. 2005).

3.5. Aleppo pine as a model forest tree

Aleppo pine (*Pinus halepensis* Miller) is an important forest tree in the Mediterranean region, and the only pine species native to Israel (Quezel 2000). Temperature and precipitation requirements generally confine its distribution to sub-humid areas of the Mediterranean. In light of predictions of global drying and warming for this region, there is some concern about the physiological ability of *P. halepensis* to persevere in large afforestations in the future (Oliveras et al. 2003, Maestre et al. 2004). This ability mainly depends on the hydraulic properties of *P. halepensis*, which have already attracted the attention of several research programs in Mediterranean countries. Under induced drought, seedlings of Italian *P. halepensis* ecotypes from more xeric habitats had greater g_s and Transpiration (T) rates than ecotypes from more mesic habitats (Tognetti et al. 1997). A subsequent trial (Calamassi et al. 2001) on younger seedlings of European ecotypes confirmed this observation, and added that the 'xeric' ecotypes displayed strategies typical of drought-tolerant species. Associations between the hydraulic characteristics and tree function were the focus of another study (Royo et al. 2001), that showed that growth parameters (e.g. height, diameter) of young seedlings in the greenhouse were very sensitive to the irrigation regime. Yet after planting in the field under natural conditions differences diminished and became insignificant, suggesting that the hydraulic systems of *P. halepensis* are highly plastic. Assessments of vulnerability to xylem embolism, together with field measurements of leaf water potential, lead to predictions of high values (>75%) of xylem embolism under drought (Oliveras et al. 2003). However, the authors concluded, also in contrast to earlier studies (Calamassi et al. 2001, Atzmon et al. 2004), that *P. halepensis* is a drought-avoiding species. A parallel comparative study confirmed this conclusion by analysis of carbon isotope discrimination in tree rings (Ferrio et al. 2003). While these works provided ample information, results and interpretations regarding the hydraulic regulation in *P. halepensis* varied. Perhaps one of the reasons for this is the lack of a mechanistic description of hydraulic regulation in *P. halepensis*.

3.6. A forest in the dry timberline

Forest function under drought has been studied intensively in semi-arid pine afforestation in Southern Israel for the past decade indicating relatively high forest productivity (Gruenzweig et al. 2007). This was associated with adjustments to the dry conditions, such as a shift in maximum assimilation rates to early spring, (Maseyk et al. 2008, Rotenberg and Yakir 2010). It was also shown that low rates of water loss were associated with increasing sensitivity of stomatal conductance (g_s) to soil moisture below a relative extractable water (REW) value of 0.4, and decreased g_s sensitivity to vapor pressure deficit (VPD) below REW of 0.2. These eco-physiological responses raise questions concerning the underlying hydraulic mechanisms allowing the trees to withstand regular long and intense drought periods.

3.7. Research Objectives

The objective of this study was to identify the complex interactions between the hydraulic properties of a major forest tree species in the Mediterranean (*Pinus halepensis*), its physiology, and the forest ecosystem water availability. These interactions potentially create a feedback cycle, in which both tree physiology and the ecosystem water availability affect the hydraulic properties of the trees, which in turn feedback on the tree physiological response and ultimately on water availability. During the course of the study the original objectives were partly modified to reflect preliminary results. Within this framework, the specific goals were to:

1. Identify and quantify the mechanisms of hydraulic adjustments involved in the drought resistance of *Pinus halepensis*
2. Test the hypothesis that plasticity in physiological and hydraulic traits will help sustaining growth and survival of *P. halepensis* and its provenances under climate change in the Mediterranean.
3. Identify and quantify the factors influencing soil water availability to tree water use and its dynamics in a water-limited pine forest.
4. Quantify the impact of *P. halepensis* on the forest water balance, specifically in relation to stomatal regulation and stand density.

4. Materials and Methods

In this study we combined several scientific approaches at four different scales (leaf → tree → plot → forest), to study the multiple aspects of tree water use. First, the responses of young trees to induced soil drought were tested in a greenhouse experiment. Second, hydraulic adjustments (identified in the greenhouse and in the field) were quantified in the field. Third, we measured the contribution of hydraulic and physiological adjustments to tree survival and growth under a climatic gradient. For this we used similar genotypes growing in three forest sites in Israel and Italy. Forth, soil water availability for tree transpiration in a semi-arid forest was quantified and its relations to tree water use dynamics were studied. Fifth, we quantified the impact of *P. halepensis* on the forest water balance, specifically in relation to stomatal regulation (inter-species comparison) and stand density (thinning experiment).

4.1. Forest sites and plant material

The majority of the study was conducted in Yatir forest, a 40-year-old Aleppo pine (*Pinus halepensis* Miller) plantation located at the northern edge of the Negev desert, Israel (31°20'N, 35°20'E). The forest covers an area of 2,800 ha and lies on a predominantly light brown Rendzina soil (79 ± 45.7 cm deep), overlying a chalk and limestone bedrock. The climate is hot (40-year average mean annual temperature is 28°C) and dry (40-year average mean annual precipitation is 285 ± 88 mm). Stand density is ca. 300 trees ha^{-1}, mean tree height is 10.2 ± 2.49 m and mean diameter at breast height is 19.8 ± 5.61 cm, leading to an average leaf area index of about 1.50 (Sprintsin et al. 2011). Surface runoff (R) and deep drainage (D) are negligible (Shachnovich et al. 2008, Raz-Yaseef et al. 2010b) and the water table is below 300 m, eliminating the possibility of groundwater recharge (S) or other sources than precipitation (P) for evapotranspiration (ET). The long-term hydrological balance between the ecosystem water components ($P = R + S + ET + D$) can therefore be simplified in Yatir to $P \approx ET$. In 2000, an instrumented flux tower was erected in the geographic center of the forest, allowing continuous measurements of both P and ET (Rotenberg and Yakir 2010).

The climatic gradient study included five provenances of *P. halepensis* grown from seeds collected from mature trees in natural stands of each provenance and sown in three sites of the UN FAO seed collection provenance program (SCM/CRFM/4 bis project, http://www.fao.org/docrep/006/k1203e/K1203E08.htm; see database in:

http://147.100.66.194/ForSilvaMed). Out of 32 provenances 5 were selected to allow in-depth study while maintaining sufficient representation of the variety of habitats in which *P. halepensis* grows. Seed sources included contrasting sites from different areas around the Mediterranean starting with mean annual precipitation (P) of 830 mm in Otricoli, Italy, to 310 mm in Senalba, Algeria. All five provenances were represented by 10-12 actively growing trees in each of three experimental plots in three different climates: meso-Mediterranean (MM, in Castel Di Guido, Rome), thermo-Mediterranean (TM, in Beit Dagan), and semi-arid (SA, in Yatir), see a summary of climate characteristics for the sites in Table 1. The Castel Di Guido farm is located in the coastal plains15 km west of Rome, Italy, 10 km east of the Tyrrhenian Sea shore, and its soil is mostly clay. The experimental plot was planted in 1975 in a randomized block design, with 9-25 replicates x 6-9 blocks at 3 x 3 m spacing. The Beit Dagan ARO Volcani Center farm is located in the coastal plains, 20 km south-east of Tel-Aviv, Israel, 20 km east of the Mediterranean Sea shore, and its soil is deep sandy to sandy-loam. The 1-ha experimental plot was planted in 1991 with 11 provenances in parallel rows with 12 replicates x 1 block at 2 x 4 m spacing. The Yatir experimental plot was planted in 1989-1990 with 17 provenances in parallel rows with 12 replicates x 4 blocks with 4 x 4 m spacing. Previous reports about performance of *P. halepensis* provenances in Yatir (Atzmon et al. 2004; Schiller and Atzmon 2009) refer to another experimental provenance plot, where micro-climatic conditions are drier than in the plot reported here. All three plots were not thinned, and with the exception of several tree mortalities, plot densities were kept as planted. To account for differences in trees' age among plots, field performance was measured in trees at the same age, but in different years. To avoid edge effects, sampling excluded trees growing in the margins of plots.

The pine-oak water use comparison was performed on trees that were selected in the 1-ha experimental plot (EP) of ARO Volcani Center in Beit Dagan, Israel (31°59'N 34°48'E, elevation 20 m) and in an afforestation plot (AP) at Harel forest, Israel (31°43'N 34°57'E, elevation 320 m). In Beit Dagan, diameter at breast height (DBH) of *P. halepensis* trees ranged between 13.7 cm and 19.9 cm; diameter of the main coppice at 0.5 m (DMC) of *Quercus calliprinos* trees was 11.5-18.5 cm. The Harel forest plot is located on a hilltop 4 km south-west of Beit Shemesh, and its soil is shallow light rendzina overlying white chalk and flint bed. Mean annual temperature and precipitation are 20°C and 490 mm respectively. Selected trees are

young (10-15 years) second generation trees which grew naturally from seeds of the first generation of trees which were planted in the 1930's. DBH of *P. halepensis* trees was 8.7-20.7 cm; DMC of *Q. calliprinos* trees was 6.4-9.6 cm. In both plots no irrigation was provided and water supply was permitted by precipitation alone.

For the greenhouse experiment, *P. halepensis* trees were grown from seed (source: Mount Carmel, Israel) in 4 cm diameter cylinders in Styrofoam blocks at KKL-JNF Eshtaol nursery. In February 2009 one hundred 16-months saplings with a height to meristem of 44.6 ±4.2 cm and root collar diameter of 3 ±0.4 mm were taken from one block. In April 2009 trees were transplanted into 5L pots at the Weizmann Institute of Science greenhouse facility in Rehovot. Young trees were kept under optimal growth conditions (ambient light, 24ºC, RH = 70%, ultra-optimal irrigation) for a 3-week acclimation period.

4.2. Experimental set-up and design of the greenhouse experiment

The experiment was on 100 actively growing 18-months trees in 5L pots. Trees were divided into 10 irrigation treatments as shown in Table 1, 10 trees per treatment. A three weeks pilot trial characterized the tree water requirement under greenhouse conditions to be 350 ml wk^{-1} per pot. This was used as the standard 100% irrigation amount (A_0) given once a week to trees in the control group. The water portion given in a treatment (A_i) was 75, 50, or 25% of that, creating four discrete levels of drought intensity. Treatments differed also in the duration of their drought cycle, which was 7, 14, or 21 days. This means that while control trees had three irrigation events in 21 days (D_0), the number of irrigation events given in a treatment (D_i) was 3, 1.5, or 1 in 21 days. Treatments are indicated by their index number (T1 to T9) and their respective irrigation regime (x:y, where x is amount, in % of control, and y is time between irrigations, in weeks). Trees were grown together in one greenhouse over a 30 week period. Other environmental factors (air temperature (T), relative humidity (RH), vapor pressure deficit, photosynthetically active radiation) were maintained at reasonable conditions for young tree growth. Average T was 22°C ±6.5°C and average RH was 71% ±15

4.3. Experimental design of the thinning experiment

During December 2009 twenty forest plots (70x70m) were thinned to three stand density levels: 100, 200, and 300 trees ha^{-1} plus unthinned control. Among these plots,

four neighboring plots, sharing a NE aspect, were selected for seasonal gas exchange measurements. In each plot, five trees were selected according to the following criteria: 1. 19<DBH<25 cm; 2. 10<Height<14 m (one exception); 3. Healthy phenotype; 4. Leaves accessible for measurement. In each tree, W and E facing needle cohorts were marked for repeated measurement. Leaf-scale conditions (photosynthetic active radiation, PAR, and vapor pressure deficit, VPD) and gas exchange rates (Net photosynthesis, A, and transpiration, T) were measured before (10:30-11:30) and after (13:30-14:30) noontime in three trees at each plot during five field days along the year.

4.4. Tree water use

Between September 2009 and March 2010 sap flow sensors were installed on sixteen trees in Yatir forest, 70 m from the flux tower. Lab-manufactured thermal dissipation sensors (Granier and Loustau 1994) were applied to all trees, and commercial heat balance sensors (EMS, Brno, Czech Republic; Cermak et al. 2004) were also used on six of these trees (pioneering application in a semi-arid forest). Measurements were taken every 30 s and the 30 min average was saved on a local CR1000 data-logger (Campbell Scientific Inc., Utah, USA) and transmitted via internet to the lab at the Weizmann Institute of Science. Sap flow rates (kg hr^{-1}) were calculated in relation to the minimum sap flux during the day, as shown in the empirical equation of Granier and Loustau (1994), modified by Kaneti (2010):

(4) $$SF = LCF \times CF \times 0.04284 \times [(\Delta T_{max} - \Delta T_r)/ \Delta T_r]^{1.231}$$

where SF is the half hourly sap flow rate; LCF is the length compensation factor due to the inability of the 2 cm probes to capture the entire active sapwood depth, but rather 65% of it (for *P. halepensis* in Yatir; Cohen et al. 2008) and calculated specifically for individual trees; CF is a calibration factor of 2.5 (Steppe et al. 2010; Kaneti, 2010); ΔT_r is the average half hourly temperature difference between heated and non-heated probes, and ΔT_{max} the maximum temperature difference measured during the day (assumed to be at a negligible sap flow rate, below sensor sensitivity threshold). The calibrated SF values correlated well with SF measurements using the heat balance method (r^2=0.90). The radial gradient of sap velocity in these trees was quantified in an earlier study (Cohen et al. 2008), indicating a quasi-linear decrease from maximum sap velocity at 5 mm below the cambium down to zero at 40 mm.

Diurnal totals were further calculated and transformed into sap flux densities, according to:

(5) $SFD = \Sigma^{d}(SF)*1{,}000 / A_{sw}$

where SFD is the diurnal sap flux density ($cm^3\ d^{-1}\ cm^{-2}$) and A_{sw} is the sapwood area of each individual tree. Tree transpiration (T_t, mm d^{-1}) was calculated as the mean sap flux density of all trees multiplied by stand density (300 trees ha^{-1}) and the mean sapwood area of 216 cm^2. T_t was identified as one of four components of total evapotranspiration:

(6) $ET = T_t + T_u + I + E_s$

where T_t is tree transpiration; T_u is transpiration from understory vegetation (usually confined to the rainy season); I is evaporation of water intercepted by plant foliage; and E_s, evaporation from soil.

4.5. Xylem hydraulic conductivity and cavitation

Hydraulic conductivity was measured in five to nine trees per treatment, under low pressure (0.02 MPa) before and after perfusing the xylem tissue at a high pressure of 0.5 MPa. In order to eliminate variations at the time of sampling due to the treatment-specific irrigation program, trees were watered 24 hr prior to measurement. We can assume that any reversible reductions in conductance were not measured and the measurement captured the mid-term steady-state developmental responses (and not short-term embolism). A 30 cm stem section was cut from the base of the stem and resin secretion from the cuts was eliminated by placing both ends (5 cm from cut tips) in a water bath at 95°C for 10 min. (adapted from Waring and Silvester 1994). Next, stem sections were submerged in distilled water for 10 min. The root collar end of each stem was then fitted with a rubber gasket, while still submerged, to a latex pipe fed by 10 mM KCl solution in double distilled water reservoir. A hydrostatic pressure of 0.02 MPa was applied by placing the reservoir exactly 2 m above the stem section. For two hours, water dripping from the distal end of the stem section was collected and weighed every 20 min. The water flow rate (kg s^{-1}) was divided by the pressure gradient (0.02 MPa) along the 30 cm stem length to provide the hydraulic conductivity K_h (kg m $MPa^{-1}\ s^{-1}$), as described by Tyree and Alexander (1993). K_h was further divided by the xylem cross-sectional area to provide the specific hydraulic conductivity K_s (kg $m^{-1}\ MPa^{-1}\ s^{-1}$). Stem sections (1-4 per treatment) were then fitted with a high pressure valve to a pressure-resistant pipe fed by 10 mM KCl solution

reservoir placed inside a Scholander pressure chamber. Pressurizing the solution through the segment at 0.5 MPa for 5 min. followed by a second measurement of K_s determined the maximum specific conductivity, $K_{s\ max}$. Measurements of K_s and $K_{s\ max}$ were further used to identify loss of conductivity which can be attributed to xylem cavitation according to equation (7), (Tognetti et al. 1997):

(7) $PLC = 100 * (K_{s\ max} - K_s) / K_{s\ max}$

where PLC is the percent loss of conductivity (%) due to cavitation. Branches were sampled every 1-2 hours during three field days between Jan and Jun 2011

4.6. Leaf gas exchange and water potential

Leaf stomatal conductance (g_s, in mol H_2O m^{-2} s^{-1}), net carbon assimilation (A, in µmol CO_2 m^{-2} s^{-1}) and transpiration (T, in mmol H_2O m^{-2} s^{-1}), were measured on pre-marked needle cohorts. Three to four cycles of measurements were made from 8:30 to 14:00 using a LI-6400 Photosynthesis System (Licor Inc., Lincoln, NE, USA), also simultaneously measuring air temperature, photosynthetically active radiation (PAR, in µmol m^{-2} s^{-1}) and vapor pressure deficit (VPD, in kPa). These measurements were used in the calculation of water use efficiency (WUE, in mmol CO_2 mol^{-1} H_2O) according to:

(8) $WUE = A / T$

And intrinsic water use efficiency (WUE_i, in µmol CO_2 mol^{-1} H_2O) according to:

(9) $WUE_i = A / g_s$

Gas exchange measurements were accompanied by measurements of leaf water potential (Ψ_l) using the pressure chamber technique (Scholander et al. 1965, Holbrook et al. 1995). Small (5-7 cm long) shoots were cut from the same trees used for the gas exchange measurements and put in pressure chamber (Model 600; PMS instrument Co., Albany, OR, USA) fed by nitrogen gas cylinder and equipped with a lamp-carrying magnifying glass. Gas pressure within the chamber was gradually increased (~1 MPa min^{-1}) until water emerged from the protruding twig surface, and the pressure value was recorded as leaf water potential (Ψ_l).

4.7. Field Performance and growth phenology

Periodic measurements of tree height and diameter at breast height (DBH, 1.3 m) were performed every 1-3 years from the time of planting on 10 trees of each provenance and site. Height was measured using a PM-5 clinometer (Suunto, Sylvan

Lake, MI, USA) and DBH was estimated from tree circumference. Since planting density differed among sites, individual measurements of DBH were normalized by the standard stand density of 1,343 trees ha^{-1} (3 x 3 m spacing). Dendrometers were prepared using stem circumference increment tape (EMS, Brno, Czech Republic) fitted with custom-made 50 mm steel tension coil springs (Hakfitz, Ramat Gan, Israel). During December 2008 dendrometers were installed on five trees of each provenance growing in Beit Dagan and Yatir. Trunk circumference increment was measured once in two weeks using a digital caliper (indication error 0.03 mm; Fuji, Japan). Observed growth rate in mm $month^{-1}$ was calculated from consecutive measurements divided by the time in between individual measurements. In order to estimate trunk growth-season length (GSL), increments in circumference were expressed as percent of the total annual increment for each individual tree, and GSL was defined as the time (in days) between 2 periods where increment was ≥ 5% of the total annual increment.

4.8. Tree- ring $\delta^{13}C$

Tree cores were sampled between December 2008 and December 2009 using a 200 mm increment borer (core diameter 5.15 mm) equipped with starter (Haglof, Sweden). From each tree, two trunk cores were collected, at breast height at 0° (N) and 180° (S). The sampling design was 3 sites x 5 provenances x 8-10 trees x 2 sides = 270. Tree-rings of the growth years 1997-2000 were identified, cut into 7-12 equal intra-annual sub-sections and their $\delta^{13}C$ values analyzed as described in Klein et al. (2005). To minimize analysis time and resources, isotopic analysis was performed on whole wood samples rather than cellulose, which is generally coherent (McCarroll and Loader 2004 and references therein). The $\delta^{13}C$ results were used to calculate the tree discrimination against ^{13}C (Δ) expressed in delta notation as parts per thousand (‰) deviations from the international carbon isotope standard (Coplen 1994):

(10) $\Delta = (\delta^{13}C_a - \delta^{13}C_t) / (1 + \delta^{13}C_t)$

where $\delta^{13}C = (\delta^{13}C/\delta^{12}C)_{sample} / (\delta^{13}C/\delta^{12}C)_{reference} - 1$ and the reference is PDB carbonate, and subscripts a and t stand for atmospheric air and the tree-ring material, respectively. *Pinus halepensis* is a drought avoiding species and therefore deposition of carbon into tree-rings is typically restricted to Oct-May (Klein et al. 2005). This means that the annual $\delta^{13}C$ maxima occurred in Mar-May, when soil and atmospheric humidity were declining while still permitting leaf gas exchange. From intra-annual

sub-sections, annual maxima Δ values of trees from each provenance and climate were further used in the derivation of the tree's intrinsic water use efficiency (WUE_i) using the following equation (adapted from Farquhar et al. 1982; Seibt et al. 2008):

(11) $WUE_i = C_a / r \{[b - \Delta - f(\Gamma^* / C_a)] / [b - a + (b - a_m) * (g_s / g_i\, r)]\}$

where C_a is the atmospheric CO_2 concentration in ppm (an annual global average; Robertson et al. 2001); r is the ratio of the diffusivities of CO_2 and water in air (1.6); a, a_m, b and f are the leaf-level discriminations against ^{13}C in the diffusion through the stomata (4.4‰), during dissolution and liquid phase diffusion (1.8‰), during biochemical CO_2 fixation (29‰), and in photo-respiratory CO_2 release (8‰), respectively; Γ* is the temperature-dependent CO_2 compensation point of *ca.* 30-45 ppm (Maseyk et al. 2008); g_s / g_i is the ratio between stomatal and internal conductances to CO_2 respectively (0.5, according to Maseyk et al. 2011).

4.9. Leaf chlorophyll concentration

During May 2009 and April 2010 healthy 1 year old needles were collected in 3 replications from 3 trees per provenance in Yatir and Beit Dagan. Needles (50 mg leaf tissue per sample) were cut into 5 mm segments and immersed in 1 ml 80% aqueous acetone solution together with 2 bearing balls (diameter = 3 mm). Leaf specimens were ground using a ball mill (Retsch, Hann, Germany) at a frequency of 25 s^{-1} until full extraction was achieved (~5 min.), followed by centrifugation at 14,000 rpm for 10 min. The supernatant of each specimen was transferred into a micro-well in a 96 well plate, where its absorbance was measured at 663.6 and 646.6 nm using a tunable micro-plate reader (Molecular Devices, Sunnyvale, CA, USA). Concentrations of chlorophylls *a* and *b* were determined following subtraction of the absorbance of a blank sample (containing solution but not leaf sample) according to Porra et al. (1989). Results were expressed on a dry weight (DW) basis following the drying of remaining needles in the sample at 60°C for 48 hr.

4.10. Soil mechanical arrangement and water retention

In June 2009, six uninterrupted soil samples were taken from the flux tower plot in Yatir using 53-mm rings (Eijkelkamp, Giesbeek, Netherlands). Mechanical arrangement of the soil and particle size distribution were analyzed according to the equivalent diameter scale used by the International Soil Science Society (Marshall 1947). The analysis was done by the density method with variable depth, based on

Stock's law (Bouyoucos 1962). Approx. 40 g oven-dried soil samples were weighted and mixed with 100 ml dispersing solution of 2.5% $Na_4P_2O_7*10H_2O$ (Merck chemicals, Darmstadt, Germany) and 100 ml distilled water, as described by Klute (1986). After 10 minutes, the suspension was transferred into a 1L measuring tube and the remaining volume was filled with distilled water. S uspensions were left overnight to reach equilibrium temperature. Then, preliminary readings of temperature and density were taken in order to determine time intervals for further density measurements, using a hydrometer on well mixed soil suspensions. Particle size distribution was determined for four depths: 0-10, 10-20, 20-40, and 40-60 cm, denoted as layer *i* to *iv* respectively.

The mechanical arrangement analysis at each depth allowed computation of discrete approximated water retention curves, describing the relationship between the soil water capillary head (Ψ) and the respective water content ($\theta_{(\Psi)}$), as described by Gupta and Larson (1979). The approximation was done by the RETC software package (http://epa.gov/ada/csmos/models/retc.html) using the van Genuchten - Mualem model (van Genuchten et al. 1991):

$$\theta(\psi) = \theta r + \frac{\theta s - \theta r}{\left[1 + \alpha |\psi|^n\right]^m} \quad (12)$$

where θr and θs are the residual and saturation water content respectively, and α, n and m are the soil parameters (m = 1-1/n, n>1). The robustness and accuracy of this pedo-transfer function and specifically the RETC software has been demonstrated at various soil types in numerous studies (e.g. Yates et al. 1992, Woesten et al. 1995, Ritter et al. 2004, Matula and Spongrova 2007).

4.11. Root depth distribution

During a forest-scale soil survey in September 2011, twenty two trenches, 1-1.8 m deep and 5-7 m long, were dug in Yatir forest. In each trench three vertical profiles were chosen, 0.1-1 m from tree trunk bases. Root diameter was measured using a digital caliper (indication error 0.03 mm; Fuji, Japan) for all roots larger than 0.5 mm diameter and captured within a 20cm x 20cm frame that was placed onto the trench's wall in 5-9 consecutive soil depths. Root density (roots m^{-2}) was then calculated for five different root diameter classes. Soil depth and stone fraction were also measured and recorded.

4.12. Simulation of soil water content dynamics

Soil water content was simulated using the multilayer, multi-leaf process-based biosphere-atmosphere gas exchange model MuSICA (Ogée et al. 2003). The model is well suited for studies on conifer trees because it explicitly accounts for needle clumping of various needle cohorts, and the version 2.0.x used in this study has been upgraded compared to the versions 1.x.x used in previous publications (e.g. Ogée et al. 2003, Ogée et al. 2009). Most MuSICA parameters were taken from published measurements of soil physical parameters (profiles of soil porosity, soil matric potential and Ks at saturation), hydraulic parameters and rooting profiles.

4.13. Upscaling from leaf- to forest stand-scale transpiration

Measurements of leaf transpiration (T) were used for the estimation of diurnal tree-scale transpiration amounts for each species and field day, according to:

(13) $T_d = T_m \times LA \times t_T \times LC \times 0.0648/1{,}000$

where T_d is the diurnal transpiration (mm tree^{-1} d^{-1}), T_m is the average transpiration rate of 3-4 measurements in the morning and afternoon (mmol H_2O m^{-2} s^{-1}), LA is the mean total leaf area of a mature, 15-cm DBH/DMC tree (40.0 and 37.7 m^2 for *Q. calliprinos* and *P. halepensis*, respectively) calculated with allometric equations (Schiller et al. 2003 for *Q.* calliprinos; Grunzweig et al. 2007 for *P. halepensis*), t_T is the diurnal fraction of time allocated for transpiration (8-11 hours per 24 hours, depending on the season), and LC is the time-averaged portion of leaf cover (100% for *P. halepensis*, 87.5% for *Q. calliprinos*, due to ~50% defoliation 3 months a year). An annual total tree-scale water use amount, T_t (mm tree^{-1} year^{-1}), was calculated for each species by integration of the T_d values of the seven field days across an entire year.

T_t was identified as one of four components of stand-scale evapotranspiration (ET):

(14) $ET = T_t \times sd + T_u + I + E_s$

where sd is stand density (trees ha^{-1}); T_u is transpiration from understory vegetation; I is evaporation of water intercepted by plant foliage; and E_s, evaporation from soil. The magnitude of the three non-tree fluxes (T_u, I, and E_s) largely depends on the local annual precipitation (P) at each forest site. Therefore, for a preliminary assessment of the stand-scale ET flux, we estimated T_u, I, and E_s at 0.13, 0.11, and 0.30 of P,

respectively (Raz-Yaseef et al. 2010, Raz-Yaseef et al. 2011, Klein et al. 2012b). The difference between P and ET for a particular area is defined as water yield (WY), which, using Eq. (14) is described as:

(15) $WY = P - (T_t \times sd + T_u + I + E_s)$

Eq. (15) defines a framework in which the interdependence between mean annual precipitation (P), stand density (sd) and water yield (WY) can be assessed.

4.14. Statistical analysis

Data were analyzed by analysis of variance (ANOVA) using JMP software (Cary, NC, USA). Measurements of individual trees were used as observations, where climate type (3 levels, nominal variable), provenance (5 levels, nominal variable) and their interaction were defined as factors. Differences between responses were considered significant when type 3 sum of squares met the F-test criterion at probability <0.05. The effect of climate in individual provenances and the effect of provenance in the three climate types were also analyzed. Means were compared using the Tukey HSD test, reported as letters indicating significant differences. To test the relationship between variance in field performance (increment growth) and variance in physiological traits, data were analyzed by partial least square regression (PLS) and the relative percent of variation in performance explained by each of six parameters is reported.

5. Results

The results below are divided into four chapters, according to the four research objectives above:

1. Hydraulic adjustments underlying drought resistance of *Pinus halepensis*.
2. The role of trait plasticity in sustaining growth and survival of *P. halepensis* under climate change in the Mediterranean.
3. The role of soil and tree hydraulics in the success of a water-limited pine forest.
4. From leaf to forest scale: water use of *P. halepensis* and the coexisting, anisohydric *Quercus calliprinos* and the impact of a semi-arid pine forest on local water yield.

5.1. Hydraulic adjustments underlying drought resistance of *Pinus halepensis*.

In order to identify the mechanisms and quantify the hydraulic adjustments involved in drought resistance of *Pinus halepensis*, two scientific approaches were applied:

(i) Testing the responses of 2-year trees to induced soil drought, in a greenhouse experiment.

(ii) Measuring tree hydraulics of 40-year trees in the field, in the semi-arid forest at Yatir, Israel.

The results of the greenhouse experiment are described in Klein et al. (2011, see below), followed by description of the results of the field observations.

Tree Physiology 31, 637–648
doi:10.1093/treephys/tpr047

Research paper

Hydraulic adjustments underlying drought resistance of *Pinus halepensis*

Tamir Klein[1,3], Shabtai Cohen[2] and Dan Yakir[1]

[1]Department of Environmental Sciences and Energy Research, Weizmann Institute of Science, Rehovot 76100, Israel; [2]Institute of Soil, Water and Environmental Sciences, Volcani Center ARO, Beit Dagan 50250, Israel; [3]Corresponding author (tamir.klein@weizmann.ac.il)

Received January 5, 2011; accepted April 26, 2011; published online June 27, 2011; handling Editor Roberto Tognetti

Drought-induced tree mortality has increased over the last decades in forests around the globe. Our objective was to investigate under controlled conditions the hydraulic adjustments underlying the observed ability of *Pinus halepensis* to survive seasonal drought under semi-arid conditions. One hundred 18-month saplings were exposed in the greenhouse to 10 different drought treatments, simulating combinations of intensities (fraction of water supply relative to control) and durations (period with no water supply) for 30 weeks. Stomata closed at a leaf water potential (Ψ_l) of –2.8 MPa, suggesting isohydric stomatal regulation. In trees under extreme drought treatments, stomatal closure reduced CO_2 uptake to –1 μmol m^{-2} s^{-1}, indicating the development of carbon starvation. A narrow hydraulic safety margin of 0.3 MPa (from stomatal closure to 50% loss of hydraulic conductivity) was observed, indicating a strategy of maximization of CO_2 uptake in trees otherwise adapted to water stress. A differential effect of drought intensity and duration was observed, and was explained by a strong dependence of the water stress effect on the ratio of transpiration to evapotranspiration T/ET and the larger partitioning to transpiration associated with larger irrigation doses. Under intense or prolonged drought, the root system became the main target for biomass accumulation, taking up to 100% of the added biomass, while the stem tissue biomass decreased, associated with up to 60% reduction in xylem volume.

Keywords: carbon reallocation, drought tolerance, embolism, transpiration ratio, tree mortality.

Introduction

Water deficiency is the main factor limiting plant production worldwide (Boyer 1982, Flexas et al. 2004) and drought is an important driver of eco-physiological adaptations in plants. Future climate warming is expected to elevate atmospheric water demand; however, changes will not be restricted to increases in mean temperature, but will also include increases in the frequency and intensity of droughts (Christensen et al. 2007, Seager et al. 2007, Sterl et al. 2008). The fate of many forest ecosystems will depend on the ratio of the rate of the climate changes to the rate of adaptation to such changes. A ratio larger than one means that the rate of climate change exceeds the rate of plant adaptation. Accumulating evidence of drought-induced tree mortality in recent years (Allen et al. 2009 and references therein) might be the result of this scenario.

Forest function under drought has been studied intensively in semi-arid pine afforestation in Southern Israel for the past decade, indicating relatively high forest productivity (Grunzweig et al. 2007). This was associated with adjustments to the dry conditions, such as a shift in maximum assimilation rates to early spring (Maseyk et al. 2008, Rotenberg and Yakir 2010). It was also shown that low rates of water loss were associated with increasing sensitivity of stomatal conductance (g_s) to soil moisture below a relative extractable water (REW) value of 0.4, and decreased g_s sensitivity to vapor pressure deficit (VPD) below a REW of 0.2. These eco-physiological responses raise questions concerning the underlying hydraulic mechanisms

allowing the trees to withstand regular long and intense drought periods.

In natural ecosystems, drought is typically driven by restriction in either the amount or the frequency of precipitation. This entails a dual parameterization of drought. While the reduction in precipitation amount below a certain threshold (e.g., the negative deviation from a multi-annual average) defines drought intensity, the reduction in precipitation frequency defines drought interval (IPCC 2001). Together, these two parameters determine the drought impact on the ecosystem and agricultural productivity of the affected region. High-intensity drought episodes, consequently bearing a profound impact on forest and plant function, have been studied extensively (Breshears et al. 2005, Ciais et al. 2005). Yet the distinction of drought interval as an equally important drought parameter has been described only in a few studies (e.g., Mueller et al. 2005), in spite of the fact that it plays a major role in determining responses in semi-arid ecosystems, where precipitation often arrives in sporadic events, which can be described as pulses.

Plant resistance to drought relies on two hypothetical contrasting physiological approaches: drought avoidance and drought tolerance. The underlying mechanism of either approach involves stomatal response and regulation of water status, named isohydric or anisohydric, respectively (Tardieu and Simonneau 1998, McDowell et al. 2008). Isohydric plants reduce g_s as soil and atmospheric conditions dry, maintaining relatively constant leaf water potential regardless of drought intensity. Anisohydric species, in contrast, allow leaf water potential to decline as soil water potential declines with drought (West et al. 2008). The soil–tree–atmosphere continuum also includes the tree hydraulic system, from the water uptake sites at the root hairs, up the xylem conduits in the stem and on to the transpiration sites in the leaf stomata. Water is transported through this system following a water potential (Ψ) gradient which considerably increases with drought. Both approaches enable plant survival under harsh drought conditions; however, each has an inherent pitfall that can lead to failure in certain conditions. Prolonged reductions of g_s expose isohydric species to carbon starvation, while very negative leaf water potentials in anisohydric species result in xylem cavitation and embolism and subsequent hydraulic failure (McDowell et al. 2008). A basic risk assessment of these mechanisms reveals that not only drought intensity but also the duration of drought plays a key role in determining the fate of the plant.

Aleppo pine (*Pinus halepensis* Miller) is an important forest tree in the Mediterranean region, and the only pine species native to Israel (Quezel 2000). Temperature and precipitation requirements generally confine its distribution to sub-humid areas of the Mediterranean. In light of predictions of global drying and warming for this region, there is some concern about the physiological ability of *P. halepensis* to persevere in large afforestations in the future (Oliveras et al. 2003, Maestre and Cortina 2004). This ability mainly depends on the hydraulic properties of *P. halepensis*, which have already attracted the attention of several research programs in Mediterranean countries. Under induced drought, seedlings of Italian *P. halepensis* ecotypes from more xeric habitats had greater g_s and transpiration (T) rates than ecotypes from more mesic habitats (Tognetti et al. 1997). A subsequent trial (Calamassi et al. 2001) on younger seedlings of European ecotypes confirmed this observation, and added that the 'xeric' ecotypes displayed strategies typical of drought-tolerant species. Associations between the hydraulic characteristics and tree function were the focus of another study (Royo et al. 2001), which showed that growth parameters (e.g., height, diameter) of young seedlings in the greenhouse were very sensitive to the irrigation regime. Yet after planting in the field under natural conditions, differences diminished and became insignificant, suggesting that the hydraulic systems of *P. halepensis* are highly plastic. Assessments of vulnerability to xylem embolism, together with field measurements of leaf water potential, led to predictions of high values (>75%) of xylem embolism under drought (Oliveras et al. 2003). However, the authors concluded, also in contrast to earlier studies (Calamassi et al. 2001, Atzmon et al. 2004), that *P. halepensis* is a drought-avoiding species. A parallel comparative study confirmed this conclusion by analysis of carbon isotope discrimination in tree rings (Ferrio et al. 2003). While these works provided ample information, results and interpretations regarding the hydraulic regulation in *P. halepensis* varied. Perhaps one of the reasons for this is the lack of a mechanistic description of hydraulic regulation in *P. halepensis*. Such a description will have to include the underlying mechanism, i.e., the type of stomatal regulation of water status, and tie it to the relevant physiological processes. To accomplish this goal, more complex drought scenarios must be tested, robust techniques must be used, and the use of very young seedlings should be limited.

Based on field observations, we hypothesize that the mode of stomatal regulation in *P. halepensis* is isohydric. Yet this gives rise to additional questions, e.g., how is carbon uptake sustained under long drought, and how is the tree water supply ensured so as to postpone stomatal closure. By integrating a mechanistic approach, combining high-resolution measurements and using state-of-the-art methodology, we wish to deepen our understanding of water use by forest trees under drought. Ultimately this should facilitate forestry planning in the face of contemporary challenges, i.e., global warming and drying in many regions.

Materials and methods

Plant material

Pinus halepensis trees were grown from seed (source: Mount Carmel, Israel) in 4 cm diameter cylinders in Styrofoam blocks at KKL-JNF Eshtaol nursery. In February 2009 one hundred 16-month saplings with a height to meristem of 44.6 ± 4.2 cm and a root collar diameter of 3 ± 0.4 mm were taken from one block. In April 2009 trees were transplanted into 5 l pots at the Weizmann Institute of Science greenhouse facility in Rehovot. Young trees were kept under optimal growth conditions (ambient light, 24 °C, RH = 70%, ultra-optimal irrigation) for a 3-week acclimation period.

Experimental set-up and design

The experiment was on 100 actively growing 18-month trees in 5 l pots. Trees were divided into 10 irrigation treatments as shown in Table 1, 10 trees per treatment. A 3-week pilot trial characterized the tree water requirement under greenhouse conditions to be 350 ml week^{-1} per pot. This was used as the standard 100% irrigation amount (A_0) given once a week to trees in the control group. The water portion given in a treatment (A_i) was 75, 50 or 25% of that, creating four discrete levels of drought intensity. Treatments differed also in the duration of their drought cycle, which was 7, 14 or 21 days. This means that while control trees had three irrigation events in 21 days (D_0), the number of irrigation events given in a treatment (D_i) was 3, 1.5 or 1 in 21 days (Table 1). Treatments are indicated by their index number (T1–T9) and their respective irrigation regime (*x*:*y*, where *x* is amount, in % of control, and *y* is time between irrigations, in weeks). Trees were grown together in one greenhouse over a 30-week period. Other environmental factors (air temperature (T), relative humidity (RH), photosynthetically active radiation (PAR)) were maintained at reasonable conditions for young tree growth. Average T was 22 ± 6.5 °C and average RH was 71 ± 15%.

Soil and water parameters, including soil salinity

Pots contained 20 cm deep enriched sandy loam on top of a 2 cm gravel infiltration layer. Soil water content (SWC) was determined by the oven-drying method on samples taken three times in the course of the experiment. Every pot was weighed twice a week (morning and evening of the same day) using a Sartorius 3808 MP8 wide-range balance (up to 30 kg with 0.1 g precision; Gottingen, Germany). Calibration of pot mass values with periodic measurements of SWC allowed its determination for every week along the experiment. The long-term hydrological balance of a system can be represented by

$$S = D + R + \mathrm{ET} \quad (1)$$

where S is supply inputs (precipitation and irrigation), D is drainage, R is runoff and ET is evapotranspiration. While Eq. (1) provides the overall hydraulic perspective, in our experiment the relatively small irrigation amounts were found to result in D and R being below detection limits, and at the experimental time-scale measurements of SWC indicated that SWC declined continuously (Figure 1a). Over this time-scale ET > S and ET was therefore quantified from

$$\mathrm{ET}_j = W_{j-1} - W_j + S_j \quad (2)$$

where ET in week j was calculated from the difference in pot weight (W, measured each Thursday at 18:30, prior to irrigation) between week j and the previous week ($j - 1$) plus the irrigation supplied during the past week (Sj). Mean weekly ET, which was calculated for each treatment, was further used in the analysis (Table 1). In order to check whether the drought

Table 1. Summary of treatments and hydrological components of the 30-week experiment. Treatments are indicated by their index number (T1–T9) and their respective irrigation regime (*x*:*y*, where *x* is amount, in % of control, and *y* is time between irrigations, in weeks). *A* indicates amount of irrigation water; *D* indicates number of irrigation events in 3 weeks (control, Ctrl, treatment was irrigated weekly); D_i/D_0 indicates the irrigation frequency of treatment *i* relative to control ($D_0 = 3$); *S* indicates total water supply; T and ET indicate transpiration and evapotranspiration, respectively; PDI indicates plant drought index, as defined in Eq. (4). Note that ETj > *S*j because the initial, standard, pot water content was not included in *S*.

	Ctrl	T1	T2	T3	T4	T5	T6	T7	T8	T9
	1:1	0.75:1	0.75:2	0.75:3	0.5:1	0.5:2	0.5:3	0.25:1	0.25:2	0.25:3
A (g)	350	262.5	262.5	262.5	175	175	175	87.5	87.5	87.5
A_i/A_0	1.00	0.75	0.75	0.75	0.50	0.50	0.50	0.25	0.25	0.25
D	3	3	1.5	1	3	1.5	1	3	1.5	1
D_i/D_0	1.00	1.00	0.50	0.33	1.00	0.50	0.33	1.00	0.50	0.33
Si	1.00	0.75	0.38	0.25	0.50	0.25	0.17	0.25	0.13	0.08
T_i/ET_i	0.18	0.21	0.22	0.24	0.16	0.19	0.22	0.09	0.13	0.15
PDI	0.00	0.14	0.55	0.67	0.54	0.74	0.79	0.88	0.92	0.91
Sj (g week^{-1})	350	263	131	88	175	88	58	88	44	29
ETj (g week^{-1})	366	291	157	93	197	113	72	116	71	56
Tj (g week^{-1})	67	60	34	22	32	21	16	10	9	10

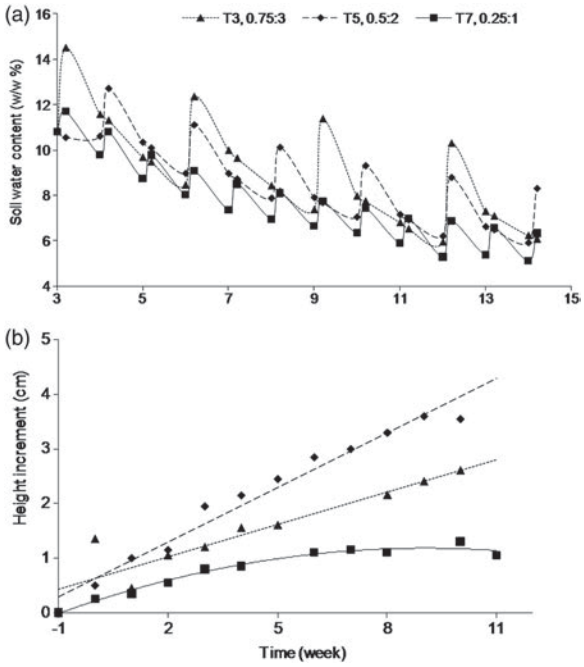

Figure 1. Changes in SWC (a) and tree height (b) with time during the drought experiment, for treatments with identical total irrigation amounts: T3, T5 and T7 ($n = 10$). Height measurements started before the onset of the experiment (last simultaneous irrigation to all treatments). Equations of the regression lines were $y = 0.33x + 0.63$, $R^2 = 0.97$ for T3; $y = 0.20x + 0.62$, $R^2 = 0.86$ for T5; and $y = 0.01x^2 + 0.21x + 0.21$, $R^2 = 0.98$ for T7. Saplings were 1.5 years old.

effect was confounded by a salinity effect, electrical conductivity (EC) of the soil and irrigation water was determined with a YSI 3200 EC meter (Yellow Springs, OH, USA). Average EC of irrigation water (tap water at the Weizmann Institute) was 0.8 dS m^{-1}, indicating a very 'slight salinity problem' according to the Food and Agriculture Organization of the United Nations irrigation guidelines (Ayers and Westcot 1985). At the end of the experiment, 5 g soil samples were taken from pots of control or T9 (0.25:3) trees and thoroughly mixed with 5 g of double-distilled water. Slurries were shaken at 200 rpm for 2 h followed by centrifugation and EC was determined as described above. Average EC values of the slurries ranged from 0.35 dS m^{-1} for soil from control pots to 1.4 dS m^{-1} for soil taken from pots from the lowest irrigation (T9). Since *P. halepensis* is salt tolerant at levels of 6–8 dS m^{-1} (Miyamoto et al. 2004), this indicates that soil salinity was not a major factor affecting plant physiology in this experiment.

Morphological measurements and biomass accumulation

During the course of the experiment, height to meristem and root collar diameter were measured for all trees once a week. At the end of the experiment, trees were dissected; root system and leaves were carefully collected and laid out inside transparent plastic bags and scanned using a Toshiba e-studio 282 scanner (Toshiba Corp., Tokyo, Japan). Scanned images were analyzed using GNU image manipulation program 2.6 (www.gimp.org) to give total projected root and leaf area estimates. Detached root systems were also used for measurement of root volume by the water displacement method using a collection tube attached to a nozzle-fitted Erlenmeyer flask. Upon initiation of the experiment, five additional trees were sacrificed; root systems were cleaned from soil particles and cut from the stem, and needles were collected. The three fractions (leaves, stem and roots) were dried at 60 °C for 48 h and later weighed on a Precisa 62A balance (Precisa Gravimetrics, Dietikon, Switzerland) to give the dry mass of each fraction. By the end of the experiment the dry mass of each fraction was determined for each tree. The increase in biomass over time was calculated by subtracting mean initial dry mass from final dry mass.

Leaf gas exchange and water potential

During the course of the experiment, leaf gas exchange, i.e., stomatal conductance (g_s), transpiration (T) and net assimilation (A_n), were measured once a week on three trees per treatment. Measurements were made on a pre-marked twig terminus carrying juvenile needles with a total projected area of 2 cm^2, using a LI-6400 Photosynthesis System (Licor Inc., Lincoln, NE, USA) equipped with an LED lamp set to 1000 µmol m^{-2} s^{-1} PAR. This PAR value was shown as saturating by light response curves of seedlings of three Mediterranean pine species (Awada et al. 2003). Mean weekly amounts of transpiration (T_j, g week^{-1}) were estimated from leaf-level measurements according to

$$T_j = T_{mean} \times t_T \times k \times MW_w \times \{L_{a\,j-1} + [(L_{a\,week30} - L_{a\,week0})/40]\} \quad (3)$$

where T_{mean} is an average of three transpiration measurements (in mmol m^{-2} s^{-1}) between 8:00 and 12:00, t_T is the cumulative time (in s) of transpiration during the week (assuming 12 h/day), k is a correction factor that was used to account for the fact that T was measured at least 1 week after each irrigation event (thereby underestimating T by a factor of 2), MW_w is the molar mass of water (18 g mol^{-1}), and L_a is the calculated leaf area based on measurements at the beginning ($L_{a\,week0}$) and end ($L_{a\,week30}$) of the experiment and assuming a linear increase in between. Once in 1 or 2 weeks gas exchange measurements were accompanied by measurements of leaf water potential (Ψ_l) using the pressure chamber technique (Scholander et al. 1965; Holbrook et al. 1995). Small (5–7 cm long) twigs were cut from the same trees used for the gas exchange measurements (three per treatment) and put in a pressure chamber (Arimad 2; A.R.I., Kfar Charuv, Israel) fed by a nitrogen gas cylinder and equipped with a lamp-carrying magnifying glass. Gas pressure within the chamber was gradually increased (~1 MPa min^{-1}) until water

emerged from the protruding cut branch surface, and the pressure value was recorded as leaf water potential (Ψ_l).

Xylem hydraulic conductivity

Hydraulic conductivity was measured in five to nine trees per treatment, under low pressure (0.02 MPa) before and after perfusing the xylem tissue at a high pressure of 0.5 MPa. In order to eliminate variations at the time of sampling due to the treatment-specific irrigation program, trees were watered 24 h prior to measurement. We can assume that any reversible reductions in conductance were not measured and the measurement captured the mid-term steady-state developmental responses (and not short-term embolism). A 30 cm stem section was cut from the base of the stem and resin secretion from the cuts was eliminated by placing both ends (5 cm from cut tips) in a water bath at 95 °C for 10 min (adapted from Waring and Silvester 1994). Next, stem sections were submerged in distilled water for 10 min. The root collar end of each stem was then fitted with a rubber gasket, while still submerged, to a latex pipe fed by 10 mM KCl solution in a double-distilled water reservoir. A hydrostatic pressure of 0.02 MPa was applied by placing the reservoir exactly 2 m above the stem section. For 2 h, water dripping from the distal end of the stem section was collected and weighed every 20 min. The water flow rate (kg s^{-1}) was divided by the pressure gradient (0.02 MPa) along the 30 cm stem length to provide the hydraulic conductivity K_h (kg m MPa^{-1} s^{-1}), as described by Tyree and Alexander (1993). K_h was further divided by the xylem cross-sectional area to provide the specific hydraulic conductivity K_s (kg m^{-1} MPa^{-1} s^{-1}). Stem sections (1–4 per treatment) were then fitted with a high-pressure valve to a pressure-resistant pipe fed by 10 mM KCl solution reservoir placed inside a Scholander pressure chamber. Pressurizing the solution through the segment at 0.5 MPa for 5 min followed by a second measurement of K_s determined the maximum specific conductivity, $K_{s\,max}$.

Statistical analysis

Data were subjected to analysis of variance (ANOVA) using JMP software (Cary, NC, USA). Measurements of individual trees were used as observations, where drought intensity (water amount) and drought interval (irrigation frequency) were defined as factors. Differences between treatments were considered significant when type 3 sum of squares met the *F*-test criterion at probability <0.05.

Results

Differential effect of drought intensity and duration on tree survival and growth

The differential effect of drought intensity and duration was first assessed by comparing growth rates in T3 (0.75:3), T5 (0.5:2) and T7 (0.25:1) treatments. These treatments had identical total irrigation amounts ($Si = 0.25$), but clearly different growth patterns (Figure 1b). These effects on growth were linked to changes in SWC (Figure 1a): in T7 (0.25:1), the frequent small irrigation doses resulted in increasingly lower SWC values, reflecting the effects of 'drought intensity' (Figure 1b). Comparing T5 and T3 indicated that in this case the higher irrigation dose (T3) was not sufficient to compensate for the 'drought duration' effect (3 weeks vs. 2 weeks), and its mean SWC and growth rates were lower.

We further assessed the observed links between irrigation patterns and SWC by partitioning the ET fluxes. Based on integrated leaf scale gas exchange measurements, mean weekly transpiration (T_j) ranged from 9 to 67 g $week^{-1}$, compared with 56–366 g $week^{-1}$ for ET_j (76–91% of the water demand) depending on the treatment (Table 1). Partitioning between T_i and ET_i was linearly related to the relative water amount at each event (A_i/A_0) for a given drought duration. For example, where drought duration was 1 week, T_i/ET_i of T1 (0.75:1), T4 (0.5:1) and T7 (0.25:1) was 0.21, 0.16 and 0.09, respectively, yielding the regression equation $T_i/ET_i = 0.24 \times A_i/A_0 + 0.03$ ($R^2 = 0.99$). The partitioning ratio increased with A_i/A_0 also under higher drought duration, albeit with lower regression slopes (Figure 2).

To assess the integrated drought intensity/duration effects, a simple empirical plant drought index (PDI) that considers their combined effect was used:

$$\mathrm{PDI} = 1 - S_i \times T_i \,/\, \mathrm{ET}_i \qquad (4)$$

where the relative total water supply in treatment *i*, Si, was obtained from $Si = A_i/A_0 \times D_i/D_0$, where A_i is the water amount for the treatment, A_0 is the control amount (which was predetermined as indicated in Materials and methods), and D_i and D_0 are the number of irrigation events in 21 days (maximum drought duration in this study) in a treatment and control,

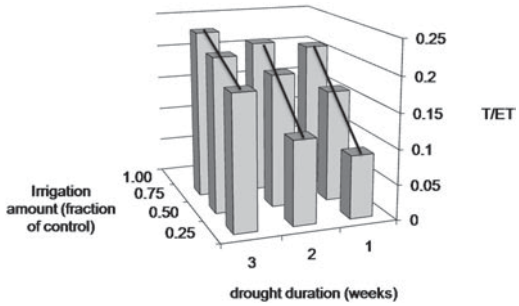

Figure 2. Change in the ratio of transpiration, T, to evapotranspiration, ET (T/ET, transpiration ratio), as a function of irrigation amount (% of control) and drought duration. Equations of the regressions lines were $T/ET = 0.24 \times A_i/A_0 + 0.03$ ($R^2 = 0.99$) for 1 week, $T/ET = 0.20 \times A_i/A_0 + 0.08$ ($R^2 = 0.95$) for 2 weeks and $T/ET = 0.10 \times A_i/A_0 + 0.17$ ($R^2 = 0.99$) for 3 weeks.

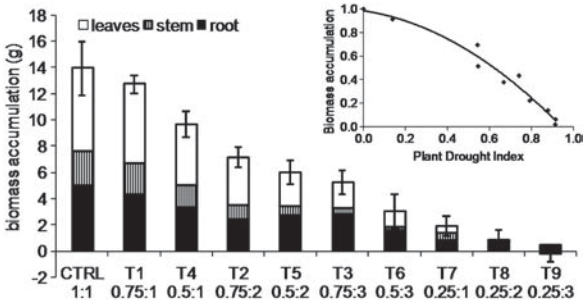

Figure 3. Dry biomass accumulation in leaves, stems and roots, in response to drought treatments (T1–T9; see Table 1). Results were arranged according to the treatment's Plant Drought Index (PDI, Eq. (4)), with total biomass relative to control in response to PDI shown in the inset ($BA = 1 - 0.82 \times PDI^2 - 0.27 \times PDI$). Error bars indicate the standard error of the mean mass in all three organs combined ($n = 6$).

respectively (Table 1; i.e., *Si* and PDI ranged between zero and 1 with $S = 1$ and PDI = 0 for optimal conditions). Weight-based estimates of ET were simplified in our system since runoff, *R*, and drainage, *D*, could be ignored (see Eq. (1)) and transpiration (T) rates were calculated based on gas exchange measurements as described above. Within 30 weeks of exposure to drought, all trees receiving 25% of optimal irrigation (T7–T9) died, while if total irrigation input was 50% of optimum, most (60%) trees survived even the lowest irrigation frequency (T6). Accordingly, the threshold PDI value for tree survival was $0.74 < PDI < 0.79$.

Trees started the experiment with ~6 g of biomass, and hence the accumulation of 14 g in control trees means that 230% was the potential growth in the course of the trial (Figure 3). Drought reduced this growth to 50% in T6 (0.5:3) trees, and lower in trees that received only 25% irrigation and died before the end of the trial. The empirical drought index, PDI, predicted well reductions in biomass accumulation (BA, as a fraction of control; Figure 3, $R^2 = 0.97$), yielding the following regression equation:

$$BA = 1 - 0.82 \times PDI^2 - 0.27 \times PDI \quad (5)$$

The non-linear nature of Eq. (5) suggested that tree growth was less sensitive to drought at low PDI values, but sensitivity increased at high PDI. The differential effects of drought intensity and drought interval were also apparent based on the analysis of variance reported in Table 2.

Response of the tree's hydraulic structure to drought parameters

Root, stem and leaf biomass were measured in order to understand the structural response of each hydraulic component. Figure 3 shows the biomass partitioning for all treatments, ordered according to their PDI value. When water supply was optimal, biomass partitioning to leaves, stem and roots was 50, 20 and 30%, respectively. Biomass distribution was similar for mild drought, in T1 (0.75:1), T2 (0.75:2) and T4 (0.5:1). Under more intense drought, as for T5 (0.5:2), diversion of biomass to roots increased while decreasing to stems, with this trend further increasing in T3 (0.75:3). At the limit of tree survival in

Table 2. Response means for the drought treatments, slopes of linear regression fits and their significance levels, from ANOVA of the parameters indicated, as a function of 'drought duration' (irrigation frequency) and 'drought intensity' (water amount). Responses not connected by the same letter are significantly different. Slopes express a change (percent of control) for each 1-week extension of the drought period or for each 25% reduction in irrigation amount. All measurements were made at the end of the 30-week experiment, except for g_s (Week 8) and height increment (Ht. increm.) and diameter (Week 17).

	Ht. increm. (cm)	Diameter (mm)	Total biomass increm. (g)	Stem biomass increm. (g)	Leaf biomass increm. (g)	Root biomass increm. (g)	K_s (kg m^{-1} MPa^{-1} s^{-1})	g_s (mol m^{-2} s^{-1})	A_r (cm^2)
Means									
Control	5.6^{a}	5.27^{a}	12.20^{a}	2.56^{a}	6.36^{a}	5.01^{a}	0.13^{a}	0.06^{a}	24.6^{ab}
T1	4.7^{ab}	5.20^{ab}	12.20^{a}	2.33^{ab}	6.07^{ab}	4.32^{ab}	0.11^{a}	0.06^{ab}	27.3^{a}
T2	4.4^{abc}	4.55^{cd}	6.49^{bc}	1.08^{cd}	3.61^{cd}	2.45^{cd}	0.05^{a}	0.04^{cd}	19.1^{c}
T3	2.9^{bcde}	4.12^{de}	4.70^{cd}	0.50^{def}	1.96^{ef}	2.79^{cd}	0.04^{a}	0.02^{cde}	25.2^{ab}
T4	4.3^{abc}	4.78^{bc}	9.34^{ab}	1.66^{bc}	4.63^{bc}	3.37^{bc}	0.04^{a}	0.04^{bc}	28.4^{a}
T5	4.0^{abcd}	4.34^{cde}	6.00^{bc}	0.66^{de}	2.60^{de}	2.76^{cd}	0.03^{a}	0.03^{cde}	19.7^{bc}
T6	2.4^{cde}	4.25^{de}	1.92^{de}	0.20^{ef}	1.26^{efg}	1.61^{de}	n.a.	0.01^{de}	18.1^{c}
T7	3.8^{abcd}	4.33^{cde}	1.63^{de}	0.60^{def}	0.50^{fg}	0.80^{e}	n.a.	0.01^{e}	12.8^{d}
T8	2.0^{de}	3.87^{ef}	0.98^{e}	0.01^{ef}	0.10^{g}	0.73^{e}	n.a.	0.01^{e}	11.1^{d}
T9	1.1^{e}	3.65^{f}	0.56^{e}	−0.14^{f}	−0.10^{g}	0.46^{e}	n.a.	0.01^{de}	12.1^{d}
Regression slope									
Duration	−21.9	−8.6	−26.3	−31.9	−26.8	−18.0	−29.1	−22.5	−10.0
Intensity	−17.2	−7.3	−29.4	−27.1	−30.2	−26.4	−35.8	−25.5	−19.9
Significance									
Duration	n.s.	<0.001	<0.001	<0.001	<0.001	<0.005	n.s.	<0.005	<0.05
Intensity	n.s.	<0.01	<0.01	<0.01	<0.05	<0.01	n.s.	<0.05	n.s.

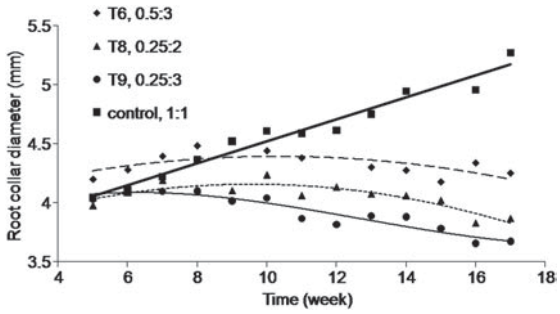

Figure 4. Change with time in mean root collar diameter of trees under drought treatments where biomass allocation to stem was ≤0 and under control treatment ($n = 10$). Equations of regression lines were $y = 0.09x + 3.59$, $R^2 = 0.96$ for control; $y = 0.004x^2 + 0.09x + 3.93$, $R^2 = 0.41$ for T6; $y = 0.006x^2 + 0.11x + 3.61$, $R^2 = 0.77$ for T8; and $y = 0.0004x^3 + 0.016x^2 + 0.15x + 3.66$, $R^2 = 0.89$ for T9.

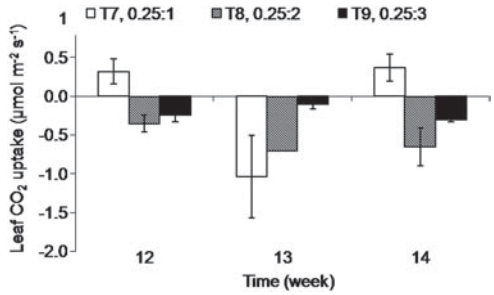

Figure 5. Mean rates of net leaf CO_2 uptake (A_n) under fatal drought treatments (T7–T9; see Table 1), measured at three times during the experiment. Error bars indicate the standard error of the mean ($n = 3$).

T6 (0.5:3), new tissue was formed almost entirely in roots and none in the stem. When drought intensity was fatal, biomass allocation was only to roots, first at the expense of the stem and later at the expense of the leaves, up to a negative biomass accumulation in stem tissue (see the bar representing T9 (0.25:3) in Figure 3). An average T9 (0.25:3) tree started the experiment with a stem biomass of 2290 mg dry weight and ended it with 2150 mg, a net biomass loss of 140 mg.

Unexpectedly, whereas stem height increased in all trees during the experiment (Figure 1b), stem diameters peaked for some treatments on Weeks 6–10 and shrank continuously thereafter (Figure 4), also reflected by very low to negative stem biomass accumulation (Figure 3). Similarly, leaf area increased during the trial in all trees (data not shown), while in treatments T8 and T9 there was no accompanying increase in leaf biomass. Figure 4 shows that stem diameter decreased in a non-linear fashion, initially increasing up to Week 6, which means that while the net observed stem biomass loss for a T9 (0.25:3) tree was 140 mg, the effective loss was larger (approximation of stem dry biomass on Week 6 was possible since stem density before and after the experiment was similar). Using weekly measurements of stem height and diameter in calculation of stem volume (assuming a conical shape) during the course of the experiment yielded a stem biomass value of 2750 mg for a T9 (0.25:3) tree on Week 6. This means that stem biomass potentially decreased by ~600 mg between Week 6 and the time of mortality. Loss of biomass was partly explained by negative carbon balance between emission of CO_2 in respiration and uptake in photosynthesis. Slow rates of CO_2 emission were found in trees under the highest drought intensity (T7–T9), i.e., ~0.2 µmol m^{-2} s^{-1} at midday (Figure 5) and 0.4 µmol m^{-2} s^{-1} in the late evening in the leaves of T9 (0.25:3) trees. These snapshot measurements were used to approximate the weekly leaf CO_2 exchange (FC, in mg $week^{-1}$) according to

$$FC = L_a \times MW_c \times (A_{n\,fs} \times t_{fs} + A_{n\,d} \times t_d) \quad (6)$$

where L_a is projected leaf area (0.015 ± 0.004 m^2), MW_c is the molar mass of CO_2 (44 g mol^{-1}), $A_{n\,fs}$ and $A_{n\,d}$ are net assimilation rates (–0.2 and –0.4 µmol m^{-2} s^{-1}, respectively) under full sunlight (9:00–15:00) and partial sunlight or dark (15:00–9:00) conditions, and t_{fs} and t_d are cumulative times (in s) of full sunlight and partial sunlight or dark, respectively, along the week. It was estimated, for a first approximation, that ~120 ± 32 mg CO_2 $week^{-1}$ was emitted per tree. Assuming a respiration quotient for carbohydrates of 1.0 and a carbohydrate molar mass of 30 g mol^{-1}, this CO_2 net loss translates into ~81 mg carbohydrates $week^{-1}$, or a total of ~320 mg stem biomass during the 4 weeks prior to tree mortality. This amount is markedly below the estimated stem biomass loss of 600 mg, suggesting that other processes, including translocations of biomass, also took place. For example, the net biomass accumulation of 460 mg in the root tissue of T9 (0.25:3) trees may have partly relied on reallocation of biomass from the stem.

Hydraulic regulation of different plant organs

We measured traits underlying hydraulic activities for the three main hydraulic components of the trees: changes in root system area; in xylem conductivity; and in stomatal conductance to water vapor. Figure 6 shows that the total area of the root system (A_r) increased in all trees, including trees that suffered the highest drought intensity and did not survive. Based on an initial root area of 5.2 cm^2, a 400% increase in root system area was observed in T1 (0.75:1) and T4 (0.5:1), higher than in the control.

Specific hydraulic conductivity of the xylem, K_s, measured after stems were allowed to rehydrate for 24 h, decreased dramatically with drought, although values varied greatly (see the black bars in Figure 7). K_s decreased by 15, 50, 65 and 75% with increasing drought in T1 (0.75:1), T2 (0.75:2), T4 (0.5:1) and T5 (0.5:2), respectively. The magnitude of reduction in xylem conductivity did not correlate linearly with PDI: for SWC <10% the effect was similar irrespective of irrigation regime, indicating a fixed SWC threshold for loss of xylem conductivity. Loss of K_s could be due to shrinkage of the total volume/diameter of the tracheids or due to embolisms that the plant was

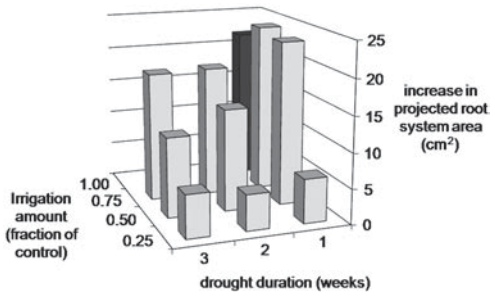

Figure 6. Mean growth in projected root system area in the course of the drought experiment in treatments T1–T9 (see Table 1; $n = 5–8$).

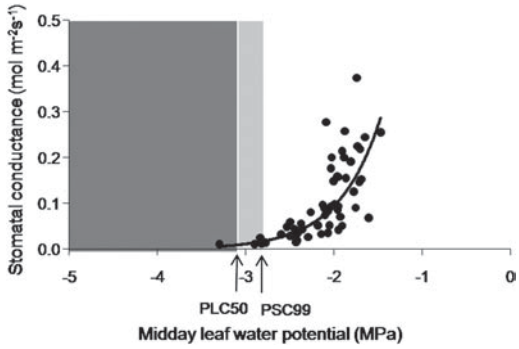

Figure 8. Response of stomatal conductance to water vapor to midday leaf water potential. Data from all drought treatments were obtained from weekly measurements during Weeks 1–8 at midday (each point represents the mean of three replicate measurements). Hydraulic safety margin, between Ψ99PSC and Ψ50PLC, is indicated by light gray background, and PLC > 50 is indicated by dark gray.

not able to refill during rehydration. In order to distinguish between these processes, we repeated the conductivity measurements after perfusion at high pressure, in which water was forced through the xylem. This treatment presumably refilled embolized tracheids, giving $K_{s\,max}$, which should only be related to the total volume of the tracheids. Indeed $K_{s\,max}$ values for each treatment were higher than K_s values, and had greater uniformity within a treatment. The white bars in Figure 7 show that T1 (0.75:1) trees maintained the $K_{s\,max}$ of control trees and with increasing drought $K_{s\,max}$ dropped by 60–65%, depending on the treatment (and also under fatal drought). This was interpreted as indication that xylem volume decreased following drought, in agreement with measurements of decreased stem diameter under drought (Figure 4).

Leaf stomatal conductance also decreased in response to drought, in relation to PDI:

$$g_s = 0.07 - 0.02 \times \mathrm{PDI}^2 - 0.04 \times \mathrm{PDI} \qquad (7)$$

The effects of drought intensity and duration on g_s (in percent of the control value; see Table 2) were summarized by the regression equations $g_s = 100–25 \times (A_0/A_i)$ ($P < 0.05$) and $g_s = 100–22 \times (3/D_i)$ ($P < 0.005$). A reduction of 25% in g_s was observed by reducing water input by 25%. Alternatively, a reduction of 22% in g_s was observed by extending the interval between irrigations by 1 week (Table 2). The second equation also indicated that $g_s = 0$ when $D_i = 0.67$, i.e., one irrigation event in 31.5 days, which is the longest drought duration still allowing stomatal activity in this experiment. Leaf conductance was closely related to leaf water potential (Figure 8): g_s fell as midday leaf water potential declined. g_s was highly correlated with the decrease in SWC ($R^2 = 0.79$; data not shown), and at –2.8 MPa conductance approached zero. Thus, –2.8 MPa is the leaf water potential that resulted in 99% stomatal closure (Ψ99PSC). This tight regulation is characteristic of isohydric plant species.

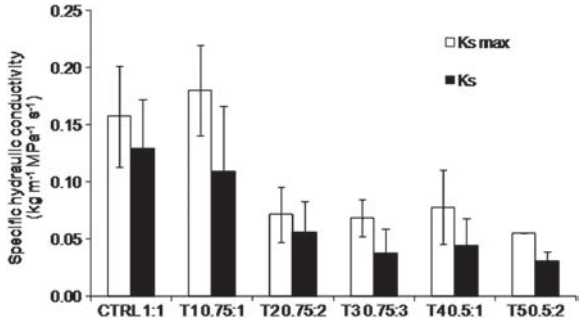

Figure 7. Mean xylem specific and maximal hydraulic conductivity (K_s and $K_{s\,max}$, respectively) in treatments with surviving trees (indexed as shown in Table 1). Error bars indicate the standard error of the mean ($n = 5–9$ for K_s and $n = 1–4$ for $K_{s\,max}$).

Discussion

Hydraulic regulation at the whole tree level

The Ψ99PSC value of –2.8 MPa that we measured for *P. halepensis* is a relatively high value in comparison with other arid coniferous tree species. For example, *Callitris rheomboidea* of Eastern Australia has a Ψ99PSC of –4.3 MPa (Brodribb and Cochard 2009), and *Juniperus scopulorum* of New Mexico, USA has a Ψ99PSC of –5.5 MPa (McDowell et al. 2008). High Ψ99PSC may be related to high sensitivity of the xylem to embolism or to a wide safety margin taken by the plant, since cavitation occurs when Ψ declines below a threshold value. Indeed, in this experiment we found that treatments that resulted in higher loss of xylem conductivity also exposed it to lower midday leaf water potentials (Figure 9). This is in agreement with values reported in the past for *P. halepensis*: 37% PLC at –2 MPa, 48% at –3 MPa and 67% at –4 MPa (Oliveras et al. 2003).

Xylem sensitivity to embolism is often expressed by the Ψ value where 50 percent conductivity loss (Ψ50PLC) occurs. Martinez-Vilalta et al. (2004) listed Ψ50PLC values of 40

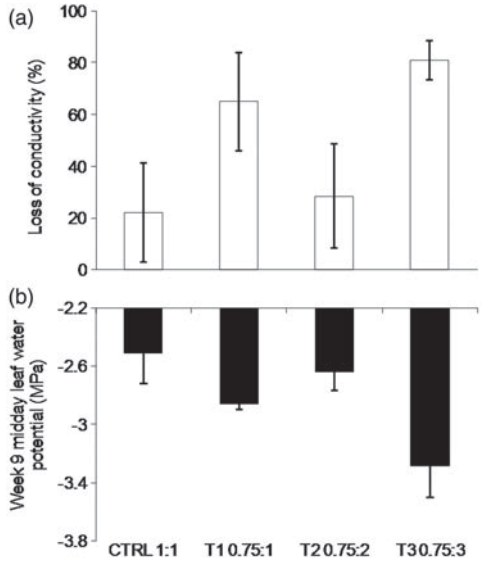

Figure 9. Loss of xylem hydraulic conductivity (%; where PLC = 100 – ($K_s/K_{s\ max}$ × 100)) measured at the end of four drought treatments (indexed as indicated in Table 1; a), and mean midday leaf water potential, measured on Week 8 of the experiment (b). Error bars indicate the standard error of the mean (n = 2–4).

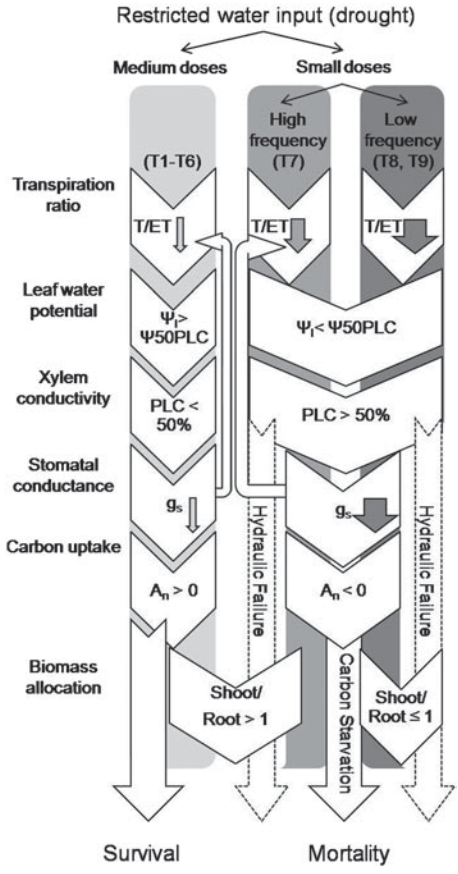

Figure 10. Effects of the main drought scenarios on hydraulic components, carbon management and the tree's fate. Arrow width indicates magnitude of response in T/ET and g_s. Dotted outline indicates a possible pathway without sufficient evidence.

coniferous species; *P. halepensis*, with a Ψ50PLC of –3.11 MPa, ranked at the 9th place, with 80% of the species characterized by lower Ψ50PLC. Tyree et al. (1994) showed a positive relationship between conduit diameter and xylem vulnerability to embolism. Accordingly, a lower Ψ50PLC was expected in the case of *P. halepensis*, where tracheids are only 10 μm in diameter (Oliveras et al. 2003). However, the reported Ψ50PLC of –3.11 MPa (Oliveras et al. 2003) was similar to that estimated from our potted trees (–2.9 MPa) and close to that of other narrow-tracheid pine species. The conductivity loss described in Figure 9 can be linked to xylem cavitation and embolism processes, in turn causing hydraulic dysfunction which may result in tree mortality (Cochard 2006). It is therefore possible that hydraulic failure played a role in the mortality of stressed *P. halepensis* trees, as presented in Figure 10.

The transpiration ratio, T/ET, appears to integrate the intensity and duration effects of the drought, and influences the trees' response to it (Figure 10). In treatments with less frequent but larger irrigation doses, T/ET was 22–24%, while for frequent, smaller water applications, transpiration ratios were as small as 9% (Figure 2). Apparently, even in pot experiments the transpiration ratio is sensitive to water infiltration depth associated with the irrigation dose. This provided a strong link to field measurements. The results of Raz Yaseef et al. (2009) in the Yatir forest showed that small precipitation events were sufficient to maintain the topsoil layer wet during the rainy season, but only more intensive storms infiltrating to the root zone increased T/ET. This demonstrated the importance of precipitation patterns, as opposed to the total amount, on the forest functioning, similar to the results obtained here. The combined greenhouse and field measurements indicate, therefore, that drought effects may be better predicted by assessing its effect on the transpiration ratio than by assessing the absolute amount of water input.

Tree-level hydraulic processes downstream of the transpiration ratio can be described as a cascade of responses, eventually determining the tree's fate (Figure 10). The significance of maintaining Ψ_l above Ψ50PLC is twofold: first, exposing the xylem to extreme tension can result in hydraulic failure; and second, the resulting stomatal closure may lead to carbon loss. Unless the drought stress is relieved, mortality cannot be avoided, despite hydraulic adjustments, such as prioritization of root growth.

Hydraulic safety margin of P. halepensis

The relatively high xylem vulnerability to embolism displayed by trees in this study was not expected in a tree species successfully growing on the dry timberline (Maseyk et al. 2008). Martinez-Vilalta et al. (2004) reported a Ψ50PLC of –9.20 MPa for *C. rheomboidea*, and –7.40 MPa for *J. scopulorum*, both arid coniferous species as well. Notably, while these PLC values are

much lower than the value for *P. halepensis*, they are also considerably lower than the values of Ψ99PSC of these exact species, –4.3 and –5.5 MPa, respectively (McDowell et al. 2008). The gap between stomatal closure (Ψ99PSC) and xylem dysfunction (Ψ50PLC) is considered the hydraulic safety margin of the species (Sperry 2004). Note that this gap is very narrow (0.3 MPa) for *P. halepensis* (Figure 8, marked by light gray background), in comparison with the two other species noted above, which are 1.9 and 4.9 MPa, respectively, or 2.4 MPa for the isohydric *Pinus edulis* (Ψ50PLC of –4.5 MPa, Ψ99PSC of –2.1 MPa; Martinez-Vilalta et al. 2004, McDowell et al. 2008).

The significance of the observed narrow safety margin in *P. halepensis* is not clear at present. It is hypothesized that it reflects opposing 'bottom-up' and 'top-down' eco-physiological adjustments. First, these trees, growing in a semi-arid environment and exposed to long seasonal droughts, adopted narrow tracheids and low hydraulic conductance to adjust to soil water availability and the prevailing soil water potential. This likely contributed to the observed trees' low water use and the relatively low mean stomatal conductance. Second, against this background, leaves adapted in order to utilize the maximal operational range available and extended stomatal conductance to CO_2 while avoiding carbon starvation as much as possible, resulting in leaf water potential approaching the 'danger zone' for the hydraulic system. In this respect, *P. halepensis* is more efficient than most tree species in terms of using the carrying capacity of the xylem (Sperry 2004).

If, hypothetically, the hydraulic safety margin of *P. halepensis* was 1.0 MPa wide and as a consequence Ψ99PSC was –2.1 MPa (instead of –2.8 MPa, and assuming Ψ50PLC = –3.1 MPa), stomatal gas exchange would cease as early as Week 4 (instead of Week 11) for T9 (0.25:3) trees, and on Week 8 (instead of ongoing carbon uptake) for T1 (0.75:1) trees. This would inevitably create a negative carbon gain (as shown in Figure 5 for a more advanced stage of the experiment) which could have an immense negative impact on tree survival rate under drought. Is this risky behavior unique to young trees, trying to maximize carbon assimilation during the juvenile phase, while adult *P. halepensis* trees potentially have a wider safety margin? Evidence to the contrary is from leaf water potential values measured in an Aleppo pine forest between October 1998 and May 1999 (Atzmon et al. 2004). There, stomatal gas exchange would not be possible before February if Ψ99PSC was –2.1 MPa. While the latter refers to *P. halepensis* growing in a Mediterranean climate, in a semi-arid forest where $\Psi_l < -2.5$ MPa all year long, the mere existence of this species there would not be possible. A tree species with relatively high xylem vulnerability to embolism like this pine could not survive drought with a wider safety margin. In practice, the semi-arid forest has been relatively highly productive over the past 45 years (Grunzweig et al. 2007, Maseyk et al. 2008, Raz Yaseef et al. 2010), and our pot experiment with the same trees indicates that xylem security was not sacrificed and hydraulic failure was usually avoided due to rapid stomatal responses (Figure 8).

Carbon management in a drought-avoiding tree

The isohydric mode of stomatal regulation indicated by our results suggests that *P. halepensis* is a drought-avoiding species. This strategy inescapably affects CO_2 uptake, and starting in Week 12 in trees under high drought intensity, signs of carbon starvation were observed (negative CO_2 uptake even at midday under optimal light; Figure 5). How can a tree sustain itself without CO_2 uptake? Biomass balance calculations (see Results) show that the loss of biomass in the stem and leaf tissues under acute drought stress (Figure 3) could be explained by CO_2 emission in respiration. Non-structural carbohydrates (NSCs) are used for storage by *P. halepensis* trees (Villar-Salvador et al. 1999) and other pine species (Guehl et al. 1993). Under acute stress associated with stomatal closure, these stored carbohydrates can be used in respiration, thus extending tree survival. Yet it cannot be ruled out that stem biomass in the form of NSCs was also reallocated to the root system, as described in the literature (Callaway et al. 1994, Canham et al. 1999). Our measurements show that there was a significant increase in root biomass of at least 0.46 g in T9 (0.25:3) trees in addition to the initial 1.35 g. This growth took place while stem and leaf tissues were shrinking, which, in turn, coincided with reducing the tree's specific conductivity (Figure 7). Theoretically, a tree exposed to limiting SWC would respond by increasing its root system area while reducing water loss through the canopy. Yet in a situation where stomatal conductance is effectively zero and hence CO_2 uptake is inhibited, the formation of new root tissue cannot rely on newly produced photosynthate and could be supported by reallocation. The carbon budget data (biomass and gas exchange) reported above suggest mobilization of carbohydrates during drought. Thus, the loss of 600 mg from the stem associated with a total net loss of 114 mg from the whole plant indicates translocation of C from the stem, and the persistent increase in root system area with drought further indicates that the target for this translocation was in the roots. This further suggests development of whole tree-level starvation in water-stressed saplings rather than the carbon mobilization disorders hypothesized by Sala et al. (2010). Furthermore, biomass balances of T8 (0.25:2) and T7 (0.25:1) trees, which also died during the experiment, show an effective stem biomass loss of 630 and 900 mg, respectively. These higher losses can be related to the respective size of carbon reserve: the maximal estimated stem biomass (which was 2750 mg in a T9 (0.25:3) tree) was 2930 and 3800 mg in T8 (0.25:2) and T7 (0.25:1) trees, respectively. This indicates that irrespective of the drought scenario, all dying trees showed a negative carbon balance as well as mobilization of carbon resources.

Relevance of greenhouse experiments to the Aleppo pine forest ecosystem

An ongoing research program has been operated for the past decade in a *P. halepensis* dominated afforestation in Yatir, Israel, in the framework of Fluxnet (www.fluxnet.ornl.gov/fluxnet/). This program included several eco-physiological field studies of the Aleppo pine forest ecosystem, in aspects of phenology, hydrology and productivity under drought (Grunzweig et al. 2007, Maseyk et al. 2008, Raz Yaseef et al. 2010, Rotenberg and Yakir 2010). While such field studies are important, they inherently involve too many variables to study mechanisms. Therefore, observed phenomena promote studies of specific effects that require investigation under controlled conditions. The greenhouse provides such a semi-controlled experimental system that allows process-based and manipulation experiments. Yet uncertainties with respect to the extent the saplings' responses represent those of mature trees in the forest require care, when results are extrapolated back to the field. For example, young trees may show different functional and structural responses than adult trees, which include the hydraulic adjustments.

To minimize these effects, precautions were taken in the design of the experiment, e.g., we used young trees (rather than seedlings) and pots fitted to root system volume. The results presented above provided several indications that the greenhouse experiment was consistent with field measurements. For example, an association between leaf water potential and the loss of xylem conductivity in this trial (Figure 9) yielded a Ψ50PLC of approximately –2.90 MPa, which is close to the value of –3.11 MPa reported for field measurements (Oliveras et al. 2003). Rates of net assimilation (A_n) and stomatal conductance (g_s), as well as their interactions, closely matched those measured in the field on the same tree species (Maseyk et al. 2008). A strong dependence of the T/ET ratio on the irrigation amount (Figure 2) corresponded well with observations of a similar association between the field T/ET ratio and the patterns of rain events (Raz Yaseef et al. 2010). These and other results from this experiment clearly demonstrated its relevance to the natural forest ecosystem.

Acknowledgments

We wish to thank Dr Ami Zehavi and Ms Ahuva Daniel of KKL-JNF, Israel, for providing the plant material. We thank Prof. Amram Eshel of Tel Aviv University, Dr Gilboa Arye and Dr Eyal Rotenberg of the Weizmann Institute of Science for scientific advice.

Funding

Jewish National Fund—Keren Kayemet L'Israel (Alberta-Israel program 90-9-608-08); Global Change and the Hydrological Cycle (GLOWA—Jordan River project 01-2061); Cathy Wills and Robert Lewis Program in Environmental Science; France-Israel High Council for Research Scientific and Technological Cooperation (project 3-6735).

References

Allen, C.D., A.K. Macalady, H. Chenchouni et al. 2009. A global overview of drought and heat-induced tree mortality reveals emerging climate change risks for forests. For. Ecol. Manage. 259:660–684.

Atzmon, N., Y. Moshe and G. Schiller. 2004. Ecophysiological response to severe drought in *Pinus halepensis* Mill. trees of two provenances. Plant Ecol. 171:15–22.

Awada, T., K. Radoglou, M.N. Fotelli and H.I.A. Constantinidou. 2003. Ecophysiology of three Mediterranean pine species in contrasting light regimes. Tree Physiol. 23:33–41.

Ayers, R.S. and D.W. Westcot. 1985. Irrigation water quality criteria. Lewis Publishers, Chelsea MI.

Boyer, J.S. 1982. Plant productivity and environment. Science 218:443–448.

Breshears, D.D., N.S. Cobb, P.M. Rich et al. 2005. Regional vegetation die-off in response to global-change-type drought. Proc. Natl Acad. Sci. USA 102:154144–154148.

Brodribb, T.J. and H. Cochard. 2009. Hydraulic failure defines the recovery and point of death in water-stressed conifers. Plant Physiol. 149:575–584.

Calamassi, R., G. Della Roccaa, M. Falusia, E. Paolettib and S. Stratib. 2001. Resistance to water stress in seedlings of eight European provenances of *Pinus halepensis* Mill. Ann. For. Sci. 58:663–672.

Callaway, R.M., E.H. DeLucia, E.M. Thomas and W.H. Schlesinger. 1994. Compensatory responses of CO_2 exchange and biomass allocation and their effects on the relative growth rate of ponderosa pine in different CO_2 and temperature regimes. Oecologia 98:159–166.

Canham, C.D., R.K. Kobe, E.F. Latty and R.L. Chazdon. 1999. Interspecific and intraspecific variation in tree seedling survival: effects of allocation to roots versus carbohydrate reserves. Oecologia 121:1–11.

Christensen, J.H., B. Hewitson, A. Busuioc et al. 2007. Regional climate projections. *In* Climate Change 2007: The Physical Science Basis. Contribution of Working Group I to the Fourth Assessment Report of the Intergovernmental Panel on Climate Change. Eds. S. Solomon, D. Qin, M. Manning, Z. Chen, M. Marquis, K.B. Averyt, M. Tignor and H.L. Miller. Cambridge University Press, Cambridge, UK and New York, NY, pp 847–940.

Ciais, P., M. Reichstein, N. Viovy et al. 2005. Europe-wide reduction in primary productivity caused by the heat and drought in 2003. Nature 437:529–533.

Cochard, H. 2006. Cavitation in trees. C. R. Physique 7:1018–1026.

Ferrio, J.P., A. Florit, A. Vega, L. Serrano and J. Voltas. 2003. Δ13C and tree-ring width reflect different drought responses in *Quercus ilex* and *Pinus halepensis*. Oecologia 442:512–518.

Flexas, J., J. Bota, F. Loreto, G. Cornic and T. Sharkey. 2004. Diffusive and metabolic limitations to photosynthesis under drought and salinity in C3 plants. Plant Biol. 6:269–279.

Grunzweig, J.M., I. Gelfand and D. Yakir. 2007. Biogeochemical factors contributing to enhanced carbon storage following afforestation of a semi-arid shrubland. Biogeosciences 4:891–904.

Guehl, J.M., A. Clement, P. Kaushal and G. Aussenac. 1993. Planting stress, water status and non-structural carbohydrate concentrations in Corsican pine seedlings. Tree Physiol. 12:172–183.

Holbrook, N.M., M.J. Burns and C.B. Field. 1995. Negative xylem pressures in plants: a test of the balancing pressure technique. Science 270:1193–1194.

IPCC. 2001. Climate change 2001: the scientific basis. Contribution of Working Group I to the Third Assessment Report of the Intergovernmental Panel on Climate Change. Cambridge University Press, Cambridge.

Maestre, F.T. and J. Cortina. 2004. Are *Pinus halepensis* plantations useful as a restoration tool in semiarid Mediterranean areas? For. Ecol. Manage. 198: 303–317.

Martınez-Vilalta, J., A. Sala and J. Piñol. 2004. The hydraulic architecture of Pinaceae—a review. Plant Ecol. 171:3–13.

Maseyk, K.S., T. Lin, E. Rotenberg, J.M. Grünzweig, A. Schwartz and D. Yakir. 2008. Physiology-phenology interactions in a productive semi-arid pine forest. New Phytol. 178:603–616.

McDowell, N.N., W.T. Pockman, C.D. Allen et al. 2008. Mechanisms of plant survival and mortality during drought: why do some plants survive while others succumb to drought? New Phytol. 178:719–739.

Miyamoto, S., I. Martinez, M. Padilla, A. Portillo and D. Ornelas. 2004. Landscape plant lists for salt tolerance assessment. USDI Bureau of Reclamation.

Mueller, R.C., C.M. Scudder, M.E. Porter, T.R. Talbot, C.A. Gehring and T.G. Whitham. 2005. Differential tree mortality in response to severe drought: evidence for long-term vegetation shifts. J. Ecol. 93:1085–1093.

Oliveras, I., J. Martínez-Vilalta, T. Jimenez-Ortiz, M.J. Lledó, A. Escarré and J. Piñol. 2003. Hydraulic properties of *Pinus halepensis*, *Pinus pinea* and *Tetraclinis articulata* in a dune ecosystem of Eastern Spain. Plant Ecol. 169:131–141.

Quezel, P. 2000. Taxonomy and biogeography of Mediterranean pines (*Pinus halepensis* and *P. brutia*). *In* Ecology, Biogeography and Management of *Pinus halepensis* and *P. Brutia* Forest Ecosystems in the Mediterranean Basin. Eds. G. Ne'eman and L. Trabaud. Backhuys Publishers, Leiden, pp 1–12.

Raz Yaseef, N., D. Yakir, E. Rotenberg, G. Schiller and S. Cohen. 2009. Ecohydrology of a semi-arid forest: partitioning among water balance components and its implications for predicted precipitation changes. Ecohydrology 3:143–154.

Raz Yaseef, N., E. Rotenberg and D. Yakir. 2010. Effects of spatial variations in soil evaporation caused by tree shading on water flux partitioning in a semi-arid pine forest. Agric. For. Meteorol. 150:454–462.

Rotenberg, E. and D. Yakir. 2010. Contribution of semi-arid forests to the climate system. Science 327:451–454.

Royo, A., L. Gil and J.A. Pardos. 2001. Effect of water stress conditioning on morphology, physiology and field performance of *Pinus halepensis* Mill. Seedlings. New For. 21:127–140.

Sala, A., F. Piper and G. Hoch. 2010. Physiological mechanisms of drought-induced tree mortality are far from being resolved. New Phytol. 186:274–281.

Scholander, P.F., H.T. Hammel, E.D. Bradstreet and E.A. Hemmingsen. 1965. Sap pressure in vascular plants: negative hydrostatic pressure can be measured in plants. Science 148:339–346.

Seager, R., M. Ting, I. Held et al. 2007. Model projections of an imminent transition to a more arid climate in southwestern North America. Science 316:1181–1184.

Sperry, J. 2004. Coordinating stomatal and xylem functioning – an evolutionary perspective. New Phytol. 162:568–570.

Sterl, A, C. Severijnes and H. Dijkstra et al. 2008. When can we expect extremely high surface temperatures? Geophys. Res. Lett. 35:L14703.

Tardieu, F. and T. Simonneau. 1998. Variability among species of stomatal control under fluctuating soil water status and evaporative demand: modelling isohydric and anisohydric behaviours. J. Exp. Bot. 49:419–432.

Tognetti, R., M. Michelozz and A. Giovannelli. 1997. Geographical variation in water relations, hydraulic architecture and terpene composition of Aleppo pine seedlings from Italian provinces. Tree Physiol. 17:241–250.

Tyree, M.T. and J.D. Alexander. 1993. Hydraulic conductivity of branch junctions in three temperate tree species. Trees 7:156–159.

Tyree, M.T., S.D. Davis and H. Cochard. 1994. Biophysical perspectives of xylem evolution: is there a tradeoff of hydraulic efficiency for vulnerability to dysfunction? IAWA J. 15:335–360.

Villar-Salvador, P., L. Ocana, J. Penuelas and I. Carrasco. 1999. Effect of water stress conditioning on the water relations, root growth capacity, and the nitrogen and non-structural carbohydrate concentration of *Pinus halepensis* Mill. (Aleppo pine) seedlings. Ann. For. Sci. 56:459–465.

Waring, R.H. and W.B. Silvester. 1994. Variation in foliar $\delta^{13}C$ values within the crowns of *Pinus radiata* trees. Tree Physiol. 14:1203–1213.

West, A.G., K.R. Hultine, K.G. Burtch and J.R. Ehleringer. 2008. Seasonal variations in moisture use in a pinon–juniper woodland. Oecologia 153:787–798.

5.1.1. Seasonal shifts in xylem hydraulics on the diurnal scale

The daily course of percent loss of specific conductivity (PLC), an indicator of xylem cavitation, shows that PLC shifted from none in the rainy season (January) to up to 40% in the dry season (May and June; Fig. 1.1). Since climate is similar during the whole summer, the measurements in May and June are representative of that season. In summer cavitation peaked two times during the day: first in the morning and later again in the afternoon (May measurement) or evening (June). At noontime and during the night cavitation declined to 0-5% and xylem conductivity was fully restored. Morning and afternoon cavitation developed within 2-3 hours and was consequently reversed within 1-2 hours.

Seasonal shifts of diurnal time-scale xylem hydraulics were reflected in the sap flow rate (Fig. 1.2). Moving from the rainy season into the dry season, the diurnal peak in SF decreased from 5-7 kg hr^{-1} in February-April to less than 1 kg hr^{-1} in July-October. The timing of the SF peak, t_{max}(SF), also changed, from ~10:00 in April to ~19:00 in October (Fig. 1.2; Table 1.1). As a result, while in April 96% of SF occurred during the daytime, during September-October as much as 70% of SF occurred at night.

These major temporal changes did not reflect leaf scale dynamics. T was always restricted to daytime throughout the year, and its peak, t_{max}(T), was in the morning in all seasons (Table 1.1), and moved from mid-day in the wet season to mid-morning (~9:00) in the dry season. Consequently, the lag time between t_{max}(T) and the less distinct t_{max}(SF) increased from 30 min in April to 9.5 hr in July (Table 1.1). Under favorable conditions, in the wet season, water transport rates in the xylem (SF) and from the leaf (transpiration, T) are relatively synchronized and the short lag can be explained by the effect of changes in Ψ_l. This synchronization was disrupted under the summer drought.

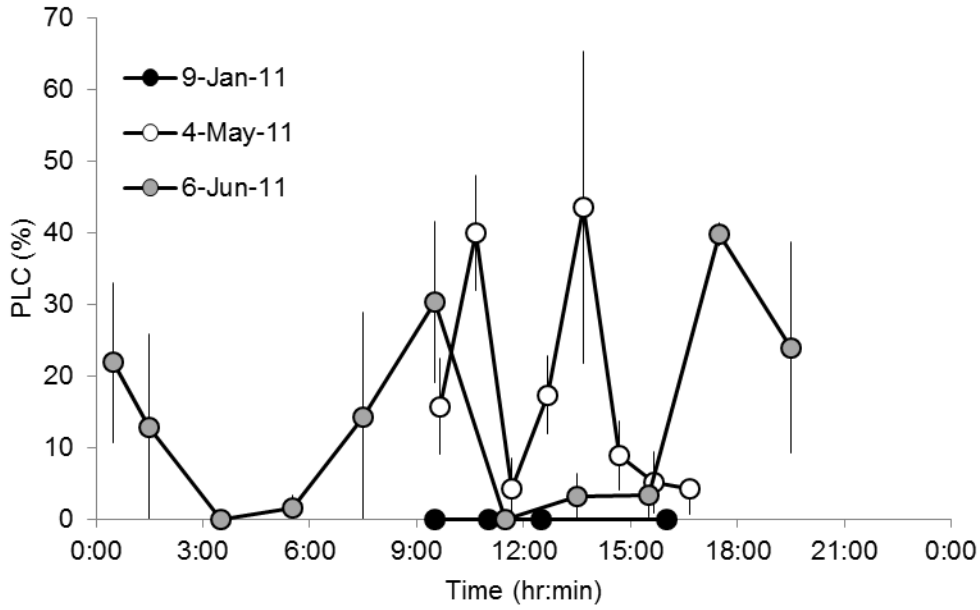

Fig. 1.1. Xylem cavitation (percent loss of conductivity, PLC) in *Pinus halepensis* branches sampled on three field days in Yatir forest. *Error bars* represent the standard error of the mean (n = 3 trees (May); 3 branches from one tree (Jan, Jun)).

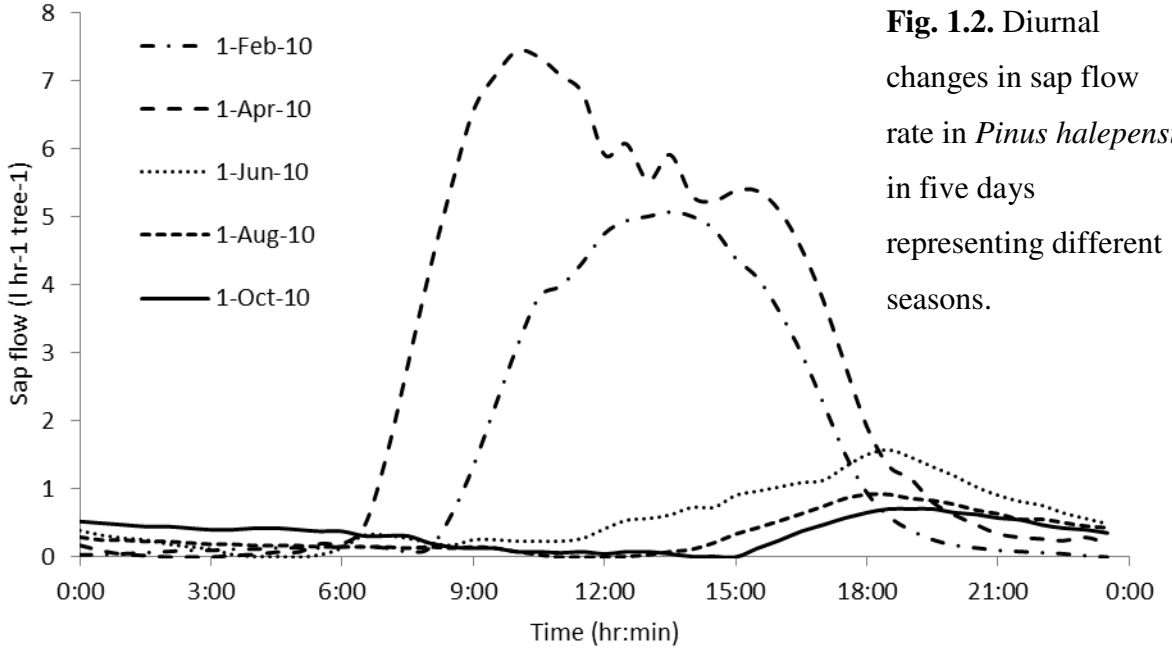

Fig. 1.2. Diurnal changes in sap flow rate in *Pinus halepensis* in five days representing different seasons.

Table 1.1. Diurnal maxima of leaf transpiration [$t_{max}(T)$] and sap flow [$t_{max}(SF)$] along the year in Yatir forest and the time difference between them.

Date	$t_{max}(T)$	$t_{max}(SF)$	Lag time, $t_{max}(SF)$- $t_{max}(T)$ (hr.)
1-Oct	11:00	19:00	8.0
1-Nov	10:30	16:30	6.0
1-Dec	10:00	12:30	2.5
1-Jan	9:00	14:30	5.5
1-Feb	9:30	13:30	4.0
1-Mar	9:30	14:00	4.5
1-Apr	9:30	10:00	0.5
1-May	9:30	13:00	3.5
1-Jun	9:30	18:30	9.0
1-Jul	9:00	18:30	9.5
1-Aug	9:00	18:00	9.0
1-Sep	9:30	18:00	8.5

To understand the drought-induced changes, we focused on the dynamics of leaf gas exchange and water use along a 24-hr period in the dry season. In our site, diurnal cycles of photosynthetic active radiation (PAR), air temperature, relative humidity, and VPD change little during summer, and hence a 24-hr period is representative. Net carbon assimilation (A) occurred in the light hours but was not synchronized with PAR (Fig. 1.3a), probably due to the development of high vapor pressure deficit around midday (VPD>3 kPa; Fig. 1.3b). In turn, the increased VPD reduced stomatal conductance (g_s) from ~0.05 µmol m^{-2} s^{-1} at 7:45 to below 0.01 µmol m^{-2} s^{-1} at 12:15 (Fig. 1.3b). In the afternoon, around 16:00, VPD decreased below 3 kPa and g_s increased to ~0.02 µmol m^{-2} s^{-1}, which was less than the morning peak, presumably due to sunset (PAR=50 µmol m^{-2} s^{-1} by 17:45). As a result, the diurnal curve of A showed a morning peak (3 µmol m^{-2} s^{-1}) followed by a midday depression and a smaller afternoon peak (1 µmol m^{-2} s^{-1}, Fig. 1.3a). The observed diurnal changes in T reflected, in contrast, the combined effects of g_s and VPD, where $T = g_s \times VPD$. Therefore T peaked at 0.73 mmol m^{-2} s^{-1} at 9:15 and declined to 0.15 mmol m^{-2} s^{-1} at 13:45 (Fig. 1.3c). Between 14:00 and 18:30 T stabilized at around 0.25 mmol m^{-2} s^{-1},

reflecting an inverse relationship between g_s and VPD. Comparing the dynamics in T and SF (Fig. 1.3c) indicated that: (1) T had large fluctuations while changes in SF were more gradual, and (2) T ceased at night whereas SF continued long after darkness (after 19:15, Fig 1.3a). Seasonal changes were observed in the T and SF dynamics, between winter and summer (Fig. 2b and Fig. 1.3c, respectively). The increase in T from 6:00 to 9:00 occurred in both seasons, but SF supply of water for T was substantially reduced in summer. The delayed refilling by SF (see Fig. 1.3c for June) meant that large (3-5 kg) water deficits developed in the xylem and needle tissues during the day (Fig. 1.3d), but the water mass balance between the leaves and the xylem was maintained on a diurnal time-scale (Fig. 1.3d), i.e. tree water content did not decline during the season. Integrating the summer diurnal water use of an average tree in Yatir forest yields a value of 15 kg. This implies that, in a summer day, 20-33% of this amount came from water storage.

Xylem cavitation (PLC) and transient decreases in needle relative water content (nRWC, from 77 to 63%, data not shown) occurred simultaneously with high g_s (compare Fig. 1.1 and Fig. 1.3b), while cavitation reversal, and nRWC (not shown) correlated with low g_s, which may indicate that refilling was dependent on reduced rates of water loss and increasing, but not recovered, nRWC.

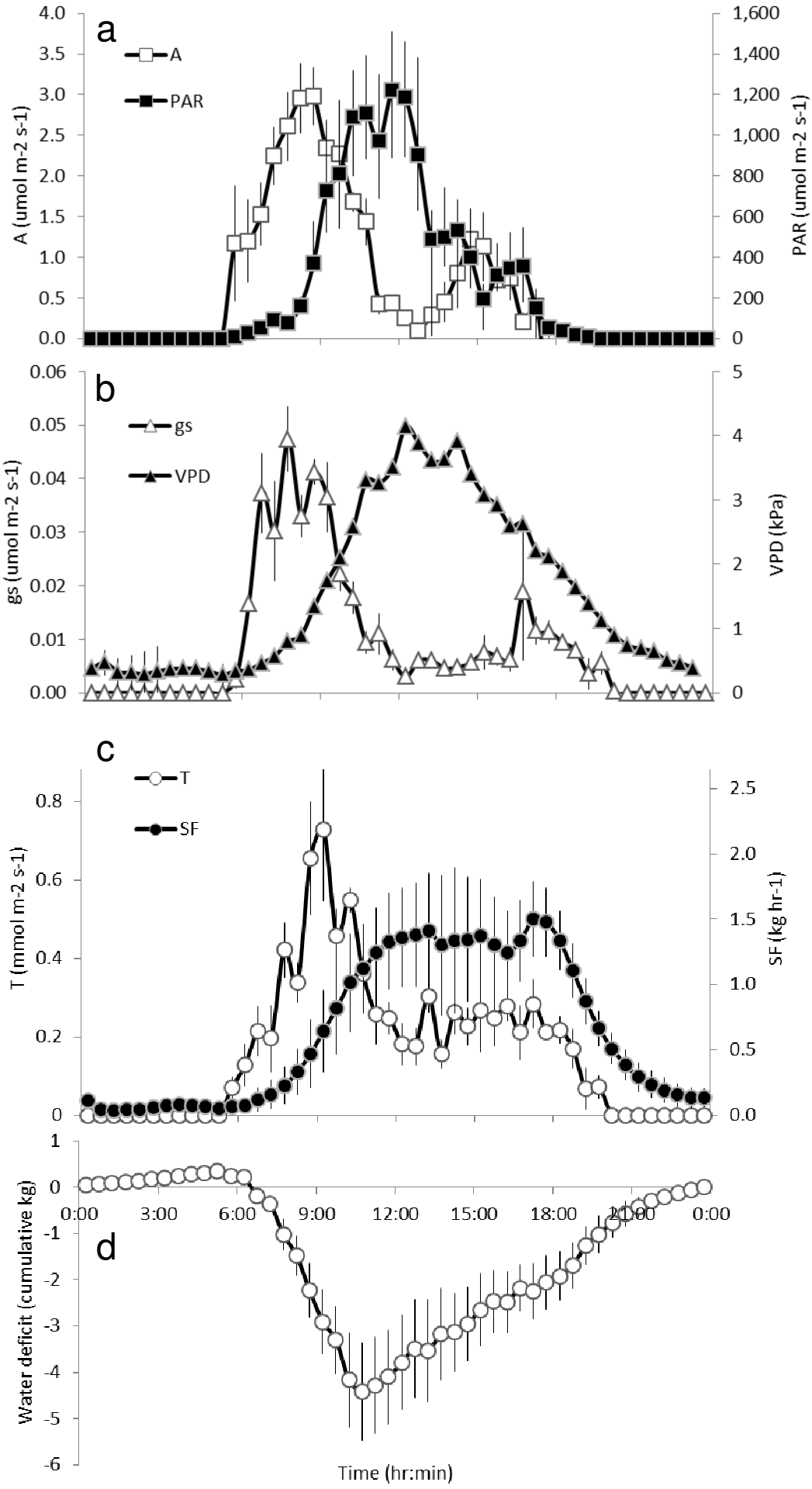

Fig. 1.3. Diurnal changes in net assimilation (A), photosynthetically active radiation (PAR) (a), stomatal conductance (g_s) , vapor pressure deficit (VPD) (b), leaf transpiration (T), sap flow (SF) (c), and cumulative water deficit (d)) in *Pinus halepensis* on 16-Jun-2011 in Yatir forest. *Error bars* represent the standard error of the mean (n = 5), not observed when smaller than symbols.

5.1.2. Comparison with previous reports of cavitation and refilling

We detected high cavitation levels (PLC of 40%) in the xylem of *Pinus halepensis* under drought, which were reversed on an hours' time scale (Fig. 1.1). Zwieniecki and Holbrook (1998) showed, in three forest tree species, about 50% recovery of cavitation overnight, but the actual time of xylem refilling was not measured and was potentially shorter. Higher resolution measurements in grapevine stems revealed a diurnal cycle of cavitation and recovery, with a 3-5-hr refilling time (Brodersen et al. 2010, Zufferey et al. 2011, respectively). Shorter refilling times (~2 hr) were reported for poplar (*Populus trichocarpa*) stems under induced embolism in the lab (Secchi and Zwieniecki 2011). But our observations of two consecutive sub-diurnal cycles of cavitation and refilling are, to the best of our knowledge, the most rapid cavitation/refilling cycles reported for trees. The kinetics of xylem refilling depends on the volume of the embolized lumen, and hence on species-specific traits like conduit diameter (Brodersen et al. 2010). With its narrow tracheids (9.4 μm; Oliveras et al. 2003), *P. halepensis* makes a good candidate for rapid refilling. The water storage capacity, contributing 20-33% of daily T, is much higher than the 2-10% reported for yellow poplar (McLaughlin et al. 2003) and within the range of 10-75% reported for potted, young Norway spruce (Zweifel et al. 2001). This also agrees with the hypothesis that isohydric, low wood density species like *P. halepensis* should have relatively high capacity to store water (Meinzer et al. 2009).

In this forest ecosystem, leaf transpiration and xylem sap flow are never quantitatively synchronized, and even at the time of peak activity, when sap fluxes surpassed 7 kg hr^{-1} (April) there was still a 30 min lag of SF behind transpiration (Table 1.1). Such short lags are expected due to changes in tree capacitance or water content as Ψ_l decreases during the morning (e.g. from -1.3 MPa at 6:30 to -1.7 MPa at 9:30 in March, data not shown). However during the summer drought these capacitance changes are augmented by the release of water from cavitated xylem. The interaction of leaf conductance with water potential can involve long response times, sometimes producing sustained stomatal cycling with an average period of approximately 70 min (Dzikiti et al. 2007). On average, diurnal peaks of T and SF (the latter peak not as distinctive) were 5.9 hr apart, compared to 0.5-3 hr reported in other studies (Zweifel et al. 2001, Meinzer et al. 2003, Fisher et al. 2007). As in the case of the refilling rate, these are exceptionally long delays, which might be expected in this case of extreme drought. The lag time was inversely related to the water flux,

peaking at 9.5 hr in the height of summer (July, Table 1.1), when peak sap fluxes never exceeded 1 kg hr^{-1}. This could partly be explained by a higher contribution of sinker roots to the tree water use in summer, thereby increasing the mean water transport path (Klein et al. 2012). The inverse relationship is in agreement with measurements in young spruce (Zweifel et al. 2001), where the lag increased from 30 min on high-flux, sunny days to 110 min on low-flux, cloudy days. Brodersen et al. (2010) showed in grapevine that refilling delays are related to water deficits, where cavitated vessels could not refill until additional water was introduced. Here we show that SF is often delayed into the night (Fig.1. 2), and consequently up to 70% of the total diurnal SF occurs after dark. This high nocturnal SF proportion, which occurs when nighttime leaf transpiration is negligible, is much larger than the values of up to 35% observed in a California oak species, *Quercus douglasii* (Fisher et al. 2007), and up to 25% in other trees (Dawson et al. 2007).

5.1.3. Stomata, VPD, leaf water potential and cavitation

For a first approximation, we validate our observations of cavitation and refilling cycles, semi-quantitatively, based on the simple, basic, flux equations for transpiration and sap flow:

(16) $T = g_s \times VPD$

(17) $SF = K \times \Delta\Psi_{soil\text{-}leaf}$

where K is the hydraulic conductivity. Under winter conditions Ψ_l = -1.5 MPa (Table 1.2), T greatly exceeds the tree capacitance, and T and SF are continuous and nearly temporally coupled (T = SF at the same point in time). In summer, the soil water potential, Ψ_s, decreases from the winter value of -0.1 MPa to -0.9 MPa (Table 1.2; Klein et al. 2012) thereby reducing $\Delta\Psi_{soil\text{-}leaf}$ from 1.4 to 0.6 MPa and, using Eq. (17), decreasing the driving force for SF. Together with the observed decrease in K, from 3.0 to 0.5 kg hr^{-1} MPa^{-1}, SF decreases from 4.5 kg hr^{-1} in winter to 1.3 kg hr^{-1} at 11:30 on a summer day (Table 1.2).

During the summer day morning, conditions change rapidly. VPD increases from 0.4 kPa at 6:30 to 1.9 kPa at 9:30 (Table 1.2). This seems to trigger two parallel processes with contrasting consequences: (1) the leaf water potential, Ψ_l, decreases from -1.5 to -3.0 MPa, approaching the *P. halepensis* threshold of Ψ_{PLC50}, -3.1 MPa, which results in xylem cavitation (30%, Table 1.2); and (2) the VPD increase, while little change is observed in g_s (0.03 µmol m^{-2} s^{-1}, Table 1.2), translates into T increase

(Eq. 16), from 0.13 mmol m^{-2} s^{-1} at 6:30 to 0.58 mmol m^{-2} s^{-1} at 9:30. Evidently, while process (1) decreases the tree hydraulic conductance, process (2) increases the tree hydraulic demand. The increased transpiration rate cavitates part of the xylem and decreases K from 0.50 to 0.35 kg hr^{-1} MPa^{-1} (Table 1.2). This further decouples SF from T, increases the water deficit (~3 kg $tree^{-1}$ by 9:30) and decreases the needle relative water content (from 77 to 63% in our case). Stomatal closure follows, reducing g_s from 0.030 µmol m^{-2} s^{-1} at 9:30 to 0.007 µmol m^{-2} s^{-1} at 11:30 (Table 1.2). This more than compensates for the VPD increase (from 1.9 to 3.4 kPa), and hence T decreases from 0.58 mmol m^{-2} s^{-1} at 9:30 to 0.25 mmol m^{-2} s^{-1} at 11:30 (Eq. 16). This decrease in the transpiration allows SF to refill the cavitated xylem even though Ψ_l is still low: SF increases from 0.7 to 1.3 kg hr^{-1} and by 11:30 cavitation is completely reversed (Table 1.2).

Table 1.2. Summary of changes in vapor pressure deficit (VPD), leaf water potential (Ψ_l), soil water potential (Ψ_s), stomatal conductance (g_s), hydraulic conductivity (K), percent loss of conductivity (PLC), leaf transpiration (T), and sap flow (SF) in *Pinus halepensis* in Yatir forest. Observed T and SF rates are compared with values calculated using Eq. (16) and Eq. (17), respectively.

Time	**Winter**	**Summer**		
	11:30	**6:30**	**9:30**	**11:30**
Observed Values				
VPD (kPa)	1.5	0.4	1.9	3.4
Ψ_l (MPa)	-1.5	-1.5	-3.0	-3.0
Ψ_s (MPa)	-0.1	-0.9	-0.9	-0.9
g_s (µmol m^{-2} s^{-1})	0.18	0.030	0.030	0.007
K (kg hr^{-1} MPa^{-1})	3.00	0.50	0.35	0.55
PLC (%)	0	7	30	0
T (mmol m^{-2} s^{-1})	3.15	0.13	0.58	0.25
SF (kg hr^{-1})	4.50	0.10	0.73	1.30
Calculated values				
$T=g_s \times VPD$ (mmol m^{-2} s^{-1})	2.70	0.12	0.57	0.24
$SF=K \times \Delta\Psi_{s\text{-}l}$ (kg hr^{-1})	4.20	0.30	0.73	1.16

The decrease in g_s in mid-morning and its subsequent increase in the afternoon seem to correspond to similar trends in VPD and inverse trends in water deficit. High VPD may serve as a signal for stomatal closure, thereby facilitating recovery from cavitation. In May, maximum daily VPD in Yatir forest is usually below 3.0 kPa (Maseyk et al. 2008) and hence the midday depression in g_s is restricted to 10:30-13:30, compared to 10:00-16:00 in June (Fig. 1.3b). This can explain the shorter cavitation/refilling cycles observed in May than in June (Fig. 1.1). While some studies claim that stomatal activity protects the xylem (Cruiziat et al. 2002, Brodribb and Holbrook 2004, Yang 2012), others propose that the xylem imposes a limit on g_s (Resco et al. 2009, Brodribb and Cochard 2009, Zufferey et al. 2011). Nardini and Salleo (2000) concluded that in very dry conditions some cavitation cannot be avoided, because it acts as a signal regulating g_s. This is consistent with the observation that stomatal responses both at 9:15 and 17:15 (Fig. 1.3b) coincided with a cavitation level of ~30% (Fig. 1.1) and indicates a possible threshold for stomatal response (e.g. Jarvis, 1976), with the value for initiation of closure corresponding to a water deficit of ~2.5 kg tree^{-1}. Based on these observations, we speculate that leaf conductance response is partly decoupled from changes in PLC, such that moderate levels of cavitation and refilling of xylem in our extremely dry conditions can be routine during daytime. This is surprising, since even if no air enters the cavitated xylem and it remains at vacuum pressure (i.e. -0.1 MPa) its pressure is much higher than that of leaves and therefore refilling requires an active, and in our case, rapid process. In *P. halepensis* (and other Mediterranean trees) roots are more vulnerable to cavitation than shoots (Oliveras et al. 2003, Froux et al. 2005). Thus, it is fair to assume that cavitation in the roots in our case is even more extensive than in the branches. Hydraulic changes (water deficit status) and atmospheric changes (VPD) are interconnected in the cavitation/refilling cycles. It is however not possible at this stage to determine the hierarchy or dominance between these signals (or others) in influencing g_s. Nevertheless, the data show that all of these processes are not dominating cavitation patterns that develop independently, as a result of the imbalance between T and SF.

We speculate that the refilling mechanism required to recover from cavitation follows the same cellular processes as demonstrated in grapevine (Holbrook and Zwieniecki 1999, Brodersen et al. 2010). That process requires live parenchyma cells adjacent to the cavitated conduits, and we assume that those cells exist in the full

cross section of our branch sections due to their young age (13±1 years, see Methods). The alternative mechanism proposed by Schenk and Espino (2011, see Introduction) might not work in this case, where nighttime transpiration is essentially zero (Fig. 1.3c). We also note that we did not observe any indication of 'cavitation fatigue' due to frequent cavitation and refilling cycles (Hacke et al. 2001, Sperry 2003). Taneda and Sperry (2008) reported repeated overnight xylem refilling throughout most of the summer in an oak species, similarly to our observations.

The combination of stomatal opening at the threshold of developing cavitation, which allows some photosynthetic gas exchange, together with rapid refilling when stomata do close, helps explain the sustained tree activity throughout the summer drought in the semi-arid Yatir forest. We suggest that the observed rapid (1-2 hr) recovery from cavitation (Fig. 1.1) can be essential to the survival of a tree species with high xylem vulnerability to embolism (Ψ_{PLC50} = -3.1 MPa), especially considering its narrow hydraulic safety margin, between stomatal closure and cavitation, of just 0.3 MPa (Klein et al. 2011). Moreover, summer carbon demand in *P. halepensis* is enhanced by fresh needle growth throughout the dry season (Klein et al. 2005, Maseyk et al. 2008).

Further research is clearly needed to focus on the different aspects of the cavitation/refilling cycle process. In addition, better tools are needed to measure cavitation in the field, which would facilitate more frequent sampling which could give insight into the different environmental and physiological factors involved in the curious phenomenon of cavitation/refilling cycles in daytime observed here.

On a more historic perspective, we show that *Pinus halepensis* trees in arid summer conditions do operate at the point of xylem dysfunction, as hypothesized by Tyree and Sperry (1988), but a highly efficient refilling mechanism seems to make such operation sustainable even in the long dry season, without serious consequences.

5.2. The role of trait plasticity in sustaining growth and survival of *Pinus halepensis* under climate change in the Mediterranean.

In order to identify the role of key traits (hydraulic, physiological and phenological) and quantify their relative contribution to sustained growth and survival of *Pinus halepensis* under climate change, five provenances were tested in three experimental forest plots in sites representing mesic to warm and very dry conditions. The results of this study are described in Klein et al. (2012a, see below). The study design, data collection and analysis, and interpretation of results are my own.

Tree Physiology 00, 1–11
doi:10.1093/treephys/tps116

Research paper

Differential ecophysiological response of a major Mediterranean pine species across a climatic gradient

Q1 Tamir Klein[1], Giovanni Di Matteo[2], Eyal Rotenberg[1], Shabtai Cohen[3] and Dan Yakir[1,4]

[1]Department of Environmental Sciences and Energy Research, Weizmann Institute of Science, Rehovot 76100, Israel; [2]CRA-PLF Research Unit for Intensive Wood Production, Agricultural Research Council, Rome, Italy; [3]Institute of Soil, Water and Environmental Sciences, Volcani Center ARO, Beit Dagan, Israel; [4]Corresponding author (dan.yakir@weizmann.ac.il)

Received August 12, 2012; accepted October 21, 2012; handling Editor: João Pereira

The rate of migration and in situ genetic variation in forest trees may not be sufficient to compete with the current rapid rate of climate change. Ecophysiological adjustments of key traits, however, could complement these processes and allow sustained survival and growth across a wide range of climatic conditions. This was tested in *Pinus halepensis* Miller by examining seven physiological and phenological parameters in five provenances growing in three common garden plots along a climatic transect from meso-Mediterranean (MM) to thermo-Mediterranean (TM) and semi-arid (SA) climates. Differential responses to variations in ambient climatic conditions were observed in three key traits: (i) growing season length decreased with drying in all provenances examined (from 165 under TM climate to 100 days under SA climate, on average); (ii) water use efficiency (WUE) increased with drying, but to a different extent in different provenances, and on average from 80, to 95, to 110 μmol CO_2 mol^{-1} H_2O under MM, TM and SA climates, respectively; (iii) xylem native embolism was stable across climates, but varied markedly among different provenances (percent loss of conductivity, was below 5% in two provenances and above 35% in others). The results indicated that changes in growing season length and WUE were important contributors to tree growth across climates, whereas xylem native embolism negatively correlated with tree survival. The results indicated that irrespective of slow processes (e.g., migration, genetic adaptation), the capacity for ecophysiological adjustments combined with existing variations among provenances could help sustain *P. halepensis*, a major Mediterranean tree species, under relatively extreme warming and drying climatic trends.

Keywords: climate change, embolism, growth phenology, provenances, water use efficiency.

Introduction

Plants are sessile and hence cannot migrate during their ontogeny when local conditions become unfavorable for their growth or survival. This selected for a remarkable ability of plants to acclimate to a changing environment through physiological, molecular and genetic responses (Reyer et al. 2012, Shaw and Etterson 2012). Trees in particular are sensitive to climate change due to their longevity, extending over time-spans from decades to centuries. For example, extreme, rare climate events (e.g., a drought year once a decade) inevitably influence tree communities more than annuals and geophytes that can, for example, avoid germination under such events. Consistent, directional climate change taking place today on a global scale highlights the importance of tree acclimation (Allen et al. 2009).

Climate predictions indicate drying trends associated with reduced precipitation in the Mediterranean and other regions (Alpert et al. 2006, Burke et al. 2006, Christensen et al. 2007). Observed increases in global drought severity since 1952 and

in evaporative demand in Israel since 1964 are expected to intensify during the 21st century (Cohen et al. 2002, Burke et al. 2006). Evidence for the impact of warming and drying on Mediterranean forests is already accumulating at an alarming pace and in 2008 alone at least five examples of distinct drought-induced forest stand dieback and decline events were observed. This includes *Abies cephalonica* forests in Greece (Raftoyannis et al. 2008); *Cedrus atlantica* in Algeria and Morroco; *Quercus*, *Pinus* and *Juniper* spp. in Turkey; and *Quercus suber* in France (Allen et al. 2009 and references therein). Impacts on Mediterranean *Pinus* spp. following the drought years of 1999–2000 are evident in Israel as well as in Greece (Koerner et al. 2005, Sarris et al. 2007) and Spain (Penuelas et al. 2001, Martinez-Vilalta and Pinol 2002). Additional implications of climate change on tree growth include reduced ability of forests to sequester carbon (Ciais et al. 2005) as well as shifting the timing of the growing season (Chmielewski and Rotzer 2001).

Common garden testing of tree populations of different origin, known as provenance trials, is a powerful tool for testing hypotheses of adaptation to climate in trees (Langlet 1971, Matyas 1996). Traditionally, provenance trials served in identifying provenances carrying the most desired phenotypes at the test location, and sometimes also as a basis for delineating seed planting and breeding zones (Raymond and Lindgren 1990). Intraspecific differences in physiological and hydraulic traits were studied in *Pinus sylvestris* (Martínez-Vilalta et al. 2009) and *Pinus pinaster* (Lamy et al. 2011). The 1975 UN FAO provenance trial program on Mediterranean conifers (www.fao.org/docrep/006/k1203e/K1203E08.htm) has a major section on Aleppo pine (*Pinus halepensis* Miller), a key forest tree across the Mediterranean region. Its distribution spans three climate types: meso-Mediterranean (MM) (Cfb, Koppen–Geiger climate classification), thermo-Mediterranean (TM) (Csa) and semi-arid (SA) (Bwh). The ability of *P. halepensis* to survive and grow in various environments indicates that it is a highly tolerant species. Field performance data of *P. halepensis* provenances collected routinely in numerous sites are being used in the selection of successful provenances for each location (Eccher et al. 1987, Fusaro et al. 2007). Ecophysiological parameters underlying *P. halepensis* provenance-level response to changes in environmental conditions were identified in seedlings (Tognetti et al. 1997, Calamassi et al. 2001, Baquedano et al. 2008), and also in field-grown trees (Schiller and Atzmon 2009). However, studies on the association between climate and adjustments in physiological traits are still scarce, and hence it is still not possible to predict provenance performance under varying climate conditions (Atzmon et al. 2004).

In this study we hypothesized that (i) ecophysiological traits should vary, both with climate and provenance; (ii) interactions of climate with provenance are expected and should result in differences in climate response thresholds and (iii) growth strategies rely on specific combinations of traits. To test these hypotheses we used five provenances originating from different environments, growing in three experimental forest plots in sites representing mesic to warm and very dry conditions. Seven eco-physiological parameters were selected to represent tree physiology (carbon assimilation rate, stomatal conductance and intrinsic water use efficiency) hydraulics (xylem conductivity and native embolism) phenology (trunk growing season length (GSL)) and integrated photosynthetic potential (leaf chlorophyll concentration). These parameters were identified as keys to *P. halepensis* functioning in previous studies (Klein et al. 2005, Maseyk et al. 2008, Klein et al. 2011). Observations were made along 2 years with focus on April–June, when plant physiological activities were intermediate between winter maxima and summer minima. Finally, we tested whether our findings could explain published data about the survival of provenances of this species under more extreme, arid conditions.

Materials and methods

Plant material and site descriptions

The study included five provenances of Aleppo pine (*Pinus halepensis* Miller) grown from seeds collected from mature trees in natural stands of each provenance and sown in three sites of the UN FAO seed collection provenance program (SCM/CRFM/4 bis project, http://www.fao.org/docrep/006/k1203e/K1203E08.htm; see database in: http://147.100.66.194/ForSilvaMed). Out of 32 provenances 5 were selected to allow in-depth study while maintaining sufficient representation of the variety of habitats in which *P. halepensis* grows. Seed sources included contrasting sites from different areas around the Mediterranean (Figure 1) starting with mean annual precipitation (*P*) of 830 mm in Otricoli, Italy, to 310 mm in Senalba, Algeria (Table 1). All five provenances were represented by 10–12 actively growing trees in each of three experimental plots in three different climates: MM (in Castel Di Guido, Rome), TM (in Beit Dagan) and SA (in Yatir), see a summary of climate characteristics for the sites in Table 1.

The Castel Di Guido farm is located in the coastal plains 15 km west of Rome, Italy, 10 km east of the Tyrrhenian Sea shore, and its soil is mostly clay. The experimental plot was planted in 1975 in a randomized block design, with 9–25 replicates × 6–9 blocks at 3 × 3 m spacing. The Beit Dagan ARO Volcani Center farm is located in the coastal plains, 20 km south-east of Tel-Aviv, Israel, 20 km east of the Mediterranean Sea shore, and its soil is deep sandy to sandy-loam. The 1-ha experimental plot was planted in 1991 with 11 provenances in parallel rows with 12 replicates × 1 block at 2 × 4 m spacing. Yatir forest is a *P. halepensis*-dominated planted forest located at the northern edge of the Negev desert, Israel and covering

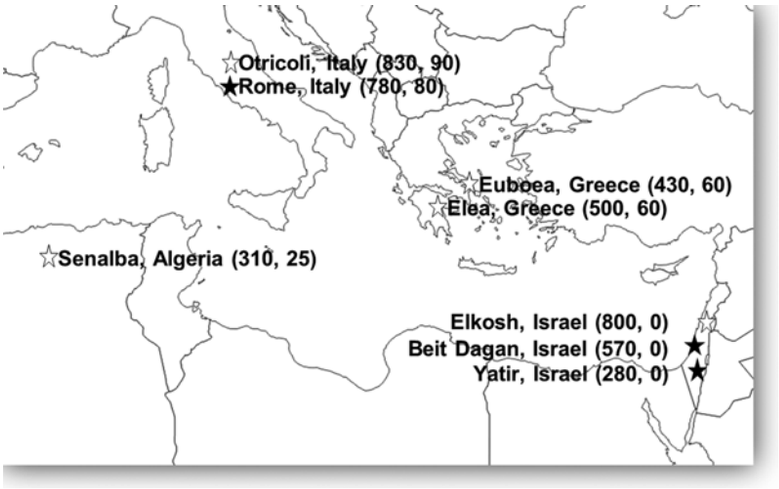

Figure 1. Geographic locations of the five *Pinus halepensis* provenances (open star symbols; Table 1) and the three experimental forest plots (closed star symbols; Table 1) included in this study and their mean annual and summer precipitation, respectively. Note that, in spite of proximity between the Beit Dagan and Yatir sites, climate types differ due to a sharp precipitation gradient.

Table 1. Summary of main geographical and climatic characteristics at the five provenances (North to South) from which seeds were collected and trees were included in this study and three experimental forest plots included in this study.

Provenance (FAO code) or site	Latitude	Longitude	*P* (mm)	PET (mm)	Aridity index (*P*/PET)	P_s (mm)
Otricoli, Italy (A 26)	42°24′N	12°38′E	830	~900	0.92	90
Euboea, Greece (A3)	38°58′N	23°18′E	430	~1250	0.34	60
Elea, Greece (A2)	37°46′N	21°32′E	500	~1350	0.37	60
Senalba, Algeria (A 30)	34°45′N	03°25′E	310	~1250	0.25	25
Elkosh, Israel (A7)	33°01′N	35°18′E	800	~1300	0.59	0
Rome, Italy	41°54′N	12°30′E	780	~1000	0.78	80
Beit Dagan, Israel	31°59′N	34°48′E	570	~1300	0.44	0
Yatir, Israel	31°20′N	35°04′E	280	~1600	0.18	0

P, mean annual precipitation; PET, mean annual potential evapo-transpiration; P_s, mean summer (May–September) precipitation. Data from: (i) FAO Forest Genetic Resources No. 5. Mediterranean Conifers, Table 1; (ii) Palutikof et al. (1994); (iii) Mejstrik and Cudlin (1983); (iv) Meteorological measurements carried out by the authors in Rome and Yatir; (v) Klein Tank et al. (2002) (data and metadata available at http://eca.knmi.nl); (vi) Cohen et al. (2002).

an area of 2800 ha on predominantly light brown Rendzina, 25–100 cm deep. The Yatir experimental plot was planted in 1989–90 with 17 provenances in parallel rows with 12 replicates × 4 blocks with 4 × 4 m spacing. Previous reports about the performance of *P. halepensis* provenances in Yatir (Atzmon et al. 2004, Schiller and Atzmon 2009) refer to another experimental provenance plot, where micro-climatic conditions are drier than in the plot reported here. None of the plots were thinned, and with the exception of several tree mortalities, plot densities were kept as planted. To account for differences in trees' age among plots, field performance was measured in trees of similar age, but in different years. To avoid edge effects, sampling excluded trees growing in the margins of plots.

Field performance and growth phenology

Periodic measurements of tree height and diameter at breast height (DBH, 1.3 m) were performed every 1–3 years from the time of planting on 10 trees of each provenance and site. Height was measured using a PM-5 clinometer (Suunto, Sylvan Lake, MI, USA) and DBH was estimated from tree circumference. Since planting density differed among sites, individual measurements of DBH were normalized by the standard stand density of 1343 trees ha^{-1} (3 × 3 m spacing). Dendrometers were prepared using stem circumference increment tape (EMS, Brno, Czech Republic) fitted with custom-made 50 mm steel tension coil springs (Hakfitz, Ramat Gan, Israel). During December 2008 dendrometers were installed on five trees of each provenance growing in Beit Dagan and Yatir. Trunk circumference increment was measured once in 2 weeks using a digital caliper (indication error 0.03 mm; Fuji, Japan). Observed growth rate in mm $month^{-1}$ was calculated from consecutive measurements divided by the time in between individual measurements. In order to estimate trunk GSL, increments in circumference were expressed as percent of the annual total for each individual tree, and GSL was defined as the sum (in days) of all 2-week periods where increment was ≥5% of the total annual increment.

Tree-ring $\delta^{13}C$

Tree cores were sampled between December 2008 and December 2009 using a 200 mm increment borer (core diameter 5.15 mm) equipped with starter (Haglof, Sweden). From each tree, two trunk cores were collected, at breast height at 0° (N) and 180° (S). The sampling design was 3 sites × 5 provenances × 8–10 trees × 2 sides = 270. Tree-rings of the growth years 1997–2000 were identified, cut into 7–12 equal intra-annual sub-sections and their $\delta^{13}C$ values were analyzed as described in Klein et al. (2005). To minimize analysis time and resources, isotopic analysis was performed on whole wood samples rather than cellulose, which is generally coherent (McCarroll and Loader 2004 and references therein). The $\delta^{13}C$ results were used to calculate the discrimination of the tree against ^{13}C (Δ) expressed in delta notation as parts per thousand (‰) deviations from the international carbon isotope standard (Coplen 1994):

$$\Delta = \frac{(\delta^{13}C_a - \delta^{13}C_t)}{(1 + \delta^{13}C_t)} \quad (1)$$

where $\delta^{13}C = (\delta^{13}C/\delta^{12}C)_{sample}/(\delta^{13}C/\delta^{12}C)_{reference} - 1$ and the reference is PDB carbonate, and subscripts a and t stand for atmospheric air and the tree-ring material, respectively. *Pinus halepensis* is a drought-avoiding species and therefore the deposition of carbon into tree-rings is typically restricted to October–May (Klein et al. 2005). This means that the annual $\delta^{13}C$ maxima occurred in March–May, when soil and atmospheric humidity were declining while still permitting leaf gas exchange. Δ values were calculated from annual $\delta^{13}C$ maxima values of trees from each provenance and climate and were further used in the derivation of the tree's intrinsic water use efficiency (WUE_i) using the following equation (adapted from Farquhar et al. 1982, Seibt et al. 2008):

$$WUE_i = \frac{C_a}{r\{[b - \Delta - f(\Gamma^*/C_a)] / [b - a + (b - a_m)(g_s / g_i r)]\}} \quad (2)$$

where C_a is the atmospheric CO_2 concentration in ppm (an annual global average; Robertson et al. 2001); r is the ratio of the diffusivities of CO_2 and water in air (1.6); a, a_m, b and f are the leaf-level discriminations against ^{13}C in the diffusion through the stomata (4.4‰), during dissolution and liquid phase diffusion (1.8‰), during biochemical CO_2 fixation (29‰) and in photo-respiratory CO_2 release (8‰), respectively; Γ^* is the temperature-dependent CO_2 compensation point of ca. 30–45 ppm (Maseyk et al. 2008); g_s/g_i is the ratio between stomatal and internal conductances to CO_2, respectively (0.5, according to Maseyk et al. 2011).

Leaf gas exchange

During March and May of 2009 and 2010, leaf stomatal conductance (g_s, in mol H_2O m^{-2} s^{-1}) and net carbon assimilation (A, in µmol CO_2 m^{-2} s^{-1}) were measured on three trees per provenance in the Yatir and Beit Dagan plots. On each field day, this was repeated 2–3 times from 9:00 to 15:00 on sunlit needles using an LI-6400 Photosynthesis System (Licor Inc., Lincoln, NE, USA) equipped with an LED lamp set on 1000 µmol m^{-2} s^{-1} PAR. These measurements were used in the calculation of intrinsic water use efficiency (WUE_i, in µmol CO_2 mol^{-1} H_2O) according to the equation:

$$WUE_i = \frac{A}{g_s} \quad (3)$$

Xylem hydraulic conductivity

Hydraulic conductivity was measured under low pressure (0.02 MPa) generated by a 2 m pressure head before and after perfusing the xylem tissue at a high pressure of 0.5 MPa. Light-exposed twig sections (30 cm long, 5 mm diameter) with 3–5 needle cohorts were cut in the field from the lower branches. From each provenance we sampled three twigs from three individual trees during morning hours (8:30–9:30) on 23 May at Yatir and on 8 June at Beit Dagan. Resin secretion from the cuts was eliminated by immediately placing both ends of the twig section (5 cm from cut tips) in a water bath at 95°C for 10 min (adapted from Waring and Silvester 1994) while still in the field. Measurements that we made in branches of *Olea europea* showed that K_s was not affected by this heat treatment. Next, the specific hydraulic conductivity K_s and maximum specific conductivity $K_{s\,max}$ (kg m^{-1} MPa^{-1} s^{-1}) were determined as described by Klein et al. (2011). Measurements of K_s and $K_{s\,max}$ were further used to identify loss of conductivity that can be attributed to xylem cavitation according to Eq. (4) (Tognetti et al. 1997):

$$PLC = 100\frac{(K_{s\,max} - K_s)}{K_{s\,max}} \quad (4)$$

where PLC is the percent loss of conductivity (%) due to cavitation.

Leaf chlorophyll concentration

During May 2009 and April 2010, healthy 1-year-old needles were collected in three replications from three trees per provenance in Yatir and Beit Dagan. Needles (50 mg leaf tissue per sample) were cut into 5 mm segments and immersed in 1 ml 80% aqueous acetone solution together with two bearing balls (diameter = 3 mm). Leaf specimens were ground using a ball mill (Retsch, Hann, Germany) at a frequency of 25 s^{-1} until full extraction was achieved (~5 min), followed by centrifugation at 14,000 rpm for 10 min. The supernatant of each specimen was transferred into a micro-well in a 96-well plate, where its

absorbance was measured at 663.6 and 646.6 nm using a tunable micro-plate reader (Molecular Devices, Sunnyvale, CA, USA). Concentrations of chlorophylls *a* and *b* were determined following subtraction of the absorbance of a blank sample (containing solution but not leaf sample) according to Porra et al. (1989). Results were expressed on a dry weight basis following the drying of remaining needles in the sample at 60°C for 48 h.

Statistical analysis

Data were analyzed by analysis of variance (ANOVA) using JMP software (Cary, NC, USA). Measurements of individual trees were used as observations, where climate type (three levels, nominal variable), provenance (five levels, nominal variable) and their interaction were defined as factors (Table 2). The relatively high number of combinations (3 × 5) together with resource limitations meant a limited sample size ($n = 3–10$). Differences between responses were considered significant when type 3 sum of squares met the *F*-test criterion at probability <0.05. In addition to the ANOVA, the effect of climate in individual provenances and the effect of provenance in the three climate types were also analyzed (Table 2). Means were compared using Tukey's HSD test, reported as letters indicating significant differences in Figures 2, 3 and 5. To test the relationship between variance in field performance (increment growth) and variance in physiological traits, data were analyzed by partial least-square regression (PLS) and the relative percent of variation in performance explained by each of the six parameters is reported in Table 2.

Results

Field performance and tree physiology

At 19 years after planting at each site, average normalized DBH was 24.1, 21.3 and 10.5 cm in the Rome, Beit Dagan and Yatir sites, respectively (Figure 2a). Trees growing in Rome reached a mean height of 12.2–15.9 m compared to 8.6–12.0 m at Beit Dagan and Yatir (data not shown), consistent with the precipitation gradient (Table 1), and especially in the Greek provenances Elea and Euboea. The reduction in annual stand-level basal area increment (BAI; $m^2\ ha^{-1}\ year^{-1}$) as a function of 100 mm reduction in precipitation, $d(BAI)/d(P_{100})$, was estimated at 0.82, 0.81, 0.31, 0.29 and 0.17 for the provenances Elea, Euboea, Elkosh, Senalba and Otricoli, respectively. Correlation coefficients between BAI and precipitation (r^2, with * indicating significant at $\alpha = 0.05$) were 0.73*, 0.68*, 0.49*, 0.44* and 0.11, respectively.

To distinguish between provenance-level physiological responses to dry conditions we used the seasonal changes in carbon isotopic composition and specifically the $\delta^{13}C$ maxima in the annual tree-rings. Such maxima can be expected to reflect the lowest seasonal discrimination against ^{13}C, which is associated with assimilation under the drier part of the growing season. While in Rome $\delta^{13}C$ values ranged between –23 and –30‰, in Beit Dagan they were between –21 and –27‰ and in Yatir between –19 and –26‰, as expected along a drying gradient. The annual maximum $\delta^{13}C$ values were then used in estimating intrinsic water use efficiency (WUE_i; μmol CO_2 mol^{-1} H_2O) using Eq. (2) (Seibt et al. 2008). WUE_i was inversely related to precipitation, but with no significant differences among provenances, except for the Beit-Dagan site (Figure 2b; $P = 0.0161$, Table 2). Across provenances, the WUE_i increase per 100 mm decrease in *P*, $d(WUE_i)/d(P_{100})$, ranged between 2.7 and 4.1 (with r^2 ranging between 0.53 and 0.87, significant at the 0.05 level in all provenances).

Leaf gas exchange measurements were used in an attempt to distinguish between the effects of *A* or g_s on WUE_i (calculated from instantaneous gas exchange measurements using Eq. 3 and derived from tree-rings). Note, however, that because of the

Table 2. *P* values (probability > *F*, an effect is significant if $P < 0.05$) from ANOVA for (i) the effects of climate, provenance and their interaction (C × P) on main response parameters, (ii) the effect of climate in individual provenances and (iii) the effect of provenance in the three climate types. Results of PLS are reported as the relative percent of variation in field performance (DBH) explained by each of the six parameters.

Variable	DBH (cm)	WUE_i (μmol CO_2 mol^{-1} H_2O)	*A* (μmol m^{-2} s^{-1})	g_s (mol m^{-2} s^{-1})	Growing season length (days)	PLC (%)	Chlorophyll conc. (mg gDW^{-1})
Climate	**<0.001**	**<0.001**	**<0.001**	**<0.001**	**<0.001**	<0.1	<0.1
Provenance	**<0.001**	n.s.	**<0.05**	**<0.05**	**<0.001**	**<0.05**	**<0.001**
C × P	**<0.001**	**<0.05**	**<0.05**	n.s.	n.s.	n.s.	**<0.05**
Otricoli	**<0.001**	**<0.001**	**<0.05**	<0.1	**<0.05**	n.s.	n.s.
Euboea	**<0.001**	**<0.05**	n.s.	n.s.	**<0.05**	n.s.	n.s.
Elea	**<0.001**	**<0.05**	n.s.	<0.1	**<0.001**	n.s.	**<0.05**
Senalba	**<0.001**	**<0.001**	n.s.	<0.1	**<0.001**	n.s.	n.s.
Elkosh	**<0.001**	**<0.001**	n.s.	**<0.05**	n.s.	n.s.	n.s.
SA	n.s.	n.s.	n.s.	n.s.	<0.1	n.s.	**<0.001**
TM	n.s.	**<0.05**	**<0.05**	<0.1	**<0.001**	**<0.05**	**<0.05**
MM	**<0.001**	n.s.					
% variation explained		39.05	16.07	7.98	18.70	4.37	13.84

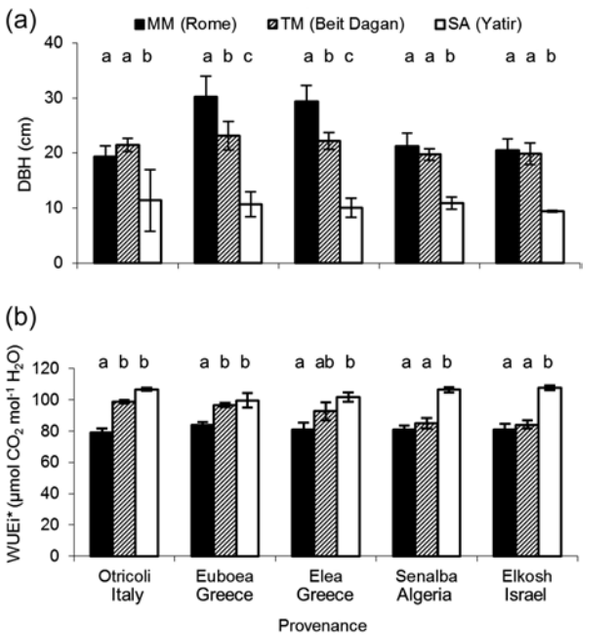

Figure 2. Mean DBH (a) and $\delta^{13}C$-derived WUE_i (b) of trees from each provenance and climate (SA, semi-arid; TM, thermo-Mediterranean; MM, meso-Mediterranean) 19 years after planting (2008–2009 in Yatir, 2010 in Beit Dagan and 1994 in Rome). WUE_i values were calculated from $\delta^{13}C$ measurements on tree-rings formed during years with precipitation within 0.5 SD of the multiannual average; 1997 in Yatir and Beit Dagan, 1999 in Rome. Similar letters indicate a non-significant difference ($\alpha > 0.05$) between trees of a provenance growing under different climate types. Error bars represent the standard error of the mean ($n = 8$–10 and 3–5, respectively).

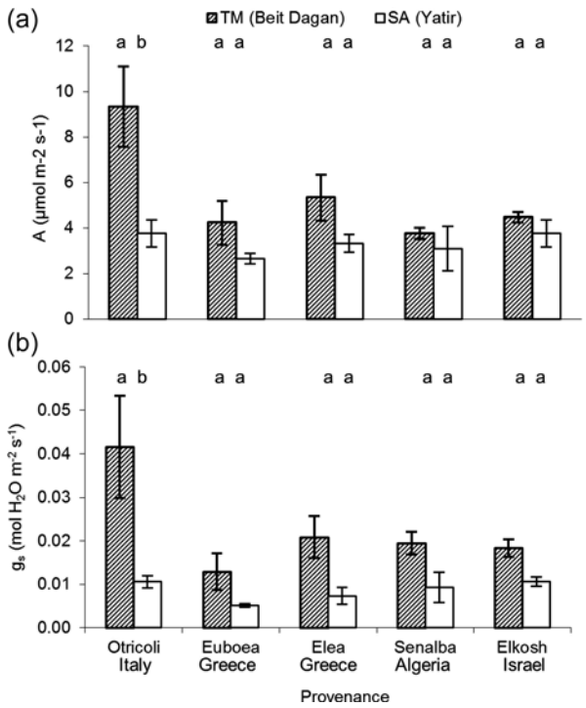

Figure 3. Mean net assimilation rates (a) and stomatal conductance (b) measured during May in leaves of trees from each provenance and two climate types (SA, semi-arid; TM, thermo-Mediterranean). Similar letters indicate a non-significant difference ($\alpha > 0.05$) between trees of a provenance growing under different climate types. Error bars represent the standard error of the mean ($n = 3$).

different time scales involved, comparing instantaneous gas exchange results with long-term integrated tree ring data only serves as an indication for the possible underlying processes. In general, values of A and g_s were comparable across provenances, with the exception of higher assimilation rates in the Italian provenance Otricoli under TM climate (Figure 3, Table 2). Along the drying climate trend across sites, A values decreased by ~40% and g_s values decreased by ~60%. The decrease in A with drying is consistent with the lower growth observed along the climatic trend (Figure 2a) and may indicate an agreement between the short and long term results. The A/g_s ratio (Eq. (3)) increased by ~100% with drying, compared to 15% increase in $\delta^{13}C$-derived WUE_i. In turn, the results indicate that the higher WUE_i under SA climate may have been the result of a greater decrease in stomatal conductance, as compared with A. Note that the decrease in A values in response to the climate gradient was not significant in Senalba and Elkosh (Table 2). This was also reflected by lower WUE_i in Senalba and Elkosh under TM climate than in other provenances, as shown above (Figure 2b).

Trunk growth phenology and leaf chlorophyll concentration

Differences in trunk growth phenology between provenances were found under identical climatic conditions in each site. Each provenance had a unique growth phenology (Figure 4) in terms of start date, end date and the GSL, defined as the sum (in days) of all 2-week periods when the increment was 5% of the annual total or more. Under TM climate, trunk growth initiation followed the beginning of the rainy season in October. At that time Elea growth rate was 2.6 ± 0.7 mm month^{-1}, and other provenances between 1.8 ± 0.6 and 2.3 ± 0.4 mm month^{-1}. Otricoli reached that rate in early December, while other provenances caught up only in early February of the following year. Growth continued in all provenances until early (Elkosh) to mid- (all others) April, with rates of up to 6.7 ± 1.0 mm month^{-1} (Euboea; Figure 4). GSL was significantly lower under SA climate ($P < 0.0001$, Table 2), predominantly due to a delayed starting date: Elea trees were again the first to resume growth, but only in mid-January, and they had the longest growing season (128 days, Figure 5a) and reached rates of 5.3 ± 0.4 mm month^{-1}, whereas other provenances' growth rates were between 2.4 ± 0.8 and 4.2 ± 0.2 mm month^{-1}. Euboea had a very short growing season (80 days). In TM climate GSL was also high for Otricoli, while Senalba and Elkosh had intermediate GSLs. Elkosh was the only provenance whose GSL did not significantly change with climate ($P = 0.1308$, Table 2).

Leaf chlorophyll concentrations were not sensitive to climatic conditions, with comparable values across sites in each

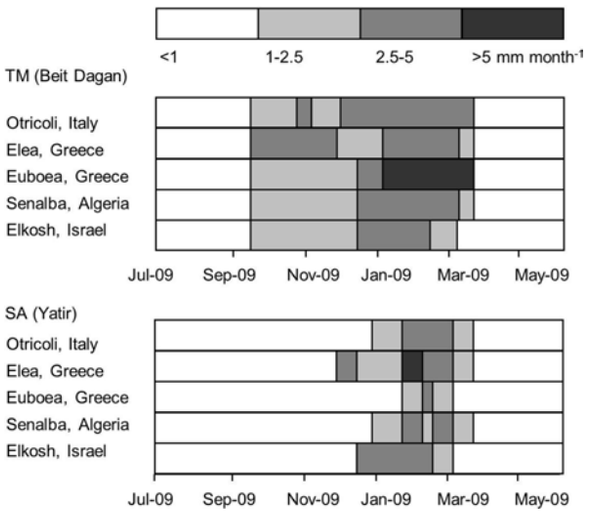

Figure 4. Quantitative trunk growth phenograms averaged across trees from each provenance and two climate types (SA, semi-arid; TM, thermo-Mediterranean).

provenance (Figure 5c; $P = 0.086$, Table 2). However, chlorophyll concentrations were 30% higher in the leaves of Euboea (Figure 5c), yielding a significant provenance effect on chlorophyll concentration ($P < 0.0001$, Table 2). The higher chlorophyll concentration in Euboea was consistent with its higher trunk growth rate, i.e., up to 6.7 mm month^{-1}, as compared with other provenances 3–5 mm month^{-1} (Figure 4), and may reflect higher integrated photosynthesis in this provenance.

Xylem hydraulic conductivity

All provenances had lower hydraulic conductivities (K_s) in SA than in TM climate: ~27 and ~120 g m^{-1} MPa^{-1} s^{-1}, respectively (Table 3). Elkosh and Elea had the highest K_s, whereas Senalba had the lowest K_s (and $K_{s\ max}$) values at both sites. Measurements of K_s and $K_{s\ max}$ were further used to identify PLC, which can be attributed to xylem cavitation, according to Eq. (4). Elkosh and Elea PLC was low (0–12%), Otricoli and Euboea was moderate (26–44%) and in Senalba PLC was high, i.e., 70% or more (Figure 5b). Provenance PLC values did not change significantly with site ($0.1083 < P < 0.8139$, Table 2).

Discussion

Ecophysiological response of Pinus halepensis to drying and warming

This study was motivated by the growing realization that the current rate of climate change may exceed the rate of evolutionary changes, genetic adaptation or migration in Mediterranean forest trees. Alternatively, the potential for ecophysiological adjustments in key traits may be sufficient to ensure the success of a genotype across a wide range of

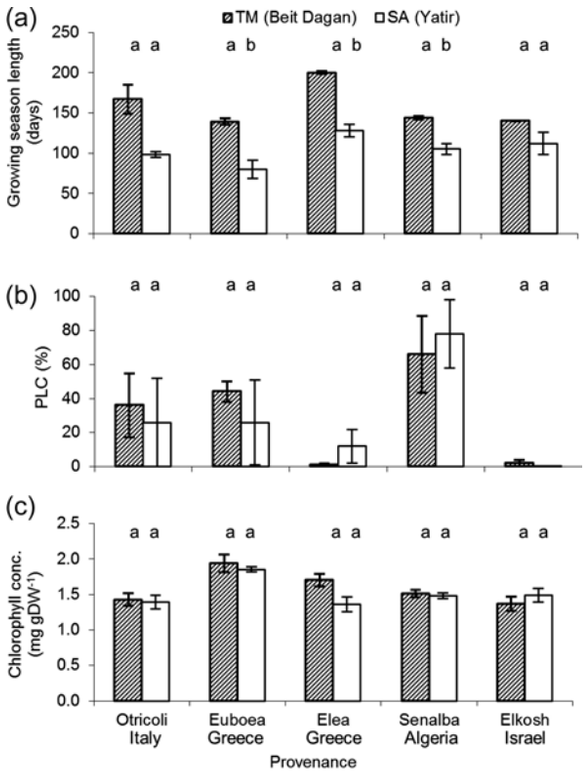

Figure 5. Mean GSL (a), percent loss of xylem conductivity (b; measured during May–June) and leaf chlorophyll concentration (c; measured during April–May) of trees from each provenance and two climate types (SA, semi-arid; TM, thermo-Mediterranean). Similar letters indicate a non-significant difference ($\alpha > 0.05$) between trees of a provenance growing under different climate types. Error bars represent the standard error of the mean ($n = 5$, 3 and 9 respectively).

climatic conditions, as described by Bradshaw (1965). The trees included in this study showed a remarkable ability to survive and grow under a range of climate conditions (Figure 2a), sometimes contrasting strongly with those prevailing at their seed source sites (Table 1).

The sources of phenotypic variance in the seven parameters were examined according to three categories: (i) environmental effects (E), represented by the three climate types (C); (ii) genetic effects (G), represented by the five provenances (P); and (iii) the interaction between the two (E × G), here (C × P). (i) The climate effect was significant in five out of the seven parameters examined (Table 2), with some traits showing marked variations in all provenances. This included the expected reductions not only in GSL (Figure 5a, ~40% decrease from TM to SA climate) and in mean stomatal conductance, g_s (Figure 2b, ~60% decrease from TM to SA climate) but also in xylem conductivity, which requires structural changes (Table 3, ~77% decrease from TM to SA climate). (ii) Differences between provenances were significant in all but one trait, WUE_i. Notably, such variations imparted some compensation for the low climate effect in traits, such as in leaf chlorophyll content and in PLC (Table 2). These two traits did

Table 3. Mean (SE)-specific xylem conductivity values (in g m^{-1} MPa^{-1} s^{-1}) before (K_s) and after ($K_{s\ max}$) perfusion at high pressure measured in twigs of trees from the five provenances in Beit Dagan and Yatir.

Climate (site)	Thermo-Mediterranean (Beit Dagan)		Semi-arid (Yatir)	
Provenance	K_s	$K_{s\ max}$	K_s	$K_{s\ max}$
Otricoli	84.5 (6.8)	146.3 (43.7)	20.4 (3.0)	27.6 (2.8)
Euboea	56.6 (4.5)	102.5 (4.0)	24.1 (9.2)	37.6 (15.4)
Elea	291.8 (76.3)	294.5 (74.0)	24.9 (0.6)	33.8 (0.2)
Senalba	18.8 (6.8)	90.5 (44.6)	7.6 (0.2)	23.5 (9.4)
Elkosh	156.2 (20.1)	159.6 (17.3)	60.0 (14.3)	61.3 (28.8)

not vary with climate but varied significantly among provenances (ranges of ~30 and ~70%, for chlorophyll and PLC, respectively). The stable PLC across climates is in agreement with the poor correlation of embolism resistance with climate reported for other pine species (Martínez-Vilalta et al. 2009, Lamy et al. 2011). The use of provenances (as opposed to identical genotypes, e.g., from clones) means that the observed variations might include some intra-provenance genetic variance, but valuable quantification of provenance-level plasticity can nevertheless be gained (e.g., Tognetti et al. 1997; Calamassi et al. 2001; Atzmon et al. 2004; Baquedano et al. 2008; Schiller and Atzmon 2009). (iii) C × P interactions include situations where a parameter changes across climates (sites), yet differences in the extent of the response are also observed among provenances. These included changes across climates in the mean rate of leaf assimilation, *A* (Table 2; Figure 3b), in WUE_i (Figure 2b) and in the maximum growth rate (Figure 4).

Nicotra et al. (2010) asked whether the incidence of adaptive plasticity may vary among types of traits (e.g., those related to anatomy versus those related to allocation or physiology). Our results show that traits related to xylem anatomy can be both plastic (e.g., K_s) and rigid (e.g., PLC). Similarly, physiological leaf parameters included the plastic A and the rigid chlorophyll level.

Interactions between specific traits

In addition to the three main categories of variations above (climate, provenances and their interactions), combinations of traits are also important: a limitation by a rigid, non-plastic, trait can be compensated for by association with another trait that has a high level of plasticity (Bradshaw 1965; Bonaparte and Brawn 1975; Sadras et al. 2009). For example, the stable PLC across climates could be compensated for by decreasing K_s in some provenances (Table 3 and Figure 5b). Combinations of traits also include GSL and PLC: a low GSL value helps avoiding unfavorable conditions, and therefore the need for high xylem resistance to embolism (low PLC). In contrast, maintaining high GSL critically depends on low PLC. Such a relationship was exemplified by the two Greek provenances: Euboea had the lowest GSL (Figure 5a) and ~35% PLC (Figure 5b), while Elea had the highest GSL and a PLC of only ~10%. The strategy of Euboea seems to rely on synchronization of cambial activity with relatively high water availability during the wet season, as previously reported for other sites (Breitsprecher and Bethel 1990; Brochert 1994), and specifically for *P. halepensis* in Yatir (Klein et al. 2005). At the other extreme, the early onset of the growing season in Elea exposes it to high water potential gradients, increasing the selective advantage of resistance to embolism (Klein et al. 2011).

Another combination of traits may exist between GSL and chlorophyll level. Assuming that the 30% higher chlorophyll content in Euboea (Figure 5c) is translated into higher integrated photosynthetic capacity, it potentially contributed to its higher trunk growth rate (up to 6.7 ± 1.0 mm $month^{-1}$ compared with 3.8 ± 0.7 to 5.0 ± 0.2 in other provenances, Figure 4). But we note that the correspondence between high chlorophyll and a high growth rate was not found in the short-term, late season, leaf gas exchange measurements (Figure 3a). Leaf chlorophyll may therefore provide a better indicator of long-term integrated photosynthetic capacity (e.g., Brougham 1960; Gratani et al. 1998). Across all five provenances, the correlation coefficient between GSL and chlorophyll content was 0.66, which was significant at $\alpha = 0.1$. Elevated chlorophyll content can be a key element in a growth strategy where trunk growth occurs in a short yet strong growth pulse, without reducing field performance (for example, Euboea DBH was similar to or higher than that of other provenances, Figure 2a).

Contribution of ecophysiological traits to growth

In contrast to the differential response in specific traits among provenances, the resulting overall tree performance was similar across provenances (Figure 2a), in agreement with an earlier *P. halepensis* study showing that trait plasticity allows different ecotypes to assume similar phenotypes (Baquedano et al. 2008). Differences in growth among provenances were usually small, and only under the wettest conditions, in the Rome site, large variations in growth rate were observed: Elea and Euboea performed better than Senalba and Elkosh. An association of growth rate with climate conditions at the seed source has been described by Fusaro et al. (2007), who found

growth inhibition of Elkosh grown in Pescara, Italy ($P = 1000$ mm), and Otricoli grown in Cagliari on the Sardinia coast ($P = 500$ mm). Note that selection of provenances under dry conditions according to growth data alone would fail in this case: high performance under MM climate (Elea, Euboea) did not carry over to drier conditions.

To quantify the relative contribution of each physiological parameter to a trait related to the overall fitness of the tree (increment growth, measured as BAI), PLS was performed. Among six parameters, 39 and 19% of the fit to BAI was explained by WUE_i and GSL, respectively (Table 2). The contribution of other parameters was 14% or lower. The ability of a genotype to succeed under climate change may depend on its overall fitness, expressed in growth and even more importantly, its survival. The survival aspects could be explored by extending the results obtained in the present study to consider two previous, consecutive studies (Atzmon et al. 2004, Schiller and Atzmon 2009). These studies examined the survival rates of the same provenances used here, planted in 1985 in an experimental plot in the Eastern Yatir area, where conditions are considerably harsher: lower elevation with strong southern aspect, and poor and drier soil. In contrast to the result reported above, high mortality ratios were observed in the Eastern Yatir site, but with large differences between provenances. These differences in mortality across a short geographical gradient are consistent with the notion that Yatir represents the 'dry timberline' for Aleppo pine and possibly for forests in general (Maseyk et al. 2008). In the Eastern Yatir site, mortality ratios in Elkosh and Elea were 18 and 26%, respectively, in 1997, increasing to 42 and 55% in the following survey in 2007. In contrast, Senalba and Otricoli showed mortality ratios as high as 55 and 59%, respectively, in 1997, and 82% mortality for both provenances in 2007 (Euboea was not included in those studies). Notably, among the seven parameters we examined, PLC levels were always lower (Figure 5b), and K_s levels were always higher (Table 3) in the surviving provenances compared to the high mortality provenances. Differential responses in other parameters, including WUE_i, did not align with the observed differences in survival. The correlation coefficient between PLC and mortality ratio was 0.78, which was significant at $\alpha = 0.1$. This finding also points to hydraulic failure as the tree mortality mechanism, rather than carbon starvation (Martinez-Vilalta and Pinol 2002, Brodribb and Cochard 2009, Sala et al. 2010, Klein et al. 2011).

Plotting PLC against WUE_i and GSL, the two traits contributing most to growth, in a 3D representation of a response space (Figure 6), demonstrates the idea of an optimal combination of traits for fitness. This optimum, corresponding to the deepest corner in the plot, is represented by low GSL (i.e., growth retention), low PLC (i.e., low embolism) and high WUE_i. The observed superiority of Elkosh and Elea over Otricoli and, to a larger extent, over Senalba, is consistent with the analysis presented in Figure 6. Furthermore, while across the climatic gradient in our study a range of combinations and tradeoffs allowed moderate growth of all provenances under SA conditions (below 300 mm annual precipitation), challenging the same provenances with yet harsher conditions (Atzmon et al. 2004, Schiller and Atzmon 2009) indicated that ultimately embolism-resistant xylem is the critical element for tree survival under dry conditions (Brodribb and Cochard 2009, Klein et al. 2011).

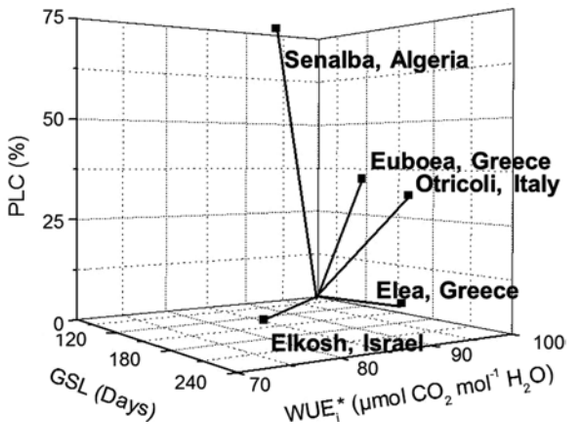

Figure 6. Mean responses of trees from the five provenances with respect to major traits: GSL in Beit Dagan and Yatir ($n = 10$), PLC in Beit Dagan and Yatir ($n = 6$) and WUE_i in Beit Dagan ($n = 6$).

Implications for forestry under climate change

Today forests around the world are challenged by an increasingly faster rate of changes in environmental conditions, already severely affecting vulnerable populations (Allen et al. 2009 and references therein). In many cases, these include trees that grow near the limit of their natural distribution, such as the dry timberline case of the Yatir forest. Our analysis suggests several implications for forestry. (i) Considering the adjustments in key traits both in any given *P. halepensis* provenance and across a range of available provenances and climates could provide a powerful management tool to address the dangers of reduced forest distribution with warming and drying climate trends, such as predicted for the entire Mediterranean and other regions (Cohen et al. 2002, Christensen et al. 2007). (ii) A single advantageous trait may be insufficient for sustainability. For example, selection of the provenance Otricoli based on high WUE_i or Senalba based on low water use in currently favorable conditions would fail under extreme conditions. (iii) Ultimately, selection for low PLC must be an important component in the face of predicted drying and warming. Our findings indicate that at least for *P. halepensis*, the existing gap between plant adaptability and the changing environment could be closed by ecophysiological response at the species and provenance level, as well as by exploiting the

range of performance offered by provenances of different seed sources. Such an approach, in turn, will potentially permit sustained forest productivity and distribution even under relatively severe climate change scenarios across the Mediterranean region. Future forest planning should consider testing for ecophysiological adjustment in key traits in candidate tree species and genotypes selected for planting today, whose growth should be ensured in the future.

Acknowledgments

The authors thank Gabriel Schiller and Ernesto Fusaro for providing access to provenance trials in Israel and in Italy, respectively; Francesco Righi and Marco Riccardi for assistance in field sampling; and Emanuela Negreanu for technical expertise and help with the $\delta^{13}C$ analyses. GDM and TK acknowledge the COST scientific programs FORMAN and SIBAE for travel grants FP0601-6298 and ES0806-05352, allowing their scientific missions in Israel and Italy, respectively. TK acknowledges the Karshon foundation grant provided through KKL-JNF.

Conflict of interest

Q7 None declared.

Funding

Jewish National Fund (Alberta-Israel program 90-9-608-08); The Sussman Center for Environmental Research; France-Israel High Council for Research Scientific and Technological Cooperation (project 3-6735); the Minerva Foundation; and the Cathy Wills and Robert Lewis Program in Environmental Science.

References

Allen CD, Macalady AK, Chenchouni H et al. (2009) A global overview of drought and heat-induced tree mortality reveals emerging climate change risks for forests. For Ecol Manage 259:660–684.

Alpert P, Baldi M, Ilani R et al. (2006) Relations between climate variability in the Mediterranean region and the tropics: ENSO, South Asian and African monsoons, hurricanes and Saharan dust. Dev Earth Environ Sci 4:149–177.

Atzmon N, Moshe Y, Schiller G (2004) Ecophysiological response to severe drought in *Pinus halepensis* Mill. trees of two provenances. Plant Ecol 171:15–22.

Baquedano FJ, Valladares F, Castillo FJ (2008) Phenotypic plasticity blurs ecotypic divergence in the response of *Quercus coccifera* and *Pinus halepensis* to water stress. Eur J For Res 127:495–506.

Bonaparte EENA, Brawn RI (1975) The effect of intraspecific competition on the phenotypic plasticity of morphological and agronomic characters of four maize hybrids. Ann Bot 39:863–869.

Bradshaw AD (1965) Evolutionary significance of phenotypic plasticity in plants. Adv Genet 13:115–155.

Breitsprecher A, Bethel JS (1990) Stem-growth periodicity of trees in a tropical wet forest of Costa Rica. Ecology 71:1156–1164.

Brochert R (1994) Water status and development of tropical trees during seasonal drought. Trees 8:115–125.

Brodribb TJ, Cochard H (2009) Hydraulic failure defines the recovery and point of death in water-stressed conifers. Plant Physiol 149:575–584.

Brougham RW (1960) The relationship between the critical leaf area, total chlorophyll content, and maximum growth-rate of some pasture and crop plants. Ann Bot 24:463–474.

Burke EJ, Brown SJ, Christidis N (2006) Modeling the recent evolution of global drought and projections for the twenty-first century with the Hadley centre climate model. J Hydrometeorol 7:1113–1125.

Calamassi R, Della Roccaa G, Falusia M, Paolettib E, Stratib S (2001) Resistance to water stress in seedlings of eight European provenances of *Pinus halepensis* Mill. Ann For Sci 58:663–672.

Chmielewski FM, Rotzer T (2001) Response of tree phenology to climate change across Europe. Agric For Meteorol 108:101–112.

Christensen JH, Hewitson B, Busuic A et al. (2007) Regional climate projections. In: Solomon S, Qin D, Manning M, Chen Z, Marquis M, Averyt KB, Tingor M, Miller HL (eds) Climate change 2007: the physical science basis. Contributions of Working Group I to the Fourth Assessment Report of the Intergovernmental Panel on Climate Change. Cambridge University Press, Cambridge, UK/New York, NY.

Ciais P, Reichstein M, Vivoy N et al. (2005) Europe-wide reduction in primary productivity caused by the heat and drought in 2003. Nature 437:529–533.

Cohen S, Ianetz A, Stanhill G (2002) Evaporative climate changes at Bet Dagan, Israel 1964–1998. Agric For Meteorol 111:83–91.

Coplen TB (1994) Reporting of stable hydrogen, carbon, and oxygen isotopic abundances. Pure Appl Chem 66:273–276.

Eccher A, Fusaro E, Pelleri F (1987) Results of Italian provenance trials of pines of the group halepensis ten years after planting. From French. For Mediterr 9:5–14.

Farquhar GD, O'Leary MH, Berry JA (1982) On the relationship between carbon isotope discrimination and intercellular carbon dioxide concentration in leaves. Aust J Plant Physiol 9:121–137.

Ferrio JP, Florit A, Vega A, Serrano L, Voltas J (2003) Δ13C and tree-ring width reflect different drought responses in *Quercus ilex* and *Pinus halepensis*. Oecologia 442:512–518. Q8

Fusaro E, Di Matteo G, Righi F (2007) Current experimental orchards of pines of the group halepensis. From Italian. Econ Mont Linea Ecol 39:2–9.

Gratani L, Pesoli P, Crescente MF (1998) Relationship between photosynthetic activity and chlorophyll content in an isolated *Quercus ilex* L. tree during the year. Photosynthetica 35:445–451.

Klein T, Hemming D, Lin T, Grunzweig JM, Maseyk K, Rotenberg E, Yakir D (2005) Association between tree-ring and needle delta C-13 and leaf gas exchange in *Pinus halepensis* under semi-arid conditions. Oecologia 144:45–54.

Klein T, Cohen S, Yakir D (2011) Hydraulic adjustments underlying drought resistance of *Pinus halepensis*. Tree Physiol. DOI 10.1093/treephys/tpr047. Q9

Klein Tank AMG, Wijngaard JB, Konnen GP et al. (2002) Daily dataset of 20th-century surface air temperature and precipitation series for the European Climate Assessment. Int J Climatol 22:1441–1453.

Koerner C, Sarris D, Christodoulakis D (2005) Long-term increase in climatic dryness in the East-Mediterranean as evidenced for the island of Samos. Reg Environ Change J 5:27–36.

Lamy J-B, Bouffier L, Burlett R et al. (2011) Uniform selection as a primary force reducing population genetic differentiation of cavitation resistance across a species range. PLoS ONE 6:e23476.

Langlet O (1971) Two hundred years of genecology. Taxon 20:653–722.

Martinez-Vilalta J, Pinol J (2002) Drought-induced mortality and hydraulic architecture in pine populations of the NE Iberian Peninsula. For Ecol Manage 161:247–256.

Martínez-Vilalta J, Cochard H, Mencuccini M et al. (2009) Hydraulic adjustment of Scots pine across Europe. New Phytol 184:353–364.

Maseyk KS, Lin T, Rotenberg E, Grunzweig JM, Schwartz A, Yakir D (2008) Physiology-phenology interactions in a productive semi-arid pine forest. New Phytol 178:603–616.

Maseyk K, Hemming D, Angert A, Leavitt SW, Yakir D (2011) Increase in water-use efficiency and underlying processes in pine forests across a precipitation gradient in the dry Mediterranean region over the past 30 years. Oecologia. DOI 10.1007/s00442-011-2010-4.

Matyas C (1996) Climatic adaptation of trees: rediscovering provenance tests. Euphytica 92:45–54.

McCarroll D, Loader NJ (2004) Stable isotopes in tree rings. Quat Sci Rev 23:771–801.

Mejstrik VK, Cudlin P (1983) Mycorrhiza in some desert plant species in Algeria. Plant Soil 71:363–366.

Nicotra AB, Atkin OK, Bonser SP et al. (2010) Plant phenotypic plasticity in a changing climate. Trends Plant Sci 15:684–692.

Palutikof JP, Goodes CM, Guo X (1994) Climate change, potential evapotranspiration and moisture availability in the Mediterranean basin. Int J Climatol 14:853–869.

Penuelas J, Lloret F, Montoya R (2001) Severe drought effects on Mediterranean woody flora in Spain. For Sci 47:214–218.

Porra RJ, Thompson WA, Kriedmann PE (1989) Determination of accurate extinction coefficients and simultaneous equations for assaying chlorophylls a and b extracted with four different solvents: verification of the concentration of chlorophyll standards by atomic absorption spectroscopy. Biochim Biophys Acta 975:384–394.

Raftoyannis Y, Spanos I, Radoglou K (2008) The decline of Greek fir. *Abies cephalonica* Loudon.: relationships with root condition. Plant Biosystems 142:386–390.

Raymond CA, Lindgren D (1990) Genetic flexibility – a model for determining the range of suitable environments for a seed source. Silvae Genet 39:3–4.

Reyer C, Leuzinger S, Rammig A et al. (2012) A plant's perspective of extremes: terrestrial plant responses to changing climatic variability. Global Change Biol (in press).

Robertson A, Overpack J, Rind D et al. (2001) Hypothesized climate forcing time series for the last 500 years. J Geophys Res 106:14783–14803.

Sadras VO, Reynolds MP, de la Vega AJ, Petrie PR, Robinson R (2009) Phenotypic plasticity of yield and phenology in wheat, sunflower and grapevine. Field Crops Res 110:242–250.

Sala A, Piper F, Hoch G (2010) Physiological mechanisms of drought-induced tree mortality are far from being resolved. New Phytol 186:274–281.

Sarris D, Christodoulakis D, Koerner C (2007) Recent decline in precipitation and tree growth in the eastern Mediterranean. Global Change Biol 13:1187–2000.

Schiller G, Atzmon N (2009) Performance of Aleppo pine (*Pinus halepensis*). Provenances grown at the edge of the Negev desert: a review. J Arid Environ 73:1051–1057.

Seibt U, Rajabi A, Griffiths H, Berry JA (2008) Carbon isotopes and water use efficiency: sense and sensitivity. Oecologia 155:441–454.

Shaw RG, Etterson JR (2012) Rapid climate change and the rate of adaptation: insight from experimental quantitative analysis. New Phytol 195:752–765.

Tognetti R, Michelozzi M, Giovannelli A (1997) Geographical variation in water relations, hydraulic architecture and terpene composition of Aleppo pine seedlings from Italian provinces. Tree Physiol 17:241–250.

Waring RH, Silvester WB (1994) Variation in foliar $\delta^{13}C$ values within the crowns of *Pinus radiata* trees. Tree Physiol 14:1203–1213.

5.3. The role of soil and tree hydraulics in the success of a water-limited pine forest.

The results of this study are described in Klein et al. (2012b), accepted for publication in *Ecohydrology* in November 2012. A PDF version of the paper should become available during December 2012.

5.3.1. Soil water content dynamics and mechanical structure

Measurements in the soil were divided into four depth layers: 0-10, 10-20, 20-40 and 40-60 cm (layers I to IV). Mean values for the 5-year study period indicated that in summer soil water content (SWC) strongly increased with depth, ranging from 7% in layer I to 21% in layer IV (Fig. 3.1a). In autumn, just before the start of the rainy season, all layers were even dryer, except for layer I, where occasionally 1-2 early rain events elevated SWC up to 11%. The sharp gradient expired in winter, when SWC was 18-20% along the entire soil profile. In spring, soil had already started to dry out, except in layer IV, where an average SWC of 18-20% prevailed all year round. Mechanical soil properties were likely to play an important role in these seasonal dynamics. Generally, there was an increase in clay content and a decrease in sand content with depth, particularly in the transition between layers III and IV (Fig. 3.1b). Layer IV was different from the other layers in its mechanical composition, with less than 5% sand and more than 50% clay. The finer soil texture (and increased water retention capacity, see below) in layer IV is associated with the maintenance of SWC above 18% all year round. Higher sand content (up to 51%) and lower clay content (down to 32%) were found in shallower layers, indicating a coarser soil texture closer to the surface.

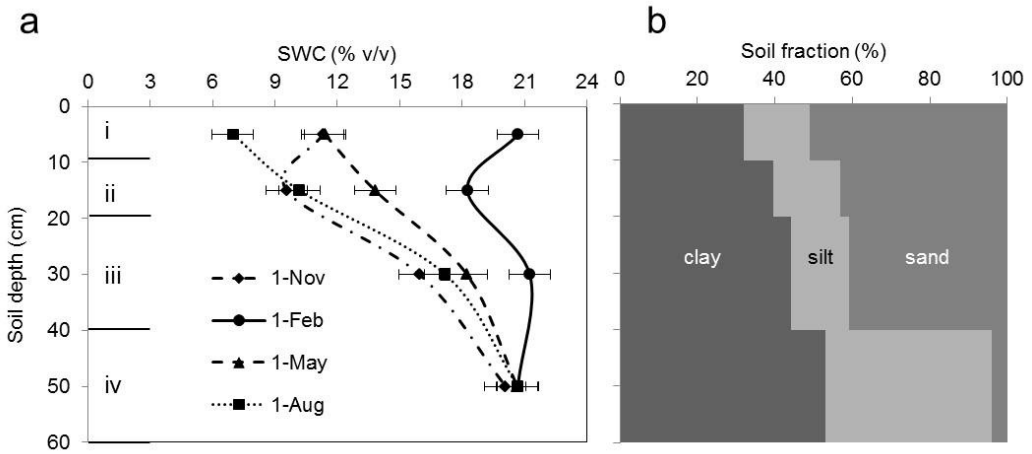

Fig. 3.1. Five-year (2006-2009) seasonal soil water content (SWC) changes (n = 5, *means* ± *SE*) in four depth layers (labeled *i* to *iv*) in Yatir forest (a), and their mechanical composition (b). Note that both SWC dynamics and sand/clay ratio decrease with depth.

5.3.2. Soil water retention properties

Based on their mechanical structure, layer-specific van Genuchten-Mualem soil parameters were calculated using the RETC software (Table 3.1), and water retention curves were plotted (Fig. 3.2). The exponential nature of all curves demonstrated that for SWC above 20%, soil water potential (Ψ_s) was high and stable (between -0.1 and -0.6 MPa depending on the layer) whereas, at low SWC values minor shifts in SWC meant major water potential changes. Applying the soil water retention curves to the layer-specific SWC measurements in a given year (Fig. 3.3a) produced layer-specific Ψ_s curves for that year (Fig. 3.3b). Errors associated with the SWC data and the retention curve estimation were propagated in this calculation according to error propagation rules (Taylor 1997), and reported in Fig. 3.3. Applying the Ψ_s threshold for T_t (-2.0 MPa, see Methods) to the layer-specific retention curves (Fig. 3.2) we then estimated SWC thresholds for T_t (ttSWC). We obtained values of 13.2±0.3%, 15.2±0.4%, 17.0±0.7%, and 17.6±0% for layers I to IV respectively. The strong increase in these thresholds with soil depth emphasizes the importance of taking into account depth-resolved soil properties. Because the ttSWC value for layer IV (17.6%) was lower than the corresponding 5-yr minimum SWC value (18.9%), unlike in other layers, we chose to use the observed minimum value as a more reliable estimate of ttSWC for layer IV, although this did not have a large impact on our results.

Table 3.1. Soil parameters of van Genuchten - Mualem model (Eq. 12) for Yatir soil, obtained by RETC software. Retention curves in Fig. 3.2 are the parameters' respective graphic solutions of Eq. 12 for discrete depths.

Soil layer	Depth (cm)	θ_r	θ_s	α	n	m
I	0-10	0.0754	0.4009	0.0245	1.2910	0.2254
II	10-20	0.0834	0.4201	0.0244	1.2579	0.2050
III	20-40	0.0867	0.4283	0.0262	1.2281	0.1857
IV	40-60	0.1050	0.5138	0.0150	1.3102	0.2368

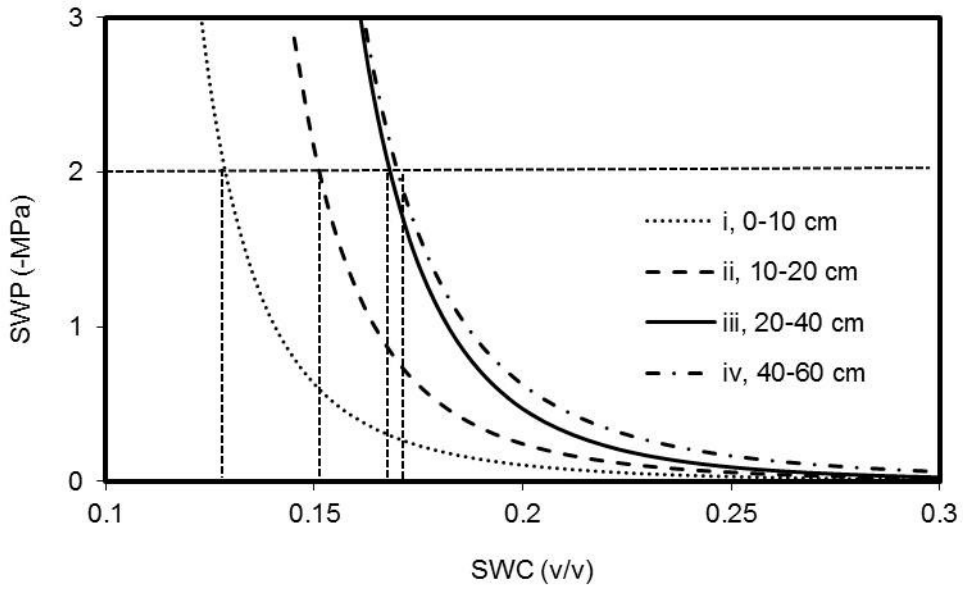

Fig. 3.2. Soil water retention curves for four depth layers in Yatir forest (based on Eq. 12 and Table 3.1). Horizontal dash line denotes the soil water potential (Ψ_s) threshold value for *Pinus halepensis* transpiration (when T_t=0). The corresponding soil water content (SWC) values were 13.2±0.3, 15.2±0.4, 17.0±0.7, and 17.6±0 % for layers I to IV respectively. The shape of the retention curves demonstrates an increasing sensitivity to small changes in SWC as the Ψ_s threshold is approached.

5.3.3. Transpirable soil water content and tree water use

Once the ttSWC thresholds estimated for each soil layer, we defined and calculated transpirable soil water content (tSWC, mm) as:

(18) $tSWC = h \times (1 - ST) \times (SWC - ttSWC)$

And for the entire soil profile:

(19) $\sum_{i \text{ to } vi} tSWC = \Sigma\, h \times (1 - ST) \times (SWC - ttSWC)$

where h is the height of the soil layer (mm), ST its stone fraction, and the summation is performed over six soil layers (layers I-IV and two deeper layers complementing for the entire soil profile in this site). This term develops the existing terms for water availability, which are discussed in the Introduction, by providing absolute quantity, rather than a fraction, which can be directly used in hydrological budgets. In addition, we link this term to species-specific root water uptake threshold and to depth-dependent soil characteristics. Soil water content data in each layer over the 5-year study period was then transformed into tSWC using Eq. 18.

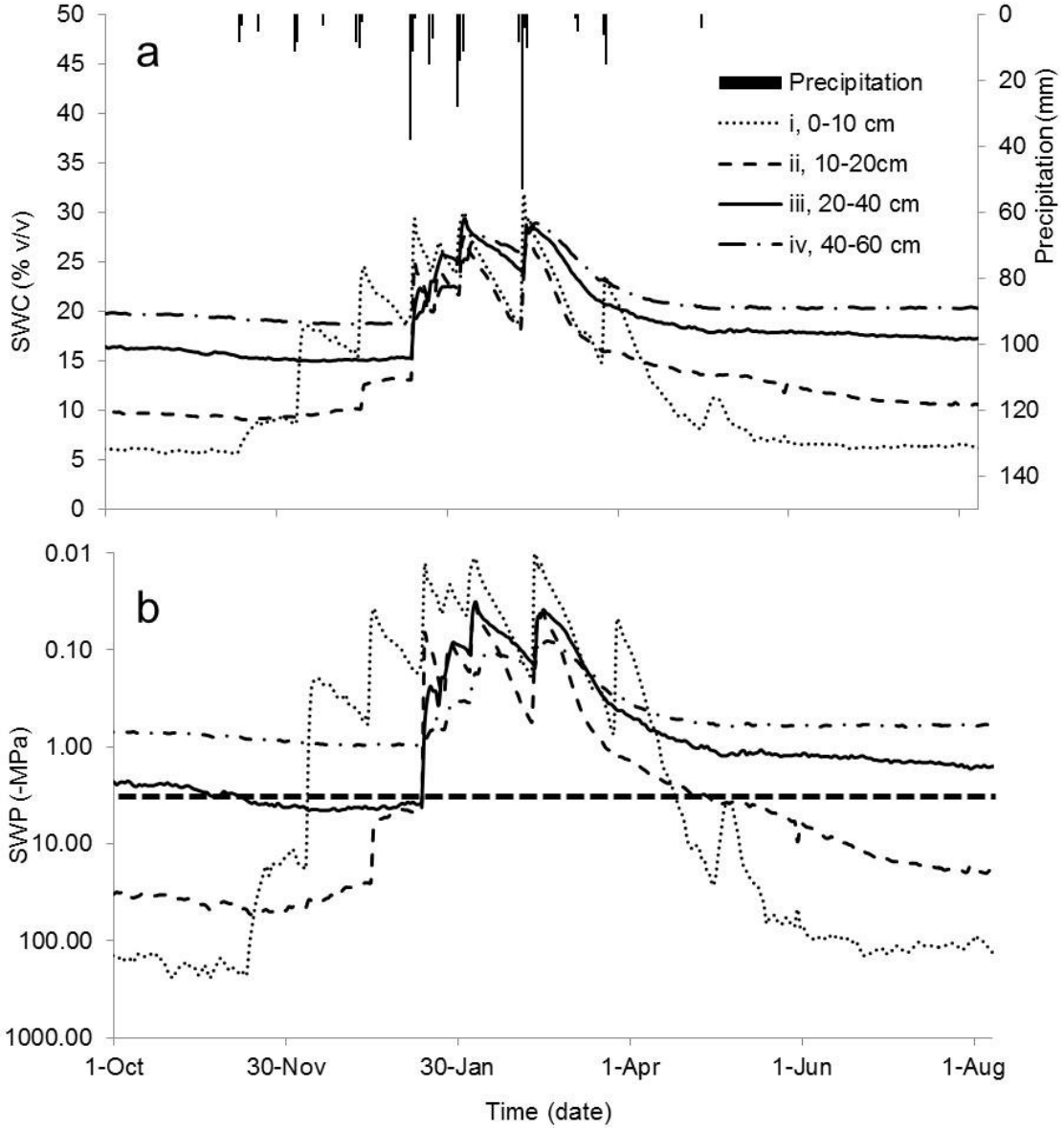

Fig. 3.3. Seasonal dynamics in precipitation and soil water content (a, SWC, n = 2-3 pits) and soil water potential (b, Ψ_s, logarithmic scale; calculated using Eq. 12 and Table 3.1) in four depth layers in Yatir forest during the 2010 growth season. Horizontal dash line in (b) denotes the soil water potential threshold value for *Pinus halepensis* transpiration (when T_t=0). *SEs* for SWC measurements are 0.1-1.6, 0.4-4.2, 0.0-4.8, and 0-4.7 % v/v for layers I-IV, respectively. Propagated *SEs* for calculated Ψ_s are 0.03-0.29, 0.08-0.65, 0.05-0.53, and 0-0.45 MPa for layers I-IV, respectively.

Errors in tSWC were calculated according to error propagation rules (Taylor 1997) and reported in Fig. 3.4. Focusing on 2010, as a representative year with the most complete measurement sets, an annual tSWC diagram showed that soil water availability was highly influenced by precipitation patterns (Fig. 3.4a). In particular

tSWC peaked in all layers following the first rain storm in January 17th-19th (P = 50 mm), marking the onset of the wet season, and diminished (in layers III and IV) or vanished altogether (in layers I and II) two weeks after the last significant rain event on March 28th, marking the onset of the drying season. Layer I also responded to the light rains marking the onset of the wetting season (November 17th-18th, P = 11 mm), despite the absence of deeper infiltration. Finally, layer II had the lowest positive values of tSWC and the shortest period. Considering the water retention properties and spatial situation of this layer, this was mainly the result of rainwater infiltration into deeper layers, as layers III and IV maintained positive tSWC values throughout the summer drought.

The tSWC diagram was further compared with continuous, parallel measurements of tree transpiration (Fig. 3.4b). During the dry period, prior to the emergence of soil water availability in layer I on December 8th, very low T_t levels (0.1-0.2 mm d^{-1}) prevailed, partly explained by a residual tSWC in layer IV. At the wetting period (prior to January 18th) low T_t levels (0.2-0.4 mm d^{-1}) were supported by layer I. After that date, high T_t levels (up to 1.6 mm d^{-1}) were observed, corresponding to positive tSWC values in all four soil layers. Non-zero T_t values after April 14th, when no soil water remained available above 20 cm, indicated a high reliance of T_t on soil water from layers III and IV. Additional water amounts were also available in deeper layers, but with smaller contribution to T_t (see next section). Above-ground conditions also affected tree transpiration. In particular the T_t peak in late spring is explained by an optimal combination of water vapor pressure deficit, solar radiation, temperature, and plant phenology (Maseyk et al. 2008). However once no soil water remained available above 20 cm, rapid decline in T_t was imposed irrespective of the other factors.

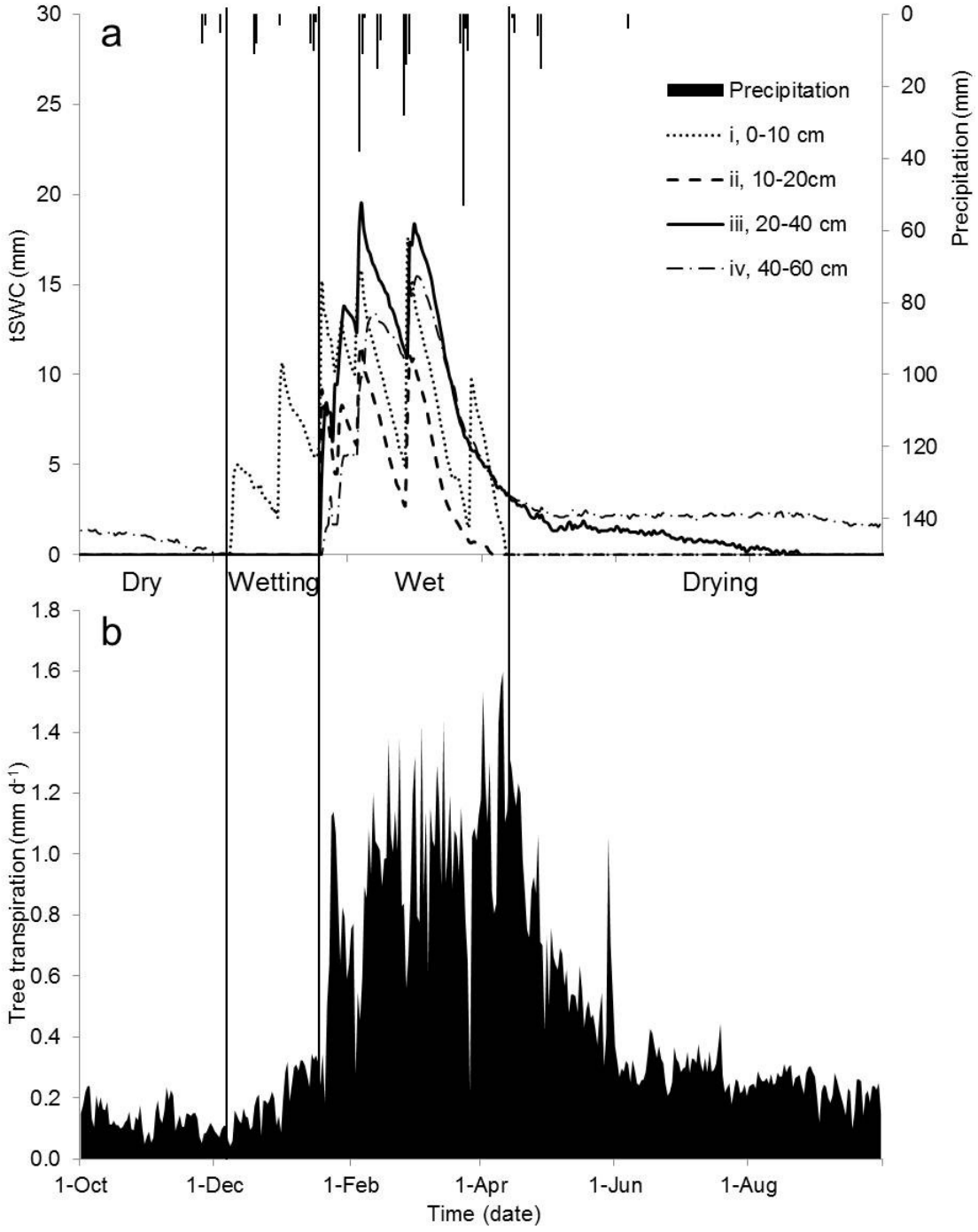

Fig. 3.4. Seasonal dynamics in precipitation and transpirable SWC (tSWC, n = 2-3 pits) in four depth layers (a), and in tree transpiration (T_t, measured in up to sixteen trees, b) in Yatir forest during the 2010 growth season. The increase in T_t during the wetting period relied on layer I; Persisted T_t throughout the dry season relied on tSWC below 20 cm. Propagated *SEs* for tSWC calculations are 0.12-0.42, 0.07-0.38, 0.50-1.05, and 0.53-0.96 mm for layers I-IV, respectively.

5.3.4. Annual soil water budget is influenced by depth-dependent infiltration

The depth-dependent change in soil water retention discussed above clearly influenced the water distribution in the soil profile and its dynamics. Layer-specific infiltration water amounts (mm) were determined using the calculation of layer-specific diurnal SWC change (dSWC, mm), as adapted from Li et al. (2002):

(20) $dSWC = h \times (1 - ST) \times (SWC_d - SWC_{d-1})$

where SWC_d and SWC_{d-1} are the soil water content values of the current and previous day, respectively. Typically to semi-arid environments, SWC fluctuations were larger in shallow layers than in deeper layers (Fig. 3.3a). In a typical precipitation event on January 17^{th}-19^{th} with a total amount of 50 mm, we calculated that 10, 11, 12, and 2 mm of water infiltrated into layers I to IV respectively and none to deeper layers, meaning that 70% of the water input reached the upper 40 cm of the forest soil and 30% was lost through evaporation from the soil, litter and leaf surfaces. The 2010 annual water budget followed an analogous partitioning: we calculated that out of 289 mm of rain, 228 mm infiltrated into the soil, and the residual 61 mm were lost in interception and soil surface evaporation. Using Eq. 19, we estimated that out of the infiltrated 228 mm, as much as 202 mm were available for transpiration (tSWC) and were partitioned into six soil layers (Fig. 3.5). Ultimately, sap flow data indicated that of the tSWC, trees actually used 164 mm, and the residual 38 mm presumably partitioned into transpiration from understory vegetation (Eq. 6).

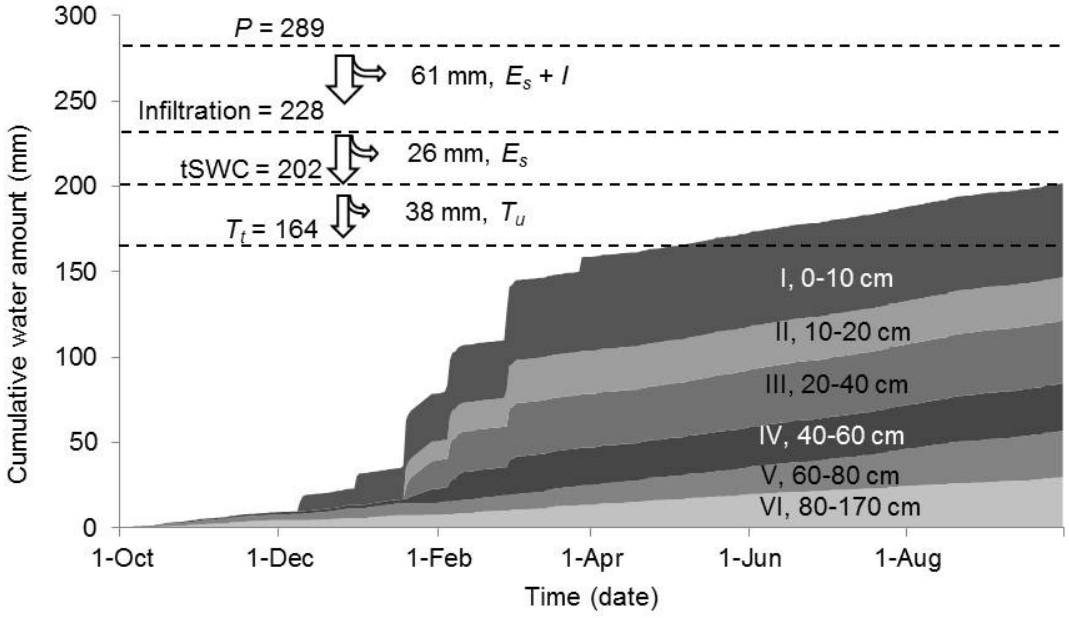

Fig. 3.5. Partitioning of precipitation water (*P*) to hydrological components at Yatir forest during the 2010 growth season (dash lines) and the accumulation over time of transpirable SWC (tSWC, n = 2-3 pits) in the different soil layers. E_s, evaporation from soil; *I,* evaporation of water intercepted by plant foliage; and T_u, transpiration from understory vegetation.

5.3.5. Root depth distribution

Root distribution across the soil profile supported the idea that T_t highly relied on tSWC in the 20-40 cm soil layer. Measurements of root distribution indicated a nearly linear decline with depth from the soil surface down to 1 m, and only very few roots were identified below that level (Table 3.2). The number of fine roots (< 2 mm) in layer III was however slightly higher than in layers I and II. Although a few fine roots were occasionally found below 1 m, the majority of the rhizosphere was confined to higher layers: 66% of roots were above 40 cm (layers I-III) and 85% above 60 cm (layers I-IV).

Table 3.2. Mean (SE) number of roots per square meter of trenched depth profile as function of soil depth, divided into five root diameter categories (n = 22 trenches).

Soil layer	Depth (cm)	0.5-2	2-5	5-10	10-20	>20 mm
I+II	0-20	317 (37)	165 (21)	74 (11)	42 (9)	9 (3)
III	20-40	334 (34)	160 (17)	52 (8)	25 (7)	8 (3)
IV	40-60	241 (32)	70 (16)	24 (5)	6 (3)	1 (1)
V	60-80	126 (21)	50 (18)	8 (3)	3 (2)	1 (1)
VI	80-100	32 (7)	7 (2)	1 (1)	1 (1)	0 (0)
VI	100-120	27 (9)	3 (2)	0 (0)	1 (1)	0 (0)
VI	120-140	7 (4)	0 (0)	1 (1)	0 (0)	0 (0)
VI	140-160	1 (1)	1 (1)	0 (0)	0 (0)	0 (0)
VI	160-180	0 (0)	0 (0)	0 (0)	0 (0)	0 (0)

5.3.6. Water $\delta^{18}O$ of soil and tree sap

Comparing the oxygen isotope composition of soil water from different depths with that of xylem water (not exposed to evaporation) can provide an indicator of the depth of water uptake, if vertical variations in oxygen isotope composition of soil water through the rooting zone are sufficiently large (Zimmermann et al. 1966, Walker and Brunel 1990, Wang and Yakir 2000). However, sap water $\delta^{18}O$ usually reflects a complex mixture of water from multiple depths, and hence a statistical approach is needed (Phillips and Gregg 2003). Results from the IsoSource mixing model applied to our $\delta^{18}O$ data indicated a seasonal shift in depth of water use over the season (Table 3.3). Specifically, the summer $\delta^{18}O$ values seem to indicate a significant contribution from layer III (~70% in average). In autumn, layer II was identified as the primary water source, while in winter the water source seemed equally partitioned among layers I to III (but with large uncertainty due to homogeneity of the soil water $\delta^{18}O$ profile). Finally in spring layer III was identified by the isotope mixing model as the primary water source (~80% in average).

Table 3.3. Partitioning of water sources for tree transpiration using a stable isotope mixing model (Phillips and Gregg 2003). Mean percent (SD) for distributions of feasible solutions of water $\delta^{18}O$ isotopic mass balance, based on tree sap as mixture and soil water as sources.

Soil layer	Depth (cm)	Summer	Autumn	Winter	Spring
I	0	5.6 (5.0)	1.4 (1.5)	7.8 (5.2)	0.1 (0.3)
I	5	10.2 (8.7)	1.9 (1.9)	7.2 (4.8)	2.8 (2.7)
I	10	7.3 (6.3)	4.3 (3.9)	26.4 (20.6)	4.8 (4.4)
II	20	6.1 (5.4)	90.5 (3.1)	29.3 (19.9)	2.4 (2.4)
III	30	14.8 (12.5)	1.9 (1.9)	29.3 (19.9)	8.0 (7.1)
III	40	56.1 (7.0)	n.a.	n.a.	82.0 (6.2)

5.3.7. Relationship between soil texture and water content from ecosystem model simulations

To study the relationship between soil texture and water content, we used the ecosystem gas exchange model MuSICA (Ogée et al. 2003). The SWC in layer III was simulated in two different scenarios: (1) using the more conventional approach of bulk hydraulic properties, applying layer II properties on the entire profile; and (2) using the observed layer-specific soil hydraulic properties as in Table 3.1. Results from the two simulations show that the bulk approach of scenario (1) yielded relatively low soil moisture during the dry season, reflecting unsustainable forest water balance, whereas the more realistic scenario (2) captured the observed, higher SWC during the dry season (Fig. 3.6). Moreover, the difference between the two simulations is emphasized considering their opposite relation to the tSWC threshold of 17%: tSWC is maintained in the root zone in scenario (2) but clearly not in (1).

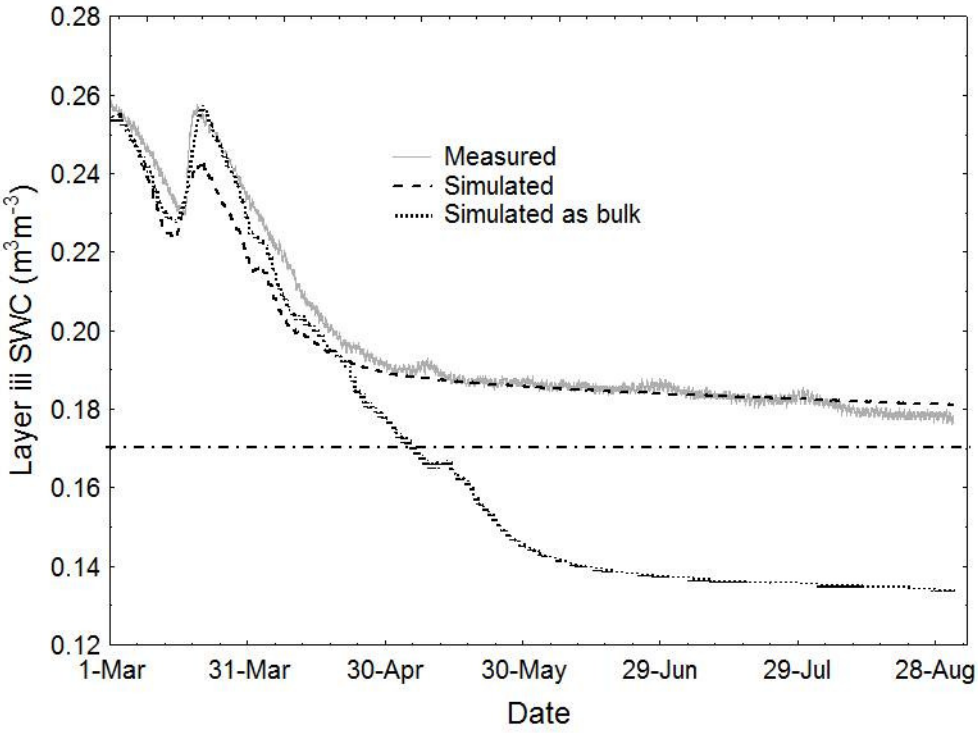

Fig. 3.6. Soil water content (SWC, n = 3) dynamics in layer III measured in Yatir forest during 2007 and simulated with MuSICA in two scenarios: (1) using layer II soil hydraulic properties for the entire profile (simulated as bulk), and (2) using observed layer-specific soil hydraulic properties as in Table 3.1 (simulated). Using the more conventional approach of bulk hydraulic properties (scenario 1) resulted with lower soil moisture during the dry season, below the tSWC threshold (horizontal line), and creating an unsustainable forest ecosystem.

5.3.8. Depth-dependent water availability

Our results indicate that for 2010, the total T_t and P values in Yatir forest were 164 and 289 mm respectively, yielding a T_t/P ratio of 0.57. This ratio is consistent with a previous estimate of 0.53 for the same forest (Raz-Yaseef et al. 2010a), but notably higher than values reported for other conifer forests (0.1-0.5; Roberts 1983) and also for different semi-arid ecosystems (0.35; Miller 1982, Paruelo et al. 2000). Considering only the water that infiltrated into the soil (228 mm, Fig. 3.5) yields even higher ratio of 0.72, indicating only little losses to recharge and soil evaporation, with most of the infiltrating water available for transpiration. We suppose that this high ratio is also strongly linked to depth-dependent soil properties. It was shown in previous forest ecohydrology studies that variability of soil texture with depth affected Ψ_s (Bréda et al. 1995, Warren et al. 2005). Specifically, high (45%) clay content layers were associated with more negative Ψ_s values (for a given SWC) and lower rooting density (Bréda et al. 1995).

Here we show that the high availability of water for transpiration is also supported by local soil structure, composed of a water holding layer III lying on top of a high retention layer IV. The relatively coarse layer III (sand fraction > 40%, Fig. 3.1b) was a major water source for T_t (Figs. 3.4 and 3.5), and was acting as a buffer by allowing a suspended release of rainfall water across weeks and months. Water availability is maintained in this layer for months after the rainy season (unlike in shallower layers, Fig. 3.4a), and its stone fraction of 21% is lower than that of deeper layers (e.g. 48% at 90 cm and up to 100% at 170 cm). In contrast to layer III, high clay content (> 50%) in layer IV (Fig. 3.1b) means that its baseline SWC of ca. 20% is essentially non-transpirable, but it minimizes infiltration and losses into deeper soil layers, thus allowing the accumulation of water in the soil above it. Evidence for such accumulation comes from SWC values exceeding field capacity in layers I and III but not in other layers. For example, at 25 cm depth, we measured SWC values of up to 31% whereas field capacity value (SWC at -0.033 MPa; Israelson and West 1922) was calculated as 30% (in contrast, at 50 cm depth, maximum SWC was 33%, still below the field capacity value of 35%). Additional evidence is provided by model simulations, where prolonged water availability in layer III is associated with the limited infiltration to depths below 40 cm and into the high water retention layer (Fig. 3.6).

The role of layers I and II in the tree water use is important during the rainy season, with both hydraulic (Fig. 3.4) and isotopic (Table 3.3) evidence.

In an ecosystem already restricted by soil depth (33-124 cm, data not shown), the rhizosphere is furthermore concentrated in the 0-60 cm layers (Table 3.2). This narrow root distribution can be explained by changes in the transpirable water content of the various depth layers: fine root density peaks in layer III and declines in the high-retention layers below. Dependence of vertical root distribution in water availability was shown in an oak stand (Bréda et al. 1995), and also in *P. halepensis* and the closely related *Pinus brutia* (Querejeta et al. 2011, Ganatsas and Tsakaldimi 2003, respectively). A similar, narrow root distribution was described in a *P. brutia* forest grown on shallow, stony soil in Greece (Ganatsas and Tsakaldimi 2003). Yet in a deep soil site (average soil depth ~100 cm), *P. halepensis* roots were concentrated between 80 and 100 cm, and none above 40 cm (van Beek et al. 2005). Note, however, that the correlation between water use and root distribution can be non-linear: a few sinker roots may dominate tree water uptake (Mickovski and Ennos 2003) especially under stress (Nadezhdina et al. 2007), and the correlation can be complicated by hydraulic redistribution, i.e. root-assisted vertical water transport (Nadezhdina et al. 2006).

5.3.9. Inter-annual variations in transpirable soil water content

On the inter-annual time scale, one of the important issues to consider is defining the growth season (i.e. delineating its onset and termination). In water-limited ecosystems such as the study site, tree growth highly coincides with water availability (Klein et al. 2005, Maseyk et al. 2008, Klein et al. 2012), and we therefore propose to define the growth season using tSWC estimates. Predictions of the onset of the growth season have so far mostly relied on precipitation data, with obvious difficulties in characterizing rainfall events by their intensity (e.g. mm d^{-1}) or their frequency of occurrence (i.e. effective time between two events; e.g. in Zeppel et al. 2008; Raz-Yaseef 2012). Figure 3.4 shows that emergence of tSWC in layers II-IV on January 18th (vertical line marking the onset of the wet season) was shortly followed by a 3-fold increase in transpiration rates starting from January 21st, potentially marking the onset of the growth season in winter (Maseyk et al. 2008). Further coordinated sap flow and SWC measurements should improve the predictability of the onset of growth season.

However, it is probably more important to examine the association between tSWC and the termination of the growth season, which can greatly influence forest sustainability and actual survival. Inter-annual variations in tSWC reflected variations in total annual precipitation as well as in the timing of the first and last rain events (Fig. 3.7a). It is the time between the last rain of a given growth year and the first rain of the following growth year that defines the length of the drought interval. During the dry season T_t relied mainly on layer III (Fig. 3.4), and to a lesser extent, on deeper layers. Therefore, maintaining T_t across the drought period depends on the water dynamics in this layer, which varied between years (Fig. 3.7a). For example, in summer 2006 trees had a continuous water supply (indicated by positive tSWC values in layer III across the entire length of the dry season). In contrast, in 2007 transpirable water was unavailable for nearly 2 months before the onset of the next active season on December 20th (Fig. 3.7a). Even longer water shortages were observed in the summer seasons of 2008 and 2009, lasting about 5 and 4 months respectively.

Notably, during the consecutive drought years of 2008 and 2009, interruptions in tSWC in layer III are correlated with increase in observed tree mortality, affecting 5-10% of the trees in Yatir. The ability of *Pinus halepensis* to survive intense and prolonged drought has been shown in the field (Maseyk et al. 2008, Schiller and Atzmon 2009). In a controlled drought experiment, *P. halepensis* saplings exposed to 3-weeks drought cycles demonstrated a 90% survival rate, even at only 25% of the optimal water supply (Klein et al. 2011). Being a drought-avoiding species, *P. halepensis* may enforce stomatal closure for periods longer than a month, risking negative carbon balance and carbon starvation, potentially leading to mortality. Our results indicate that the difference between survival and large-scale tree mortality may be related to the length of period with positive tSWC. In the study period this was reflected in the difference between 2 and 4 months of zero tSWC in 2007 vs. 2009 (Fig. 3.7a). Based on our preliminary 5-year study, we propose a threshold value of about 3 months zero tSWC for *P. halepensis* forest sustainability at our site.

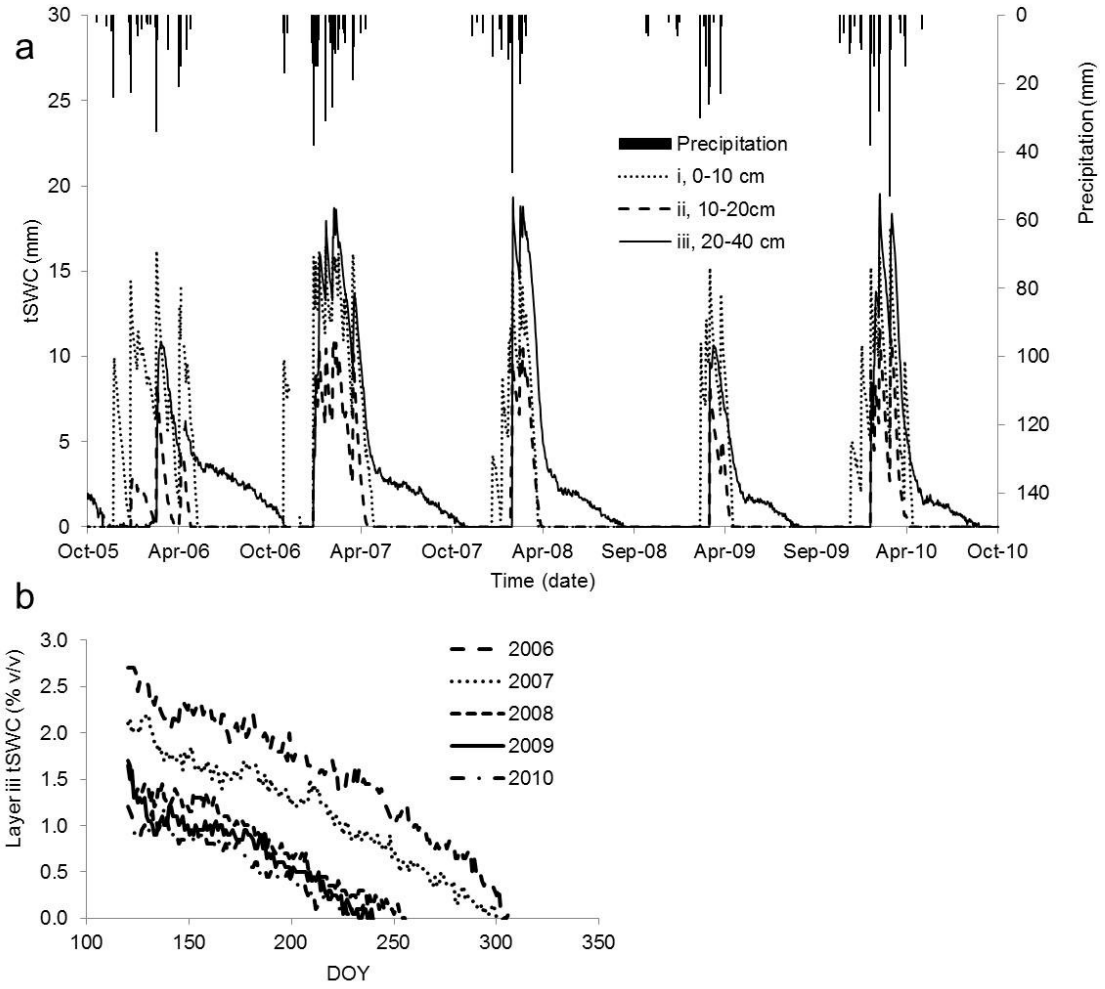

Fig. 3.7. (a) Transpirable soil water content (tSWC, n = 2-3) in three depth layers and precipitation in Yatir forest during 2006-2010 (annual precipitation amounts were 224, 308, 200, 160, and 289 mm respectively). Droughts during 2008 and 2009 resulted in long intervals (up to 5 months) of zero water availability, ultimately leading to large-scale tree mortality. (b) Zooming in on the linear decline of tSWC in layer III after April 30th. Regression slopes are -0.012, -0.011, -0.012, -0.011, and -0.009% d^{-1} for 2006-2010 respectively (R^2 = 0.92-0.97), allowing early estimate of the date of tSWC exhaustion in this forest ecosystem.

Could the date of tSWC exhaustion be estimated? It seems that this is possible at least on a seasonal basis. A careful examination of the inter-annual patterns of tSWC in layer III (Fig. 3.7b) suggests that although the spans of soil moisture availability varied between years, tSWC quenching rate followed a similar pattern. Linear regressions of layer III tSWC decline between April 30th (which was always after the last significant rain event) and the last date of water availability on

time, generated slopes of -0.012, -0.011, -0.012, -0.011, and -0.009% d^{-1} for 2006-2010 respectively (R^2 = 0.92-0.97). Therefore, the last date of positive tSWC in layer III (and the layers above it) for a given year can be estimated according to:

(21) $t_f = t_i + (tSWC_{ti} / 0.011)$

where t_f is the final date of water availability, t_i the initial date of linear quenching (April 30th), and $tSWC_{ti}$ the initial layer III tSWC on April 30th. Also, this means that a last date of water availability can be predicted by the end of April, still before summer. For example, using eq. (21), an initial layer III tSWC of 3% should suffice up to September 30th. Together with the aforementioned 3-months drought threshold this means that in such scenario, significant precipitation must come before December 30th to ensure forest sustainability. The ability to clearly define the timing of tSWC exhaustion has implications for estimating the growth season length, and forest productivity and sustainability under different climate change (precipitation) scenarios.

5.4. From leaf to forest scale: water use of *P. halepensis* and the coexisting, anisohydric *Quercus calliprinos* and the impact of a semi-arid pine forest on local water yield.

In order to upscale the hydraulic adjustments identified at the organismal scale to forest scale, and to quantify their impact on the forest water balance, two scientific approaches were applied:

(i) Comparing the water use of *P. halepensis* and the coexisting, anisohydric *Quercus calliprinos*.

(ii) Estimating the impact of a semi-arid pine forest on local water yield from transpiration rates under different stand densities.

The results of approach (i) are summarized in sections 5.4.1-8. A preliminary synthesis of the results of approach (ii) is summarized in sections 5.4.9-11.

5.4.1. Stomatal regulation in *P. halepensis* and *Q. calliprinos*

Mean (n=13) leaf water potential (Ψ_l) and stomatal conductance (g_s) at mid-day during April 2011 showed large differences between the two species, in agreement with their contrasting mode of stomatal regulation. The oak leaves had significantly lower Ψ_l than the pine leaves (-2.8±0.38 vs. -2.4±0.43 MPa respectively, P<0.01) and higher g_s (0.17±0.060 vs. 0.08±0.015 mol H_2O m^{-2} s^{-1} respectively, P<0.001). In general, for any given Ψ_l, g_s of *Q. calliprinos* was ~2-fold that of *P. halepensis*.

5.4.2. Stomatal adjustments and transpiration

The response of g_s to increasing levels of vapor pressure deficit (VPD) was measured in the two species. Under moderate VPD (from 1 to 4 kPa) both species reduced g_s in response to VPD increase (Fig. 4.1a, right panel). The oak leaves had higher g_s than the pine leaves (0.15±0.102 vs. 0.07±0.035 mol H_2O m^{-2} s^{-1} respectively, P<0.01) although the decrease rate was rather similar (-0.017 vs. -0.012 mol H_2O m^{-2} s^{-1} kPa^{-1} respectively). A continued reduction in g_s at increasingly higher VPD (from 3 to 8 kPa) was observed in *Q. calliprinos*. However in *P. halepensis* g_s was reduced to levels below 0.005 mol H_2O m^{-2} s^{-1} (Fig. 4.1a, left panel). Very low g_s levels were maintained in *P. halepensis* throughout the morning and afternoon hours of a summer day (Fig.4. 1b, left panel), in contrast with relatively large stomatal adjustments in *Q. calliprinos*. The ability of *Q. calliprinos* to open stomata in the morning (at VPD < 4 kPa), unlike *P. halepensis*, was also shown in a spring day (Fig. 4.1b, right panel).

The differences in g_s resulted in large differences in transpiration (T) rates between the two species in spring (2.1±1.09 vs. 2.9±1.65 mmol H_2O m^{-2} s^{-1} respectively, $P<0.01$), and further in summer (0.2±0.06 vs. 0.8±0.26 mmol H_2O m^{-2} s^{-1} respectively, $P<0.001$; Fig. 4.1c).

5.4.3. Seasonal gas exchange patterns of *P. halepensis* and *Q. calliprinos*

Periodic measurements of transpiration (T) and net assimilation (A) during seven field days (four in Beit Dagan and three in Harel forest) showed seasonal gas exchange patterns of the two species. In both species mean T and A rates were higher in winter and spring (1-4 mmol H_2O m^{-2} s^{-1} and 3-12 µmol CO_2 m^{-2} s^{-1} respectively) and lower in summer and fall (0.2-1.0 mmol H_2O m^{-2} s^{-1} and 1-3 µmol CO_2 m^{-2} s^{-1} respectively), as expected for trees growing in a Mediterranean ecosystem characterized by a single, short rainy season. In five out of seven field days, mean T from the oak leaves was ~2-fold higher than from the pine needles, and was equal only during winter (Fig. 4.2a). Differences in A were usually small and insignificant (Fig. 4.2b), showing that leaf-scale carbon uptake amounts were similar in the two species. Integrating the changes in T and g_s resulted with higher intrinsic water-use efficiency (WUE_i) for *P. halepensis* during most of the time (Fig. 4.2c).

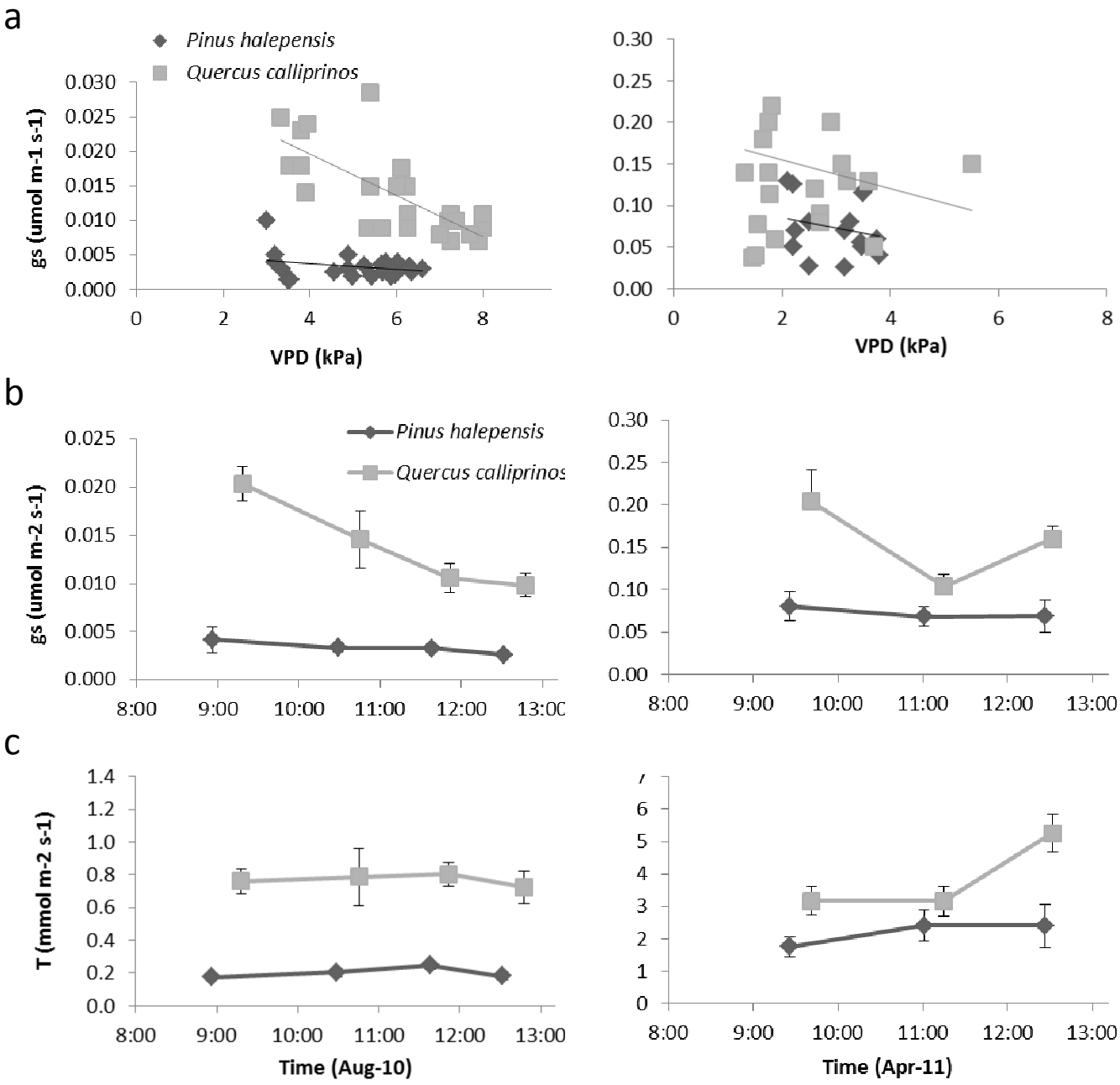

Fig. 4.1. Relationships between stomatal conductance (g_s) and vapor pressure deficit (VPD; a) in *P. halepensis* and *Q. calliprinos* along the morning and afternoon hours of a summer day (left column) and a spring day (right column) at Beit Dagan. Changes in g_s (b) and transpiration (T; c) for the two species on the respective days at Beit Dagan. *Error bars* represent the standard error of the mean (n = 6). The two species responded to increase in VPD by reduction of g_s, except for *P. halepensis* in the summer, when g_s was close to zero. g_s and T were up to 4-fold higher in *Q. calliprinos*.

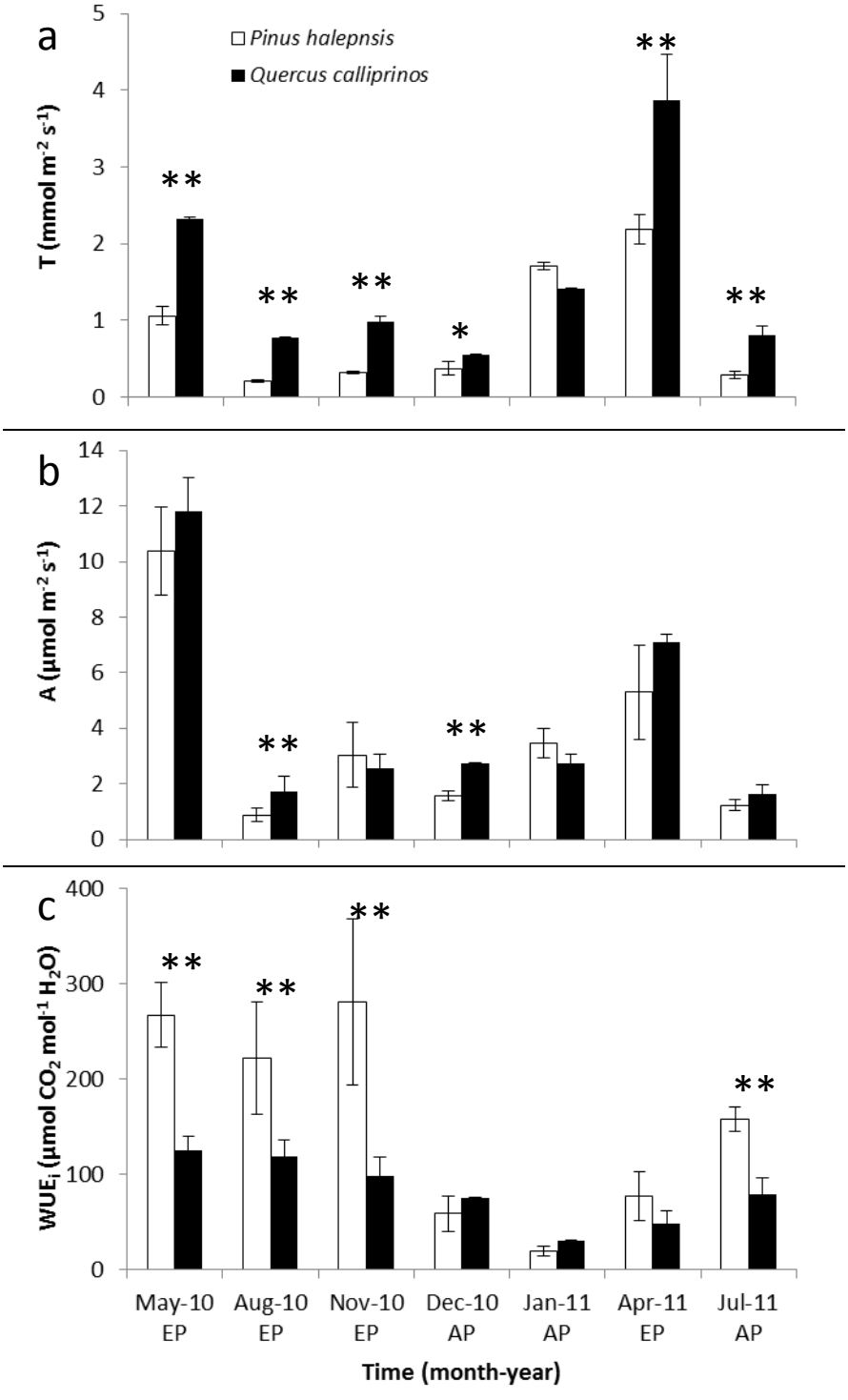

Fig. 4. 2. Mean ± SE (*n* = 12-24) transpiration (T; a), photosynthesis (A; b) and intrinsic water-use efficiency (WUE_i; c) for *P. halepensis* and *Q. calliprinos* during the seven field days at the Beit Dagan experimental plot (EP) and at the Harel afforestation plot (AP). Star symbols indicate differences between paired measurements are significant at $\alpha<0.05$ (*) or $\alpha<0.005$ (**). Significantly higher T rates in *Q. calliprinos* throughout the year (a, except in winter) and similar A rates in the two species (b) meant that *P. halepensis* had higher WUE_i during most of the time (c).

5.4.4. Tree-ring $\delta^{13}C$

The fractionation of the stable carbon isotope composition, $\delta^{13}C$, was measured in tree rings of *P. halepensis* and *Q. calliprinos* and used as a marker for stomatal regulation during photosynthesis. To test the long-term differences in tree-ring $\delta^{13}C$ between the two species, we selected a sequence of four annual tree-rings formed between 1997 and 2000, yielding 34-36 sub-annual slices (Fig. 4.3). The mean ± SE values of $\delta^{13}C$ of *P. halepensis* and *Q. calliprinos* were -24.9±0.2‰ and -26.4±0.1‰, respectively, and the 1.5‰ difference was highly significant ($P<0.001$). The ranges of $\delta^{13}C$ values of *P. halepensis* and *Q. calliprinos* were -22.6 - -26.7‰ and -24.9 - -27.4‰, yielding ranges of 4.1‰ and 2.6‰, respectively. Intrinsic water-use efficiency (WUE_i* from Eq. (11); Fig. 4.3) showed the expected annual trends, with maximum WUE_i* values at the start or end of each tree-ring, and minimum WUE_i* values at the middle of the ring. The deposition of carbon into structural tree-rings is confined to the growing season, which is governed, in our thermo-Mediterranean site, by precipitation (P). Therefore, the $\delta^{13}C$ record reproduced the discrimination against ^{13}C between October and April and not throughout the entire year. The distribution of precipitation can also explain the large inter-annual differences in the WUE_i* trends of both species: (1) Higher WUE_i* values were measured in the 1999 growing season (81.9 and 64.9 μmol CO_2 mol^{-1} H_2O vs. the overall mean 74.6 and 63.6 μmol CO_2 mol^{-1} H_2O in *P. halepensis* and *Q. calliprinos*, respectively) which was a drought year (P=289 mm) and also produced very narrow tree-rings; (2) Lower WUE_i* values were measured in 1998 (P=504 mm) and 2000 (P=485 mm, also characterized by two major rain events of P>50 mm each); and (3) Fluctuations in WUE_i* values during 1997 (P=480 mm) are related to two large (>1 month) pauses between consecutive rain events during the growing season. Evidently, the difference in WUE_i* between the two species was not constant throughout the 4-years period, and vanished altogether in course of 2000. This change is discussed below.

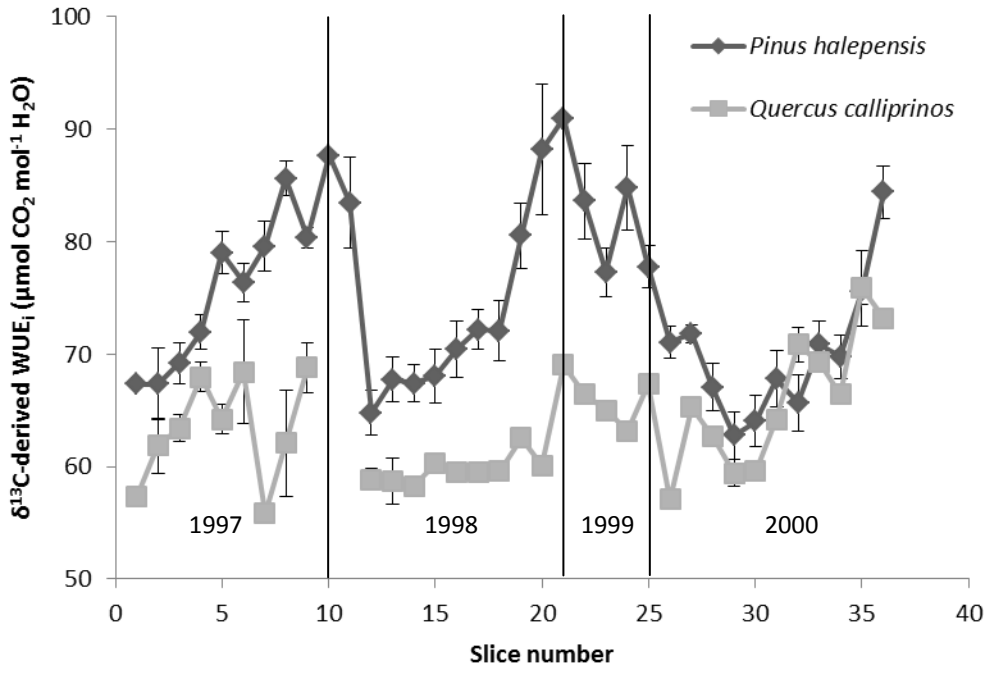

Fig. 4.3. Mean ± SE WUE_i derived from $\delta^{13}C$ of the 1997-2000 tree-rings of *P. halepensis* and *Q. calliprinos* trees (*n* = 1-5) growing at the Beit Dagan experimental plot. Annual precipitation amounts were 480, 504, 289, and 485 mm for 1997, 1998, 1999, and 2000 respectively. The tree-ring of the 1999 drought year was identified only in one of three cores sampled from *Q. calliprinos*, and hence no repetitions were available for that tree-ring.

5.4.5. Stand-scale water-use of *P. halepensis* and *Q. calliprinos*

Leaf-scale transpiration measurements (Fig. 4.2a) were used in a preliminary calculation of the diurnal tree-scale water-use for *P. halepensis* and *Q. calliprinos* during the seven field days, using Eq. (13). Water-use amounts of the pines ranged between 2.9 mm $tree^{-1}$ d^{-1} in April and 0.3 mm $tree^{-1}$ d^{-1} in August; the oaks transpired 6.5 and 0.8 mm $tree^{-1}$ d^{-1} in April and late autumn December, respectively (data not shown). An annual total tree-scale water use amount, T_t, was calculated at 6.6 and 10.0 mm $tree^{-1}$ $year^{-1}$ for *P. halepensis* and *Q. calliprinos*, respectively (Table 4.1). The 50% higher tree-scale water-use of the oak vs. the pine is in agreement with constantly higher transpiration rate in the oak leaves, considering their comparable total leaf area (37.7 and 40.0 m^2 for 15-cm DBH *P. halepensis* and 15-cm DMC *Q. calliprinos*, respectively), and in spite of partial defoliation during three months a year in the oak.

Species-specific T_t values were used in a preliminary estimate of stand-scale water-use of *P. halepensis* and *Q. calliprinos* and its impact on the local water yield. Specifically, three questions were addressed: (1) what is the maximum stand density for each forest type (pine forest and oak maquis), assuming zero water yield (i.e. no surface runoff and deep soil recharge) and for three precipitation regimes (P; 300, 500, and 700 mm); (2) what is the water yield of forest with minimum stand-density (200 trees ha^{-1}) under P = 500 mm; and (3) what is the minimum P which can support such a forest (200 trees ha^{-1}), assuming zero water yield. Table 4.1 shows that, in any of the three P scenarios, the forest stand density was moderately higher for pine. Under P = 300 mm (semi-arid climate), we calculated an oak stand density of 138 trees ha^{-1}, suggesting that mature oak maquis is unsustainable in such conditions. A minimum P requirement for *Q. calliprinos* was calculated at >400 mm, and <300 mm for *P. halepensis*. Under P = 500 mm, the water yield of the pine stand was more than 3-fold that of the oak stand.

5.4.6. Relationship between stomatal regulation and leaf gas exchange

Figures 4.1 and 4.2 confirm our first hypothesis that water amounts used by the anisohydric *Q. calliprinos* are larger than those used by the isohydric *P. halepensis*. Moreover, this was not limited to the summer drought but rather persisted during spring and fall. A typical drought avoidance strategy was demonstrated by the pine trees, restricting g_s already at VPD<3 kPa (Fig. 4.1). In contrast, the oak trees dynamically adjusted g_s even at VPD>5 kPa. The consistently higher T rates of *Q. calliprinos* are related to at least two physiological differences between the species under study: (1) higher rooting depth of *Q. calliprinos* (Oppenheimer 1957) should increase its access to soil water resources, and (2) lower Ψ_l of *Q. calliprinos*. This means that *Q. calliprinos* has higher soil water availability than *P. halepensis* at any given soil water potential (Ψ_s). For example, while *P. halepensis* is unable to extract soil water at Ψ_s<-2.0 MPa, *Q. calliprinos* may extract water even at Ψ_s<-3.5 MPa (Schiller et al. 2003). The higher water-use in *Q. calliprinos* can be related ecologically to the higher inter-species competition in the Mediterranean maquis vs. the pine forest.

Figures 4.2c and 4.3 confirm our second hypothesis that the pines have higher WUE_i than the oaks under most circumstances. The pinyon/juniper forest of SW USA

is the most studied isohydric/anisohydric forest tree system (Lajtha and Barnes 1991, West et al. 2007a, McDowell et al. 2008). In agreement with our findings, Lajtha and Barnes (1991) showed that the isohydric tree species (pinyon, *pinus edulis*) had usually higher WUE than the anisohydric species (juniper, *Juniperus osteosperma*). However a clear implication on water-use has not been shown: while juniper trees had slightly higher sap flow rates than pinyon trees without summer precipitation, a reversed trend was observed following rain events (West et al. 2007a, West et al. 2007b). It is possible that the observed difference in water-use between pines and oaks in our study is conditioned by the sharp precipitation seasonality of the Mediterranean. Stomatal conductance and water-use efficiency of oaks and pines were compared in previous studies (Guehl et al. 1995, Kolb and Stone 2000, Ferrio et al. 2003; see summary in Table 4.2). The findings of these studies were consistent with our results, except for the comparison of *Pinus pinaster* and *Quercus robur* (Guehl et al. 1995), where both species can be regarded as isohydric. This may indicate that the differences in g_s and WUE_i were not related to general differences (e.g. morphological, physiological) between oak and pine species, but rather to the specific differences between isohydric and anisohydric species, as in the case of the juniper and pinyon (Table 4.2).

Table 4.2.

Relationships between stomatal conductance (g_s), intrinsic water-use efficiency (WUE_i), and wood $\Delta^{13}C$ of *Pinus* spp. (*P.*) vs. *Quercus* (*Q.*) spp. and of isohydric (i) vs. anisohydric (an) tree species in this study and in four previous studies.

Species studied	g_s	WUE_i	$\Delta^{13}C$	Reference
P. pinaster^{i} vs. *Q. robur*^{i}	i<an	i<an	i>an	Guehl et al. 1995
P. ponderosa^{i} vs. *Q. gambelii*^{an}	i<an	i>an	-	Kolb and Stone 2000
P. halepensis^{i} vs. *Q. ilex*^{an}	-	-	i<an	Ferrio et al. 2003
P. edulis^{i} vs. *Juniperus osteosperma*^{an}	i<an	i>an	i<an	West et al. 2007b
P. halepensis^{i} vs. *Q. caliprinos*^{an}	i<an	i>an	i<an	This study

5.4.7. Relationship between tree-ring $\delta^{13}C$ and leaf gas exchange

The multiannual trends of $\delta^{13}C$-derived WUE_i* (Fig. 4.3) confirm the observed differences between the anisohydric *Q. calliprinos* and the isohydric *P. halepensis* in g_s and WUE_i. The 1.5‰ higher $\delta^{13}C$ of the pine is expected from its tight control of g_s, compared to the oak species. Ferrio et al. (2003) found 1.5‰ higher $\delta^{13}C$ in *P. halepensis* relative to *Q. ilex*, also a Mediterranean oak species. The 1.5‰ higher $\delta^{13}C$ range of *P. halepensis* is also expected, considering its large seasonal changes in WUE_i, between 20 and 280 µmol CO_2 mol^{-1} H_2O vs. 30-125 µmol CO_2 mol^{-1} H_2O in *Q. calliprinos* (Fig. 4.2c). $\delta^{13}C$-derived WUE_i* can be partly compared to WUE_i calculated from gas-exchange, noting that tree-rings provide an integrative measure, while leaf gas-exchange observations provide a transient measure. Such comparison is confined by the timing of carbon deposition into tree-rings, which is between October and April in our case. Averaging the WUE_i values corresponding to observations taken during this timeframe (November to April; Fig. 4.2c) yields 108.5±58.6 and 62.8±15.1 µmol CO_2 mol^{-1} H_2O in *P. halepensis* and *Q. calliprinos*, respectively. The $\delta^{13}C$-derived WUE_i* means are 74.6±1.2 and 63.6±0.8 µmol CO_2 mol^{-1} H_2O in *P. halepensis* and *Q. calliprinos*, respectively. The oak values are similar, but not the pine values, probably due to relatively small number of gas exchange observations, shown by excessive errors, particularly in the pine value. The inter-species differences in leaf gas exchange were smaller at the height of the wet season (Fig. 4.2) and did not carry over to the isotopic signal. However, under the very wet conditions that followed the two large rain events of the year 2000 (P>100 mm each) WUE_i* values of *P. halepensis* decreased to 62.8 µmol CO_2 mol^{-1} H_2O, similar to the *Q. calliprinos* values. This observation confirms that, conditions permitting, g_s of the pine can be as high as that of the oak, as shown in Figures 4.1 and 4.2.

5.4.8. Water-use of *P. halepensis* and *Q. calliprinos* and the forest water balance

The preliminary evaluation presented in Table 4.2, although neglecting important feedback responses (e.g. tree-scale water-use changes influenced by stand density), demonstrates how differences in stomatal regulation among forest tree species can be translated into important differences in stand-scale water balance. At P = 490 mm and considering a stand density of ~300 trees ha^{-1} (as in our afforestation site in Harel forest, Israel) annual tree water-use is 200 and 300 mm in a pine forest and oak maquis, respectively. In addition, promotion of understory vegetation growth by *Q.*

calliprinos but not by *P. halepensis*, which was not accounted for in our simplistic calculation, should potentially increase differences in stand-scale T. Our crude estimates are consistent with sap-flow based annual tree water-use amounts reported for the two species. At 230 trees ha^{-1}, an oak stand tree water-use was 293 mm (Schiller et al. 2010) and 358 mm at 470 trees ha^{-1} in a young stand (Schiller et al. 2003). These numbers mean that the oak T_t was 12.7 mm $tree^{-1}$ $year^{-1}$ in the sparse maquis and 7.6 mm $tree^{-1}$ $year^{-1}$ in the denser, young maquis. Tree water use in a semi-arid, 400 trees ha^{-1} pine forest, was calculated at 210 mm (Schiller and Cohen 1998), which was later reduced to 164 mm, following thinning to 300 trees ha^{-1} (Klein et al. 2012b). This means a *P. halepensis* T_t of 5.2-5.5 mm $tree^{-1}$ $year^{-1}$, lower than our estimate of 6.6 mm, based on *P. halepensis* transpiration in Mediterranean sites.

P. halepensis forests can grow at P<400 mm (Maestre et al. 2004, Ferrio et al. 2003) and even in semi-arid sites on the dry timberline (Rotenberg and Yakir 2009, Klein et al. 2012a), whereas *Q. calliprinos* maquis covers large areas in the more humid Galilee region of Northern Israel (P = 550-1,000 mm; Schiller et al. 2010). The observed differential distribution of the two tree species is explained by our results, showing a substantially higher P requirement for an oak maquis relative to a pine forest (Table 4.2). The higher water demand of the oak was reflected in a dramatic decrease of leaf area index, from 4.0 to 1.5, following subsequent drought years in the Galilee (Sever and Neeman 2008). Tree water-use is one of multiple hydrological fluxes that control the water balance of a forest area. The partitioning among these fluxes depends largely on determinants such as annual precipitation and stand density (Raz Yaseef et al. 2010, Klein et al. 2012b). Considering a first approximation of this partitioning, the results in Table 4.2 provide a valuable estimate of sustainable stand densities for the two species under three P regimes, and the minimum P for afforestation site selection. In general, to avoid a forest collapse scenario (e.g. following drought years), mature stands should not exceed 485 and 322 trees ha^{-1} for pine and oak, respectively.

The difference between the water yield estimates for pine and oak (Table 4.2) is substantial, especially considering the relatively small precipitation budget in our scenario (P = 500 mm). The effect of tree cover on WY was usually quantified in deforestation experiments (Sahin and Hall 1995, Stednick 1996, Zhang et al. 2001, Brown et al. 2005). In fifteen forest sites in USA where P≤700 mm and the area cut was 15-100%, increases in WY were 47±13 mm (data adapted from Stednick 1996),

still lower than the potential WY change predicted by an oak-pine conversion in our analysis. Sahin and Hall (1995), who had analyzed 145 catchment experiments around the globe, quantified 17-19 mm and 20-25 mm change in WY per 10% change in forest cover for deciduous and coniferous forest, respectively. Interestingly and in contrast to our findings, the impact on WY was larger in the coniferous forest compared to the deciduous forest. Ongoing research in our group is focused on the partitioning of hydrological fluxes in forests across a precipitation gradient in Israel, enabled by a state-of-the-art mobile laboratory. Data that will become available during the next 1-2 years should allow a better quantification of T_t and WY at various P levels between 285 and 710 mm.

Table 4.2.

Estimates of maximum stand density (sd, trees ha^{-1}), water yield (WY, mm) and minimum annual precipitation (P, mm) for mature stands of *Pinus halepensis* and *Quercus calliprinos*, based on the species-specific annual water use amount (T_t, mm $tree^{-1}$ $year^{-1}$) and using Eq. (15): $WY = P - (T_t \times sd + T_u + I + E_s)$; see Methods.

Species	T_t	Maximum **sd**			**WY**	Minimum **P**
		P=300, WY=0	P=500, WY=0	P=700, WY=0	P=500, sd=200	WY=0, sd=200
Pinus halepensis	6.6	208	347	485	97	289
Quercus calliprinos	10.0	138	230	322	30	435

5.4.9. The effect of stand density on leaf-scale conditions and gas exchange rates

Leaf-scale measurements in plots thinned to 100, 200, and 300 trees ha^{-1} indicated significant effects of stand density on environmental parameters and gas exchange rates. Average leaf-scale gas exchange measurements from 10 field days along two years show the differences between three stand density levels (Fig. 4.4a). The average photosynthetic active radiation (PAR) at the surface of the measured leaves was >50% higher at the low density stand than at the other densities. Inter-tree shading on the lower branches, where measurements took place, limited PAR to ~450 μmol m^{-2} s^{-1} in both 200 and 300 t ha^{-1}. Net photosynthesis (A) followed the changes in PAR and increased from 2.1 to 2.5 and 3.5 μmol m^{-2} s^{-1} in 300, 200 and 100 t ha^{-1}, respectively. Differences in vapor pressure deficit near the leaf surface (VPD) across densities were milder and not significant, suggesting a high level of eddy mixing within the canopy already at 300 t ha^{-1}. Similarly, average transpiration (T) rates were 10% higher at the low density stand than at the other densities, but this difference was not statistically significant. Differential effects between the major increase in A and the minor increase in T at the low density stand meant higher water use efficiency (WUE) in trees growing at that density.

5.4.10. Upscale to stand-scale gas exchange rates using leaf area index (LAI)

A first attempt to assess the implications of leaf scale observations to the stand level were made, neglecting effects such as gradients within the canopy or thinning stress. Gas exchange rates, measured per leaf area, were up-scaled to stand-scale values (rates per ground area) using concurrent LAI data. Understanding of the relationships between stand density and canopy cover in Yatir forest has been established in previous studies (Sprintsin et al. 2011). By the end of the first year following the thinning (2010), LAI values were 1.54, 1.33 and 0.90 in 300, 200 and 100 t ha^{-1}, respectively. This suggested that differences in stand architecture were higher between 200 and 100 t ha^{-1}, than between 300 and 200 t ha^{-1}, in agreement with the differences in PAR (Fig. 4.4a). Simply multiplying T and A averages in Fig. 4.4a by these LAI values yielded a preliminary estimate of stand-scale gas exchange rate (Fig. 4.4b). The thinning significantly decreased T, from 0.85 to 0.72 and 0.55 mmol m^{-2} s^{-1} in 300, 200 and 100 t ha^{-1}, respectively, but maintained A at ~3.2 μmol m^{-2} s^{-1}. This is because leaf-scale T was relatively similar across densities, while leaf-scale A increased with thinning.

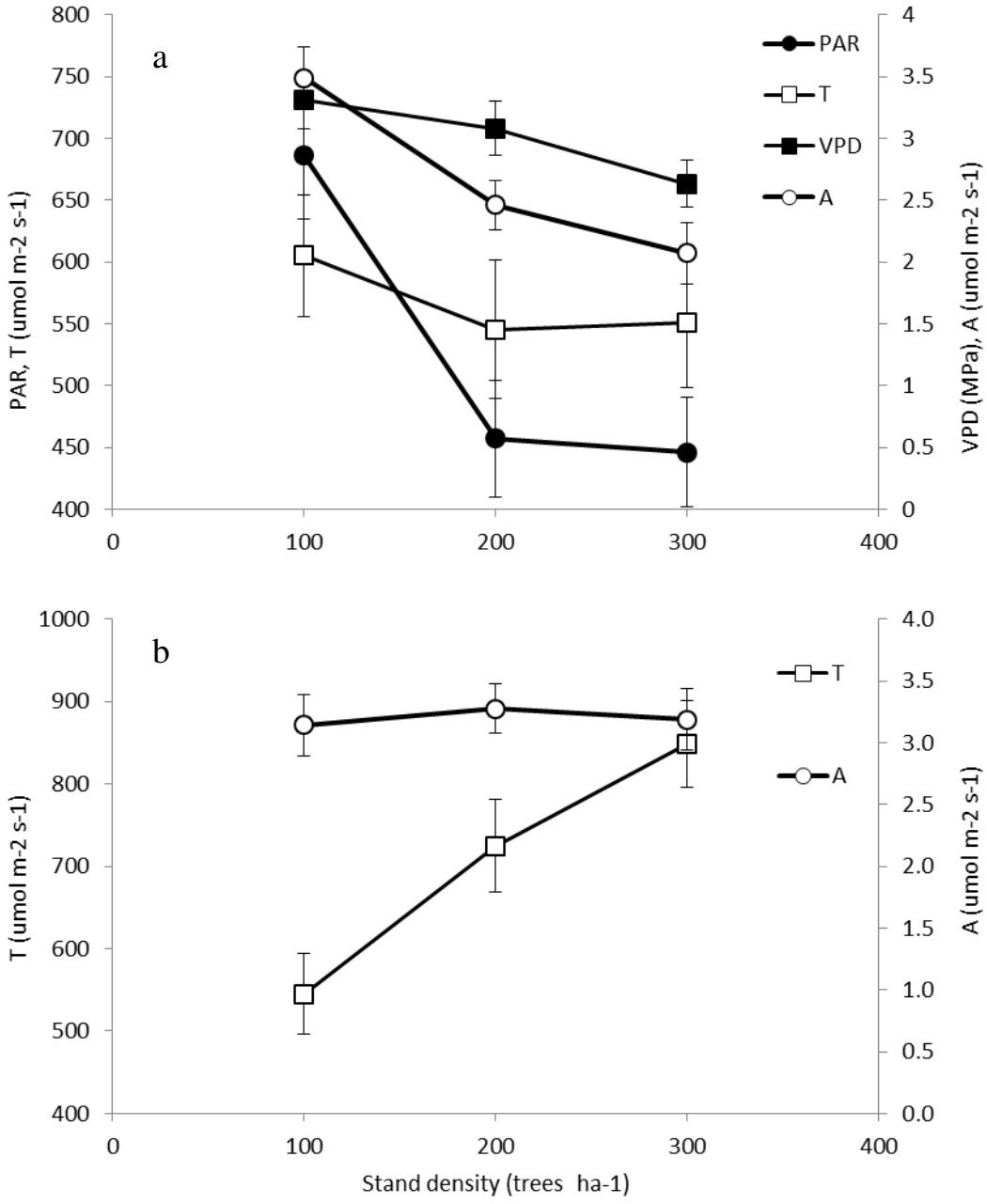

Fig. 4.4. Stand-density influence on leaf-scale photosynthetically active radiation (PAR), vapor pressure deficit (VPD), leaf transpiration (T) and net assimilation (A), (a), and stand-scale T and A (b) in Yatir forest. Each data-point is the mean (±SE) of 120 observations in 10 field days over two years.

5.4.11. The thinning bias

The thinning practice introduces some uncertainty to the effect of stand density on tree and forest activities. A stand density obtained by the dramatic, immediate,

decrease induced by thinning cannot simulate differences in native stand density, where relationships between individual trees (e.g. crowns competing on light, root systems competing on soil moisture, etc.) are often in equilibrium. We accounted for this discrepancy by including an unthinned control stand, at a native stand density of 220 t ha^{-1}. Using the average leaf-scale gas exchange rates in 300 and 200 t ha^{-1} (Fig. 4.4a), the linearly extrapolated average A and T rates in 220 t ha^{-1} are estimated from Fig. 4.4a at 2.4 μmol m^{-2} s^{-1} and 0.55 mmol m^{-2} s^{-1}, respectively. However the measured leaf-scale A and T averages in the unthinned stand were 3.1 μmol m^{-2} s^{-1} and 0.63 mmol m^{-2} s^{-1}, respectively. This meant that trees at the thinned stands were less active than trees at the control stand, suggesting the possibility of thinning stress, as described in other studies (Peltola et al. 2002, Pukkala et al. 2002, Di Mateo et al. 2010, Kariuki 2008). This effect complicated our interpretation of stand density effects and should be accounted for in the final analysis. In addition, the impact of thinning stress is often transient (Di Mateo et al. 2010), and hence stand density effects can be potentially measured directly within the timeframe of this long-term ecological research (LTER).

6. Discussion

The main findings and conclusions of this research are summarized in section 2, and the results of specific projects are discussed in their respective sections (5.1-5.4). This discussion is dedicated to two additional aspects: (1) synthesizing the conclusions of different projects into an overall perspective of the eco-physiology of water use in *P. halepensis* under semi-arid conditions; and (2) exploring the potential implications of this study in broader perspectives, e.g. for other tree species and for forests under more favorable climatic conditions. Finally, we discuss the potential implications for forest management.

6.1. Eco-physiology of water use in *P. halepensis*

This study indicates four major properties defining the eco-physiology of water use in *P. halepensis*: (1) Drought avoidance, rather than tolerance, (2) Isohydric stomatal regulation, (3) Narrow hydraulic safety margin, and (4) Remarkable ability to refill cavitated xylem and restore xylem conductivity. Drought avoidance of *P. halepensis* is strongly linked to its isohydric behavior, i.e. relatively high values of leaf water potential trigger stomatal closure (see 5.4.1-5). However, it is important to note that not all properties are inter-related. For example, the isohydric Pinyon pine (*Pinus edulis*) of North America closes stomata at -2 MPa, but loses 50% of xylem conductivity only at -4.5 MPa, which makes a relatively wide safety margin. On this background, the narrow safety margin of *P. halepensis* is interpreted as a means to maximize carbon uptake at the limits imposed by its fairly sensitive xylem. Firstly, growing in a semi-arid environment and exposed to long seasonal droughts, *P. halepensis* adopted narrow tracheids and low hydraulic conductance to adjust to the low soil water availability and prevailing soil water potential. This likely contributed to the observed low water use and the relatively low mean stomatal conductance. Secondly, leaves adapted in order to utilize the maximal operational range available and extended stomatal conductance to CO_2 while avoiding carbon starvation as much as possible, resulting in leaf water potential approaching the 'danger zone' for the hydraulic system. As a result, *P. halepensis* is more efficient than most tree species in terms of using the carrying capacity of the xylem (Sperry 2004). An inescapable side effect of such risky behavior is high levels of cavitation under drought, and the observed rapid refilling is probably a complimentary adaptation linked to living close

to the limits of hydraulic failure (see 5.1.3.). Whether this set of water use properties is unique or common to other species is discussed below.

6.2. A broader perspective

Specific projects in this research included an additional forest tree species (*Quercus calliprinos*), and the forest sites at Harel and Beit Dagan as well as Rome, Italy. Yet the majority of the study was performed in Yatir forest, on one tree species under one set of environmental conditions. Therefore, the extent of implications that can be drawn from such study is inherently limited. Here we discuss the potential implications of this study in broader perspectives, i.e. in other tree species and for forests under more favorable climatic conditions.

One approach that must be considered is to use the findings of this study as indicators of eco-physiological thresholds of forest trees under extreme conditions. We demonstrated the existence of sub-diurnal cycles of xylem cavitation and refilling, together with a narrow hydraulic safety margin. Using a threshold approach, this dynamic and risky behavior of *P. halepensis* can therefore be interpreted as an adjustment to the climatic conditions at the dry timberline. Although this could be the case, we cannot rule out the possibility that both rapid refilling and narrow hydraulic safety margin will be found in non-extreme environments and in other tree species. This is because, in contrast to the large amount of data on plant water relations, few studies calculate hydraulic safety margin and even fewer detect short-term temporal changes in xylem conductivity. Nevertheless, a relatively narrow hydraulic safety margin of 1.3 MPa was reported for the Mediterranean forest tree *Pinus nigra* (Froux et al. 2005) and Brodribb and Holbrook (2004) described narrower margins of less than 0.3 MPa, in angiosperm plant species in a tropical forest. Thus, narrow safety margins may not be uncommon. In the case of embolism recovery, refilling time of ~2 hr. was observed under induced embolism in the lab (Secchi and Zwieniecki 2011). The fact that such short refilling times were recorded in a temperate tree species (*Populus trichocarpa*), indicates that this phenomenon is not limited to semi-arid trees and conditions.

Some of the results presented above can tell us a lot about tree and forest function in the semi-arid zone, even though a single research station (Yatir forest station), as extensive as it may be, cannot represent ~30% of Earth's terrestrial biosphere. Here we provide indications that the combination of a soil structure, with

relatively high water availability and a 'water-saver' tree species is vital to the success of this forest. Ecosystem-scale processes identified in this study can be relevant in other semi-arid forests. One example is the importance of the evapotranspiration (ET) partitioning into evaporation from soil (E) and tree transpiration (T). Interpreting drought-induced changes to the water balance of potted trees in the greenhouse, we found that T/ET was 22-24% in treatments with less frequent but larger irrigation doses, and as small as 9% in frequent, smaller water applications. Apparently, even in pot experiments the transpiration ratio is sensitive to water infiltration depth associated with the irrigation dose. This provided a strong link to field measurements: Raz-Yaseef et al. (20010b) showed, in the Yatir forest, that small precipitation events were sufficient to maintain the topsoil layer wet during the rainy season, but only more intensive storms infiltrating to the root zone increased T/ET. This demonstrated the importance of precipitation patterns, as opposed to the total amount, on forest function, similar to the results obtained with the potted plants. The interplay between E and T is also central to our understanding of the expected effect of thinning on the local water yield.

On a regional scale, the sensitivity of *P. halepensis* to differences in climate is a good example of how a study of one species growing in a specific region can be applied in a broader perspective. The use of provenances allowed us to link between hydraulic characteristics (e.g. embolism sensitivity and xylem conductivity) and field performance; and between hydraulic characteristics and the plasticity of other physiological traits. As a result, we were able to identify a tradeoff between embolism sensitivity and trunk growth phenology. It is very likely that such tradeoffs exist in other tree species, also affecting their response to climate change. Similarly, the observed changes in water use efficiency (WUE) should not be viewed in the context of *P. halepensis* alone. An increase in WUE was quantitatively shown in two cases: (1) with drying and warming; and (2) with thinning. It is important to consider the latter in other scenarios, because of their potential feedbacks on field performance and the regional carbon and water cycles.

One finding that is applicable to a wide range of forest settings, also outside the semi-arid zone, is the quantification of transpirable soil water content (tSWC), as currently applied with the relative extractable water index (REW, Granier et al. 1999). By integrating soil physics and plant physiology, tSWC may ideally link between environmental (abiotic) conditions and plant (biotic) responses. Specifically, the

ability to clearly define the timing of tSWC exhaustion has implications for estimating the growth season length, forest productivity and sustainability under different climate change scenarios. The advanced tSWC definition presented here offers a mechanistic, quantitative association between soil water content and plant water use. Thus, tSWC may provide a general framework for linking between plants and soil water in studies of agriculture, ecosystem, and greenhouse alike.

6.3 Implications for forest management under change

Ongoing and future changes affecting forests in the Mediterranean and other regions include (1) the global water crisis; and (2) climate change. This study has implications for both. Recent research has focused on the impact of afforestation on water yield (Jackson et al. 2005, Farely et al. 2005) and the hydrological cycle (Ellison et al., 2011). Water use at the tree level must be considered along with other factors such as forest sustainability, and carbon sequestration. In Israel, *Q. calliprinos* and to a greater extent *P. halepensis* have been extensively recruited for afforestation during the last ~80 years (Reisman et al 2010). High fire vulnerability (Fernandes et al 2008) and negative effects on forest biodiversity (Maestre 2004) make *P. halepensis* a less desirable option. Yet the significantly lower water use of this species is of key importance at times of water crisis. In conclusion, "water savers" such as the isohydric *P. halepensis* should be nominated for future forests not only in xeric sites but also in mesic sites, where higher water yield can benefit both communities and the environment.

Today forests around the world are challenged by an increasing rate of changes in environmental conditions, already severely affecting vulnerable populations (Allen et al. 2009 and references therein). In many cases these include trees that grow near the limit of their natural distribution, such as the dry timberline case of the Yatir forest. Our analysis suggests that considering the plasticity of traits across a range of provenances and climates provides a powerful management tool, as also noted by Nicotra et al. (2010), to address the dangers of reduced forest distribution with warming and drying climate trends, such as predicted for the entire Mediterranean and other regions (Cohen et al. 2002; Christensen et al. 2007). Furthermore, it is apparent that a single advantageous trait may be insufficient for sustainability. For example, recruitment of the provenance Otricoli based on high WUE_i or Senalba based on low water use would fail under extreme conditions. Our

findings indicate that at least for *P. halepensis*, the existing gap between plant adaptability and the changing environment could be closed by phenotypic plasticity at the species and provenance level. This, in turn, will potentially permit sustained forest productivity and distribution even under relatively severe climate change scenarios across the Mediterranean region. This natural potential could be realized through informed provenance selection, which is not purely based on short term performance. Future forest planning should consider testing for plasticity in key traits in candidate tree species and genotypes selected for planting today, whose growth should be ensured in the future.

References

1. Allen, C.D., A.K. Macalady, H. Chenchouni, D. Bachelet, N. McDowell, M. Vennetier, T. Kitzberger, A. Rigling, D.D. Breshears, E.H. Hogg et al. 2009. A global overview of drought and heat-induced tree mortality reveals emerging climate change risks for forests. For. Ecol. Manage. 259:660-84.
2. Alpert P, Baldi M, Ilani R, Krichak S, Price C, Rodo X, Saaroni H, Ziv B, Kiscka P, Barkan J et al (2006) Relations between climate variability in the Mediterranean region and the tropics: ENSO, South Asian and African monsoons, hurricanes and Saharan dust. Developments in Earth Environ Sci 4:149-177.
3. Angeles et al (2004) The Cohesion-Tension Theory. New Phytologist.
4. Atzmon N, Moshe Y, Schiller G (2004) Ecophysiological response to severe drought in *Pinus halepensis* Mill. trees of two provenances. Plant Ecology 171:15-22.
5. Baquedano FJ, Valladares F, Castillo FJ (2008) Phenotypic plasticity blurs ecotypic divergence in the response of Quercus coccifera and Pinus halepensis to water stress. European J Forest Res 127:495-506.
6. Boehm T (1893) J. Ber. Bot. Ges. 11:203-212.
7. Bonaparte EENA, Brawn RI (1975) The effect of intraspecific competition on the phenotypic plasticity of morphological and agronomic characters of four Maize hybrids. Annals of Botany 39:863-869,
8. Bond BJ, Kavanagh KL. 1999. Stomatal behavior of four woody species in relation to leaf-specific hydraulic conductance and threshold water potential. *Tree Physiology* 19:503-510.
9. Bouyoucos GS. 1962. Hydrometer method improved for making particle size analysis of soils. *Agronomy Journal*, 54:464–465.
10. Boyer, J.S. 1982. Plant productivity and environment. Science 218: 443–8.
11. Bradshaw AD. 1965. Evolutionary significance of phenotypic plasticity in plants. Advances in Genetics 13:115-155.
12. Breda N, Granier A, Barataud F, Moyne C. 1995. Soil water dynamics in an oak stand. *Plant and Soil* 172:17-27.
13. Breitsprecher A, Bethel JS (1990) Stem-growth periodicity of trees in a tropical wet forest of Costa Rica. Ecology 71:1156-1164.
14. Brochert R. (1994) Water status and development of tropical trees during seasonal drought. Trees 8:115-125.
15. Brodersen CR, McElrone AJ, Choat B, Matthews MA, Shackel KA (2011) The dynamics of embolism repair in xylem: in vivo visualizations using high-resolution computed tomography. Plant Physiology 154:1088-1095.
16. Brodribb TJ and Cochard H (2009) Hydraulic failure defines the recovery and point of death in water-stressed conifers. Plant Physiology 149: 575-84.
17. Brodribb TJ and Holbrook NM (2004) Stomatal protection against hydraulic failure: a comparison of coexisting ferns and angiosperms. New Phytologist 162:663-670.
18. Brougham RW (1960) The relationship between the critical leaf area, total chlorophyll content, and maximum growth-rate of some pasture and crop plants. Annals of Botany 24:463-74.
19. Burke EJ, Brown SJ, Christidis N (2006) Modeling the recent evolution of global drought and projections for the twenty-first century with the Hadley centre climate model. J Hydrometeorology 7:1113-1125.

20. Calamassi R, Della Roccaa G, Falusia M, Paolettib E, Stratib S (2001) Resistance to water stress in seedlings of eight European provenances of *Pinus halepensis* Mill. Ann. For. Sci. 58:663–72.
21. Cermak J, Kucera J, Nadezhdina N (2004) Sap flow measurements with some thermodynamic methods, flow integration within trees and scaling up from sample trees to entire forest stands. Trees 18:529-46.
22. Chmielewski FM, Rotzer T (2001) Response of tree phenology to climate change across Europe. Agri Forest Meteorology 108:101-112.
23. Christensen JH, Hewitson B, Busuic A, Chen A, Gao X, Held I, Jones R, Kolli RK, Kwon WT, Laprise R et al (2007) Regional climate projections. In: Climate Change 2007: The Physical Science Basis. Contributions of Working Group I to the Fourth Assessment Report of the Intergovernmental Panel on Climate Change, eds Solomon S, Qin D, Manning M, Chen Z, Marquis M, Averyt KB, Tingor M, Miller HL (Cambridge University Press, Cambridge, United Kingdom/New York, NY).
24. Ciais P, Reichstein M, Vivoy N, Granier A, Ogee J, Allard V, Aubinet M, Buchmann N, Bernhofer C, Carrara A et al. (2005) Europe-wide reduction in primary productivity caused by the heat and drought in 2003. Nature 437:529–533.
25. Cochard H (2006) Cavitation in trees, C. R. Physique 7: 1018–26.
26. Cohen S, Ianetz A, Stanhill G (2002) Evaporative climate changes at Bet Dagan, Israel 1964-1998. Agri Forest Meteorology 111:83-91
27. Cohen Y, Cohen S, Cantuarias-Aviles T, Schiller G (2008) Variations in the radial gradient of sap velocity in trunks of forest and fruit trees. Plant Soil 305:49-59.
28. Coplen TB (1994) Reporting of stable hydrogen, carbon, and oxygen isotopic abundances. Pure Appl Chem 66:273–276.
29. Cruiziat P, Cochard H, Ameglio T (2002) Hydraulic architecture of trees: main concepts and results. Ann. For. Sci. 59:723-752.
30. Di Mateo G, Brugnoli E, Cherubini P, De Angelis P, Scarascia Mugnozza G (2010) Tree rings delta carbon -13 reveals the impact of past silvicultural management on water-use efficiency in a Mediterranean oak coppice. Annals of Forest Science 67:510 518.
31. Dixon HH, Joly J (1894) Philos. Trans. Royal Society of London Ser. B 186:563-576.
32. Domec JC, King JS, Noormets A, Treasure E, Gavazzi MJ, Sun G, McNulty SG. 2010. Hydraulic redistribution of soil water by roots affects whole-stand evapotranspiration and net ecosystem carbon exchange. *New Phytologist* 187:171-183.
33. Domec JC, Noormets A, King JS, Sun G, McNulty SG, Gavazzi MJ, Boggs JL, Treasure EA (2009) Decoupling the influence of leaf and root hydraulic conductances on stomatal conductance and its sensitivity to vapour pressure deficit as soil dries in a drained loblolly pine plantation. Plant Cell Environ. 32:980-991.
34. Elfving DC, Kaufmann MR, Hall AE. 1972. Interpreting leaf water potential measurements with a model of the soil-plant-atmosphere continuum. *Physiologia Plantarum* 27:161-68.
35. Ellison D, Futter MN, Bishop K (2012) On the forest cover-water yield debate: from demand- to supply-side thinking. Global Change Biology 18:806-820.
36. FAO Forest Genetic Resources No. 5. Mediterranean Conifers, Table 1: international trials of *Pinus halepensis* and *P. brutia*.
37. Farely KA, Jobbagy EG, Jackson RB (2005) Effects of afforestation on water yield: a global synthesis with implications for policy. Global Change Biology 11: 1565–76.

38. Farquhar GD, O'Leary MH, Berry JA (1982) On the relationship between carbon isotope discrimination and intercellular carbon dioxide concentration in leaves. Australian J Plant Physiol 9:121–137.
39. Fernandes PM, Vega JA, Jimenez E, Rigolot E (2008) Fire resistance of European pines. Forest Ecology and Management 256:246-255.
40. Ferrio JP, Florit A, Vega A, Serrano L, Voltas J (2003) Δ13C and tree-ring width reflect different drought responses in *Quercus ilex* and *Pinus halepensis*. Oecologia 442: 512–18.
41. Fisher JB, Baldocchi DD, Misson L, Dawson TE, Goldstein AH (2007) What the towers don't see at night: nocturnal sap flow in trees and shrubs at two AmeriFlux sites in California. Tree Physiology 27:597-610.
42. Flexas, J., J. Bota, F. Loreto, G. Cornic and T. Sharkey. 2004. Diffusive and metabolic limitations to photosynthesis under drought and salinity in C3 plants. Plant Biol. 6: 269–79.
43. Froux F, Ducrey M, Dreyer E, Huc R (2005) Vulnerability to embolism differs in roots and shoots and among three Mediterranean conifers: consequences for stomatal regulation of water loss? Trees 19:137-144.
44. Fusaro E, Di Matteo G, Righi F (2007) Current experimental orchards of pines of the group halepensis (from Italian). Economia Montana – Linea Ecologica 39:2-9.
45. Granier A, Anfodillo T, Sabatti M, Cochard H, Dreyer E, Tomasi M, Valentini R, Breda N (1994) Axial and radial water flows in the trunks of oak trees: a quantitative and qualitative analysis. Tree Physiology 14:1383–96.
46. Granier A, Breda N, Biron P, Villette S. 1999. A lumped water balance model to evaluate duration and intensity of drought constraints in forest stands. *Ecological modeling* 116:269-83.
47. Granier A, Loustau D (1994) Measuring and modeling the transpiration of a maritime pine canopy from sap-flow data. Agricultural and forest meteorology 71:61-81.
48. Grant RH (1984) The mutual interference of spruce canopy structural elements. Agri. For. Met. 32:145-56
49. Gratani L, Pesoli P, Crescente MF (1998) Relationship between photosynthetic activity and chlorophyll content in an isolated *Quercus ilex* L. tree during the year. Photosynthetica 35:445-51.
50. Gruenzweig, J.M., I. Gelfand and D. Yakir. 2007. Biogeochemical factors contributing to enhanced carbon storage following afforestation of a semi-arid shrubland. Biogeosciences 4:891–904.
51. Gupta SC, Larson WE. 1979. Estimating soil water retention characteristics from particle size distribution, organic matter percent, and bulk density. *Water Resources Research* 15:1633-5.
52. Hacke UG, Stiller V, Sperry JS, Pittermann J, McCulloh KA (2001) Cavitation fatigue. Embolism and refilling cycles can weaken cavitation resistance of xylem. Plant Physiology 125:779-786.
53. Heiskanen J, Makitalo K. 2002. Soil water retention characteristics of Scots pine and Norway spruce forest sites in Finnish Lapland. Forest Ecol. Manage. 162:137-152.
54. Holbrook NM, Zwieniecki MA (1999) Embolism repair and xylem tension: do we need a miracle? Plant Physiology 120:7-10.
55. Holbrook, N.M., M.J. Burns and C.B. Field. 1995. Negative Xylem Pressures in Plants: A Test of the Balancing Pressure Technique. Science 270: 1193-4.
56. Israelson OW, West FL. 1922. Water holding capacity of irrigated soils. *Utah State Agricultural Bulletin* 183:1-24.

57. Jackson RB, Jobbagy EG, Avissar R, Barrett DJ, Cook CW, Farely KA, le Maitre DC, McCarl BA, Murray BC (2005) Trading water for carbon with biological carbon sequestration. Science 310: 1944-7.
58. Jones MM, Turner NC. 1978. Osmotic adjustments in leaves of Sorghum in response to water deficits. *Plant Physiology* 61:122-6.
59. Kaneti (2010) Yield and physiological and environmental stress indices in persimmon trees irrigated with various grades of treated water. Thesis, The Hebrew University of Jerusalem, Rehovot, Israel.
60. Kariuki M (2008) Modelling the impacts of various thinning intensities on tree growth and survival in a mixed species eucalypt forest in central Gippsland, Victoria, Australia. Forest Ecology and Management 256:2007-2017.
61. Klein T, Cohen S, Yakir D (2011) Hydraulic adaptations underlying drought resistance of *Pinus halepensis.* Tree Physiology 31:637-48.
62. Klein T, Di Matteo G, Rotenberg E, Cohen S, Yakir D (2012) Will existing traits' plasticity sustain growth and survival of a major pine species under climate change in the Mediterranean? Oecologia.
63. Klein T, Hemming D, Lin T, Grunzweig JM, Maseyk K, Rotenberg E, Yakir D (2005) Association between tree-ring and needle delta C-13 and leaf gas exchange in Pinus halepensis under semi-arid conditions. Oecologia 144:45-54.
64. Klein Tank AMG, Wijngaard JB, Konnen GP, Bohm R, Demaree G, Gocheva A, Mileta M, Pashiardis S, Hejkrlik L, Kern-Hansen C et al (2002) Daily dataset of 20th-century surface air temperature and precipitation series for the European Climate Assessment. International J Climatology 22:1441-1453.
65. Klute (ed.) 1986. Methods of Soil Analysis, Part 1. Physical and Mineralogical Methods. Agronomy Monograph No. 9. American Society of Agronomy/Soil Science Society of America, Madison, WI.
66. Koerner C, Sarris D, Christodoulakis D (2005) Long-term increase in climatic dryness in the East-Mediterranean as evidenced for the island of Samos. Regional Environ Change J 5:27–36.
67. Lajtha K and Barnes FJ (1991) Carbon gain and water-use in pinyon pine–juniper woodlands of northern New Mexico – field versus phytotron chamber measurements. Tree Physiol 9:59–67.
68. Landsberg JJ, Powell DBB (1973) Surface exchange characteristics of leaves subject to mutual interference. Agri Meteorology 12:169-84.
69. Li Y, Fuchs M, Cohen S, Wallach R. 2002. Water uptake profile response of corn to soil moisture depletion. *Plant, Cell and Environment* 25:491-500.
70. Maestre FT and Cortina J (2004) Are *Pinus halepensis* plantations useful as a restoration tool in semiarid Mediterranean areas? Forest Ecology and Management198: 303–17.
71. Marshall TJ. 1947. Mechanical composition of soil in relation to field descriptions of texture. Council for Scientific and Industrial Research, Bulletin No. 224, Melbourne.
72. Martinez-Vilalta J, Pinol J (2002) Drought-induced mortality and hydraulic architecture in pine populations of the NE Iberian Peninsula. Forest Ecol and Manag 161:247–256.
73. Maseyk K, Hemming D, Angert A, Leavitt SW, Yakir D (2011) Increase in water-use efficiency and underlying processes in pine forests across a precipitation gradient in the dry Mediterranean region over the past 30 years. Oecologia (DOI 10.1007/s00442-011-2010-4)

74. Maseyk K, Lin T, Rotenberg E, Grünzweig JM, Schwartz A, Yakir D. 2008. Physiology-phenology interactions in a productive semi-arid pine forest. *New Phytologist* 178:603-16.
75. Maseyk K. 2006. Ecophysiological and phonological aspects of *Pinus halepensis* in an arid-Mediterranean environment. Thesis, The Weizmann Institute of Science, Rehovot, Israel.
76. Matula S, Spongrova K. 2007. Pedotransfer function application for estimation of soil hydrophysical properties using parametric methods. *Plant Soil and Environment* 53:149-57.
77. McCarroll D and Loader NJ (2004) Stable isotopes in tree rings. Quaternary Sci Rev 23:771-801.
78. McDowell N, Pockman WT, Allen CD, Breshears DD, Cobb N, Kolb T, Plaut J, Sperry J, West A, Williams DG, Yepez EA (2008) Mechanisms of plant survival and mortality during drought: why do some plants survive while others succumb to drought? New Phytologist 178: 719-39.
79. McLaughlin SB, Wullschleger SD, Nosal M (2003) Diurnal and seasonal changes in stem increment and water use by yellow poplar trees in response to environmental stress. Tree Physiology 23:1125-36.
80. Meinzer FC, James SA, Goldstein G, Woodruff D (2003) Whole-tree transport scales with sapwood capacitance in tropical forest canopy trees. Plant, Cell, and Environment 26:1147-55.
81. Meinzer FC, Johnson DM, Lachenbruch B, McCulloh KA, Woodruff DR (2009) Xylem hydraulic safety margins in woody plants: coordination of stomatal control of xylem tension with hydraulic capacitance. Functional Ecology 23:922-930.
82. Mejstrik VK and Cudlin P (1983) Mycorrhiza in some desert plant species in Algeria. Plnat and Soil 71:363-6.
83. Mickovski SB, Ennos AR. 2003. Anchorage and asymmetry in the root system of *pinus peuce*. *Silva Fennica* 37:161-173.
84. Miller PC.1982. Nutrients and water relations in Mediterranean-type ecosystems. Presented at the Symposium on Dynamics and Management of Mediterranean-type ecosystems, June 22-26 1981, San Diego, California, USA.
85. Nadezhdina N, Cermak J, Gasparek J, Nadezhdin V, Prax A. 2006. Vertical and horizontal water redistribution in Norway spruce (*Picea abies*) roots in the Moravian Upland. *Tree Physiology* 26:1277:1288.
86. Nadezhdina N, Ferreira MI, Silva R, Pacheco CA. 2007. Seasonal variation of water uptake of a *Quercus suber* tree in Central Portugal. *Plant and Soil* 305:105-119.
87. Nardini A, Salleo S (2000) Limitation of stomatal conductance by hydraulic traits: sensing or preventing xylem cavitation? Trees 15:14-24.
88. Nicotra AB, Atkin OK, Bonser SP, Davidson AM, Finnegan EJ, Mathesius U, Poot P, Purugganan MD, Richards CL, Valladares F, van Kleunen M (2010) Plant phenotypic plasticity in a changing climate. Trends in Plant Sci 15:684-92.
89. Nikolov ND, Massman WJ, Schoettle AW (1995) Coupling biochemical and biophysical processes at the leaf level: an equilibrium photosynthesis model for leaves of C_3 plants. Ecologicall modeling 80:205-35.
90. Ogee J, Barbour MM, Wingate L, Bert D, Bosc A, Stievenard M, Lambrot C, Pierre M, Bariac T, Loustau D, Dewar RC. 2009. A single-substrate model to interpret intra-annual stable isotope signals in tree-ring cellulose. *Plant Cell and Environment* 32:1071-1090.

91. Ogee J, Brunet Y, Loustau D, Berbigier P, Delzon S. 2003. MuSICA, a CO2, water and energy multilayer, multileaf pine forest model: evaluation from hourly to yearly time scales and sensitivity analysis. *Global Change Biology* 9:697-717.
92. Oliveras I, Martínez-Vilalta J, Jimenez-Ortiz T, Lledó MJ, Escarré A, Piñol J (2003) Hydraulic properties of *Pinus halepensis*, *Pinus pinea* and *Tetraclinis articulata* in a dune ecosystem of Eastern Spain. Plant Ecology 169:131–41.
93. Oren R, Ewers BE, Todd P, Phillips N, Katul G. 1998. Water balance delineates the soil layer in which moisture affects canopy conductance. *Ecological Applications* 8:990-1002.
94. Osem Y, Zangy E, Bney-Moshe E, Moshe Y, Karni N, Misna Y (2009) The potential of transforming simple structured pine plantations into mixed Mediterranean forests through natural regeneration along a rainfall gradient. Forest Ecology and Management 259:14-23.
95. Palutikof JP, Goodes CM, Guo X (1994) Climate change, potential evapotranspiration and moisture availability in the Mediterranean basin. International j climatology 14:853-869.
96. Paruelo JM, Sala OE, Beltran AB. 2000. Long-term dynamics of water and carbon in semi-arid ecosystems: a gradient analysis in the Patagonian steppe. *Plant Ecology* 150:133-43.
97. Pletola H, Miina J, Rouvinen I, Kellomaeki S (2002) Effect of early thinning on the diameter growth distribution along the stem of Scots Pine. Silva Fennica 36:813-825.
98. Penuelas J, Lloret F, Montoya R (2001) Severe drought effects on Mediterranean woody flora in Spain. Forest Sci 47:214–218.
99. Porra RJ, Thompson WA, Kriedmann PE (1989) Determination of accurate extinction coefficients and simultaneous equations for assaying chlorophylls a and b extracted with four different solvents: verification of the concentration of chlorophyll standards by atomic absorption spectroscopy. Biochemica et Biophysica Acta 975:384-94.
100. Pukkala, T., Miina, J. Palahí, M (2002) Thinning response and thinning bias in a young Scots pine stand. Silva Fennica 36(4): 827–840.
101. Quezel, P. 2000. Taxonomy and biogeography of Mediterranean pines (*Pinus halepensis* and *P. brutia*). In: Ne'eman G, Trabaud L (Eds.), Ecology, Biogeography and Management of *Pinus halepensis* and *P. brutia* Forest Ecosystems in the Mediterranean Basin. Backhuys Publishers, Leiden, pp. 1–12.
102. Raftoyannis Y, Spanos I, Radoglou K (2008) The decline of Greek fir (Abies cephalonica Loudon): Relationships with root condition. Plant Biosystems 142:386–90.
103. Raz-Yaseef N, Rotenberg E, Yakir D (2010) Effects of spatial variations in soil evaporation caused by tree shading on water flux partitioning in a semi-arid pine forest. Agri and for meteo 150:454-62.
104. Raz-Yaseef N, Yakir D, Schiller G, Cohen S. 2012. Dynamics of evapotranspiration partitioning in a semi-arid forest as affected by temporal rainfall patterns. *Agricultural and Forest Meteorology* 157:77-85.
105. Raz-Yaseef, N, Yakir D, Rotenberg E, Schiller G, Cohen S. 2010. Ecohydrology of a semi-arid forest: partitioning among water balance components and its implications for predicted precipitation changes. Ecohydrology 3:143-54.
106. Reisman O, Ben-Yair S, Bocken B (2010) Forest or gap? Establishment of *Quercus calliprinos* in pine forests in Israel. Israel Ecology and Environment 1:38-46.
107. Resco V, Ewers BE, Sun W, Huxman TE, Weltzin JF, Williams DG (2009) Drought-induced hydraulic limitations constrain leaf gas exchange recovery after precipitation pulses in the C_3 woody legume, *Prosopis velutina*. New Phytologist 181:672-682.

108. Richards CL, Bossdorf O, Muth NZ, Gurevitch J, Pigliucci M (2006) Jack of all trades, master of some? On the role of phenotypic plasticity in plant invasions. Ecology Lett 9: 981–993.
109. Ritter A, Munoz-Carpena R, Regalado CM, Vanclooster M, Lambot S. 2004. Analysis of alternative measurement strategies for the inverse optimization of the hydraulic properties of a volcanic soil. *Journal of Hydrology* 295:124-39.
110. Roberts J. 1983. Forest transpiration: a conservative hydrological process? *Journal of Hydrology* 66:133-41.
111. Robertson A, Overpack J, Rind D, Mosley-Thompson E, Zielinski G, Lean J, Koch D, Penner J, Tegen I, Healy R (2001) Hypothesized climate forcing time series for the last 500 years. J Geophys Res 106: 14783–14803.
112. Rotenberg E, Yakir D. 2010. Contribution of semi-arid forests to the climate system. *Science* 327:451-4.
113. Royo A, Gil L, Pardos JA (2001) Effect of water stress conditioning on morphology, physiology and field performance of *Pinus halepensis* Mill. Seedlings. New Forests 21: 127–40.
114. Sadras VO, Reynolds MP, de la Vega AJ, Petrie PR, Robinson R (2009) Phenotypic plasticity of yield and phenology in wheat, sunflower and grapevine. Field Crops Res 110:242-250.
115. Sarris D, Christodoulakis D, Korner C (2007) Recent decline in precipitation and tree growth in the eastern Mediterranean. Global Change Biol 13:1187–2000.
116. Schenk HJ, Espino S (2011) Nighttime sap flow removes air from plant hydraulic systems. 8th International workshop on sap flow, Voltera, Italy.
117. Schiller G and Atzmon N (2009) Performance of Aleppo pine (*Pinus halepensis*) provenances grown at the edge of the Negev desert: A review. Journal of Arid Environments 73:1051-7.
118. Schiller, G., S. Cohen, E.D. Unger, Y. Moshe and N. Herr. (2003) Estimating water use by sclerophyllous species under east Mediterranean climate: III. Tabor oak forest sap flow distribution and transpiration. For. Ecol. Manage. 238:147-155.
119. Schiller G, Unger ED, Cohen S, Herr N (2010) Water use by Tabor and Kermes oaks growing in their respective habitats in the Lower Galilee region of Israel. Forest Ecology and Management 259:1018-1024.
120. Schlichting CD (1986) The evolution of phenotypic plasticity in plants. Ann Rev Ecol Syst 17:667-693.
121. Scholander PF, Hammel HT, Bradstreet ED, Hemmingsen EA (1965) Sap Pressure in Vascular Plants: Negative hydrostatic pressure can be measured in plants. Science 148: 339-46.
122. Schwarzel K, Menzer A, Clausnitzer F, Spank U, Hantzschel J, Grunwald T, Kostner B, Bernhofer C, Feger K-H. 2009. Soil water content measurements deliver reliable estimates of water fluxes: A comparative study in a beech and a spruce stand in the Tharandat forest (Saxony, Germany). *Agricultural and Forest Meteorology* 149:1994-2006.
123. Seager, R., M. Ting, I. Held, Y. Kushnir, J. Lu, G. Vecchi, H.P. Huang, N. Harnik, A. Leetmaa, N.C. Lau, C. Li, J. Velez and N. Naik. 2007. Model projections of an imminent transition to a more arid climate in southwestern North America. Science 316:1181-4.
124. Secchi F, Zwieniecki MA (2011) sensing embolism in xylem vessels: the role of sucrose as a trigger for refilling. Plant Cell Environ. 34:514-524.
125. Seibt U, Rajabi A, Griffiths H, Berry JA (2008) Carbon isotopes and water use efficiency: sense and sensitivity. Oecologia 155:441-454.

126. Sever N, Neeman G (2008) Dehydration and recovery of *Quercus calliprinos* in Israel following consecutive drought years. Yaar 10:10-16.
127. Shachnovich Y, Berliner PR, Bar P. 2008. Rainfall interception and spatial distribution of throughfall in a pine forest planted in an arid zone. *Journal of Hydrology* 349:168-177.
128. Siqueira M, Katul G, Porporato A. 2008. Onset of water stress, hysteresis in plant conductance, and hydraulic lift: scaling soil water dynamics from millimeters to meters. *Water Resources Research* 44:1-14.
129. Sperry JS (2000) Hydraulic constraints on plant gas exchange. Agri For Meteo 104:13-23.
130. Sperry JS, Adler FR, Campbell GS, Comstock JP. 1998. Limitation of plant water use by rhizosphere and xylem conductance: results form a model. *Plant Cell and Environment* 21:347-359.
131. Sperry JS, Hacke UG, Oren R, Comstock JP (2002) Water deficits and hydraulic limits to leaf water supply. Plant Cell Environ. 25:251-263.
132. Sperry JS, Stiller V, Hacke UG (2003) Xylem hydraulics and the soil-plant-atmosphere continuum: opportunities and unresolved issues. Agron J 95:1362-1370.
133. Sperry S (2004) Coordinating stomatal and xylem functioning – an evolutionary prespective. New Phytologist 162: 568-70.
134. Sprintsin M, Cohen S, Maseyk K, Rotenberg E, Grunzweig JM, Karnieli A, Berliner PR, Yakir D. 2011. Long term and seasonal courses of leaf area index in a semi-arid forest plantation. *Agricultural and Forest Meteorology* 151:565-574.
135. Steppe K, De Pauw DJW, Doody TM, Teskey RO (2010) A comparison of sap flux density using thermal dissipation, heat pulse velocity and heat field deformation methods. Agri and For Meteo 150: 1046-56.
136. Sterl, A., et al. 2008. When can we expect extremely high surface temperatures? Geophys. Res. Lett. 35:L14703.
137. Tardieu F and Simonneau T (1998) Variability among species of stomatal control under fluctuating soil water status and evaporative demand: modelling isohydric and anisohydric behaviours. Journal of Experimental Botany 49: 419–32.
138. Tognetti R, Michelozzi M, Giovannelli A (1997) Geographical variation in water relations, hydraulic architecture and terpene composition of Aleppo pine seedlings from Italian provinces. Tree Physiol 17: 241-250.
139. Tyree MT and Alexander JD (1993) Hydraulic conductivity of branch junctions in three temperate tree species. Trees 7:156-9.
140. Tyree MT, Davis SD, Cochard H (1994) Biophysical perspectives of xylem evolution: is there a tradeoff of hydraulic efficiency for vulnerability to dysfunction? IAIW J 15: 335-60.
141. Tyree MT, Salleo S, Nardini A, Lo Gullo MA, Mosca R (1999) Refilling of embolized vessels in young stems of Laurel. Do we need a new paradigm? Plant Physiology 120:11-21.
142. Tyree MT, Sperry JS (1988) Do Woody Plants Operate Near the Point of Catastrophic Xylem Dysfunction Caused by Dynamic Water Stress? answers from a model. Plant Physiology 88:574-580.
143. Van Genuchten MT, Leij FJ, Yates SR. 1991. The RETC code for quantifying the hydraulic functions of unsaturated soils. Report No. EPA/600/2-91/065 RS Kerr Environmental Research Laboratory, US Environmental Protection Agency.
144. Waring RH and Silvester WB (1994) Variation in foliar $\delta^{13}C$ values within the crowns of *Pinus radiata* trees. Tree physiology 14:1203-13.

145. Warren JM, Meinzer FC, Brooks JR, Domec JC. 2005. Vertical stratification of soil water storage and release dynamics in Pacific Northwest coniferous forests. *Agricultural and Forest Meteorology* 130:39-58.
146. West AG, Hultine KR, Burtch KG, Ehleringer JR (2007) Seasonal variations in moisture use in a pinon–juniper woodland. Oecologia 153: 787-98.
147. Williams M, Rastetter EB, Fernandes DN, Goulden ML, Wofsy SC, Shaver GR, Melillo JM, Munger JW, Fan S-M, Nadelhoffer KJ. 1996. Modelling the soil-plant-atmosphere continuum in a *Quercus-Acer* stand in Harvard forest: the regulation of stomatal conductance by light, nitrogen and soil/plant hydraulic properties. *Plant Cell and Environment* 19:911-927.
148. Woesten JHM, Finke PA, Jansen MJW. 1994. Comparison of class and continuous pedotransfer functions to generate soil hydraulic characteristics. *Geoderma* 66:227-37.
149. Yang S-J, Zhang Y-J, Sun M, Goldstein G, Cao K-F (2012) Recovery of diurnal depression of leaf hydraulic conductance in a subtropical woody bamboo species: embolism refilling by nocturnal root pressure. Tree Physiology 32:414:422.
150. Yates SR, van Genuchten MT, Warrick AW, Leij FJ. 1992. Analysis of measured, predicted, and estimated hydraulic conductivity using the RETC computer program. *Soil Science Society of America Journal* 56:347-54.
151. Zeppel M, Macinnis-Ng CMO, Ford CR, Eamus D. 2008. The response of sap flow fluxes to pulses of rain in a temperate Australian woodland. *Plant and Soil* 305:121-30.
152. Zimmermann U, Schneider H, Wegner LH, Haase A (2004) Water ascent in tall trees: does evolution of land plants rely on a highly metastable state? New Phytologist 162:575-615.
153. Zufferey V, Cochard H, Ameglio T, Spring J-L, Viret O (2011) Diurnal cycles of embolism formation and repair in petioles of grapevine (*Vitis vinifera* cv. Chasselas). J Experimental Botany 62:3885-3894.
154. Zweifel R, Item H, Haesler R (2001) Link between diurnal stem radius and tree water relations. Tree Physiology 21:869-877.
155. Zwieniecki MA, Holbrook NM (1998) Diurnal variation in xylem hydraulic conductivity in white ash (*Fraxinus Americana* L.), red maple (*Acer robrum* L.) and red spruce (*Picea rubens* Sarg.). Plant Cell environ. 21:1173-1180.